What can we learn from transfer, and how is best to do it?

Wilton Catford
University of Surrey

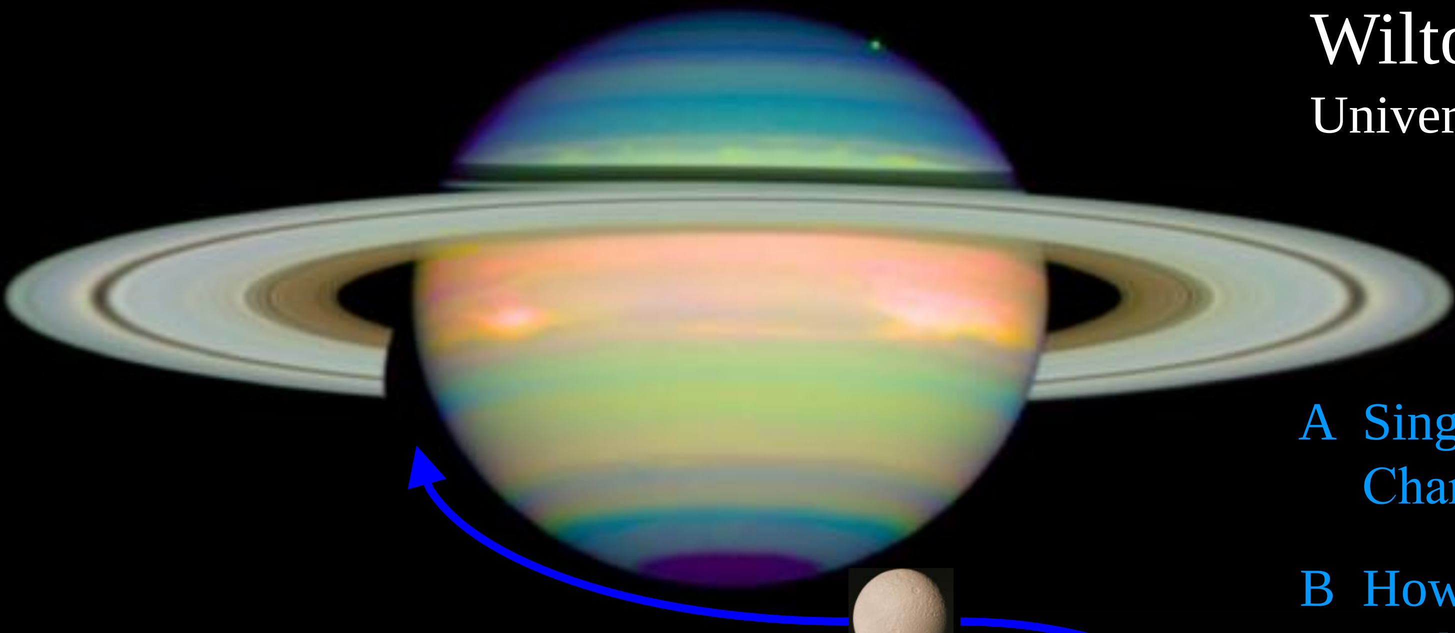

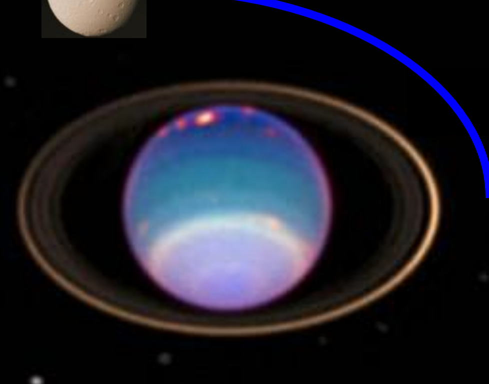

- A Single Particle States; Changing magic no.'s
- B How reactions can study this physics
- C Practicalities; Inverse Kinematics
- D Experimental setups
- E Results & Perspectives

CERN REACTIONS SCHOOL

CERN, Geneva ** 22-24 April 2014

SATURN HST/ IR 1998, TETHYS VOYAGER2 1981, URANUS HST/ IR 1986

- **Motivation: nuclear structure reasons for transfer**
- **What quantities we actually measure**
- **What reactions can we choose to use?**
- **What is a good beam energy to use?**
- **Inverse Kinematics**
- **Implications for Experimental approaches**
- **Example experiments and results**

CERN REACTIONS SCHOOL

CERN, Geneva ** 22-24 April 2014

LAKE GENEVA

Nucleon Transfer using Radioactive Beams:
results and lessons from the TIARA and TIARA+MUST2 experiments at SPIRAL

WILTON CATFORD, University of Surrey, UK

W.N. Catford, N.A. Orr, A. Matta, B. Fernandez-Dominguez, F. Delaunay, C. Timis, M. Labiche, J.S. Thomas, G.L. Wilson, S.M. Brown, I.C. Celik, A.J. Knapton *et al.*

and the TIARA+MUST2 Collaboration

(Surrey, Liverpool, Daresbury, West of Scotland, Birmingham, Orsay, Saclay, GANIL, LPC Caen)

[1] *University of Surrey, Guildford, GU2 7SH, UK*

[2] *STFC Daresbury Laboratory, Warrington, Cheshire, WA4 4AD, UK*

[3] *University of Liverpool, Liverpool, L69 7ZE, UK*

[4] *GANIL, BP 55027, 14076 Caen Cedex 5, France*

[5] *IPN Orsay, IN2P3-CNRS, 91406 Orsay, France*

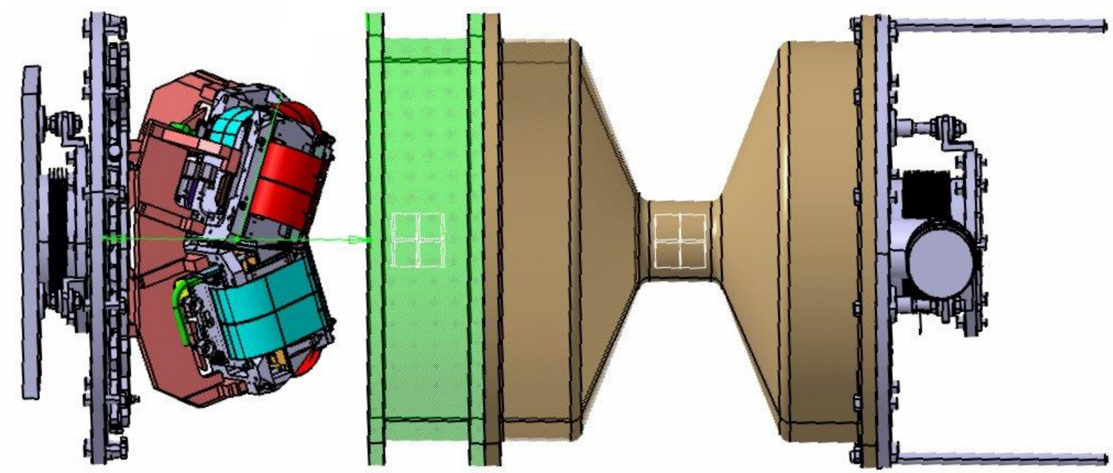

Results from SHARC+TIGRESS at ISAC2/TRIUMF

UNIVERSITY OF SURREY

WNC, G.L. Wilson, S.M. Brown

THE UNIVERSITY of York

C.Aa. Diget, B.R. Fulton, S.P. Fox
R. Wadsworth, M.P. Taggart

TRIUMF

G. Hackman, A.B. Garnsworthy, S. Williams
C. Pearson, C. Unsworth, M. Djongolov and
the TIGRESS collaboration

TIGRESS

LPC

N.A. Orr, F. Delaunay, N.L. Achouri

UNIVERSITY OF LIVERPOOL — Boston[2]

COLORADO SCHOOL OF MINES 1874 — F. Sarazin

LSU — J.C. Blackmon

UNIVERSITY of GUELPH — C. Svensson

SAINT MARY'S UNIVERSITY SINCE 1802 — R.A.E. Austin

SINGLE PARTICLE STATES in the SHELL MODEL:

Changes – tensor force, p-n

Residual interactions move the mean field levels

Magic numbers “migrate”, changing stability, reactions, collectivity

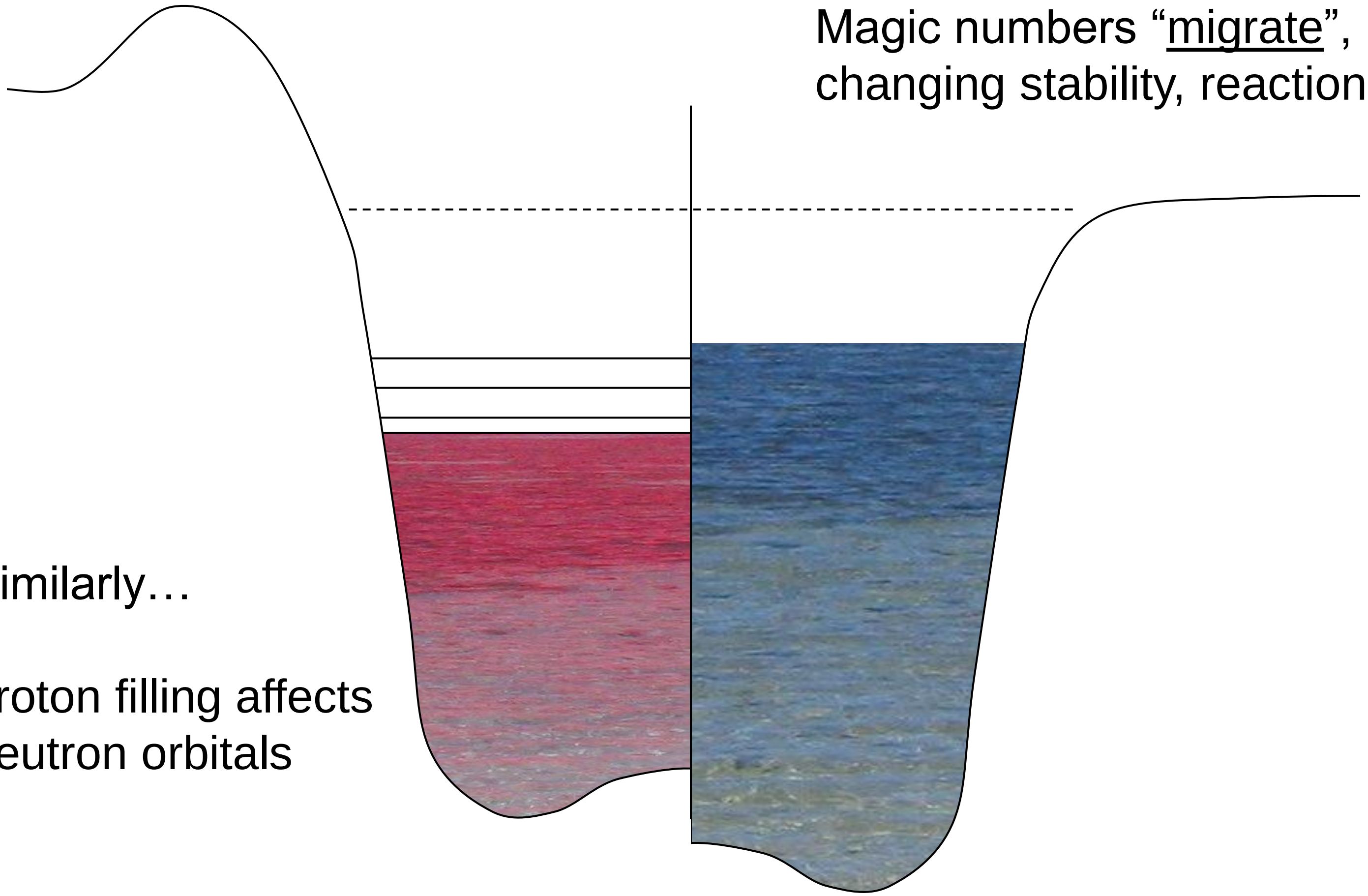

Similarly…

proton filling affects neutron orbitals

SINGLE PARTICLE STATES in the SHELL MODEL:

(d, p)

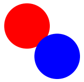

Probing the changed orbitals and their energies…

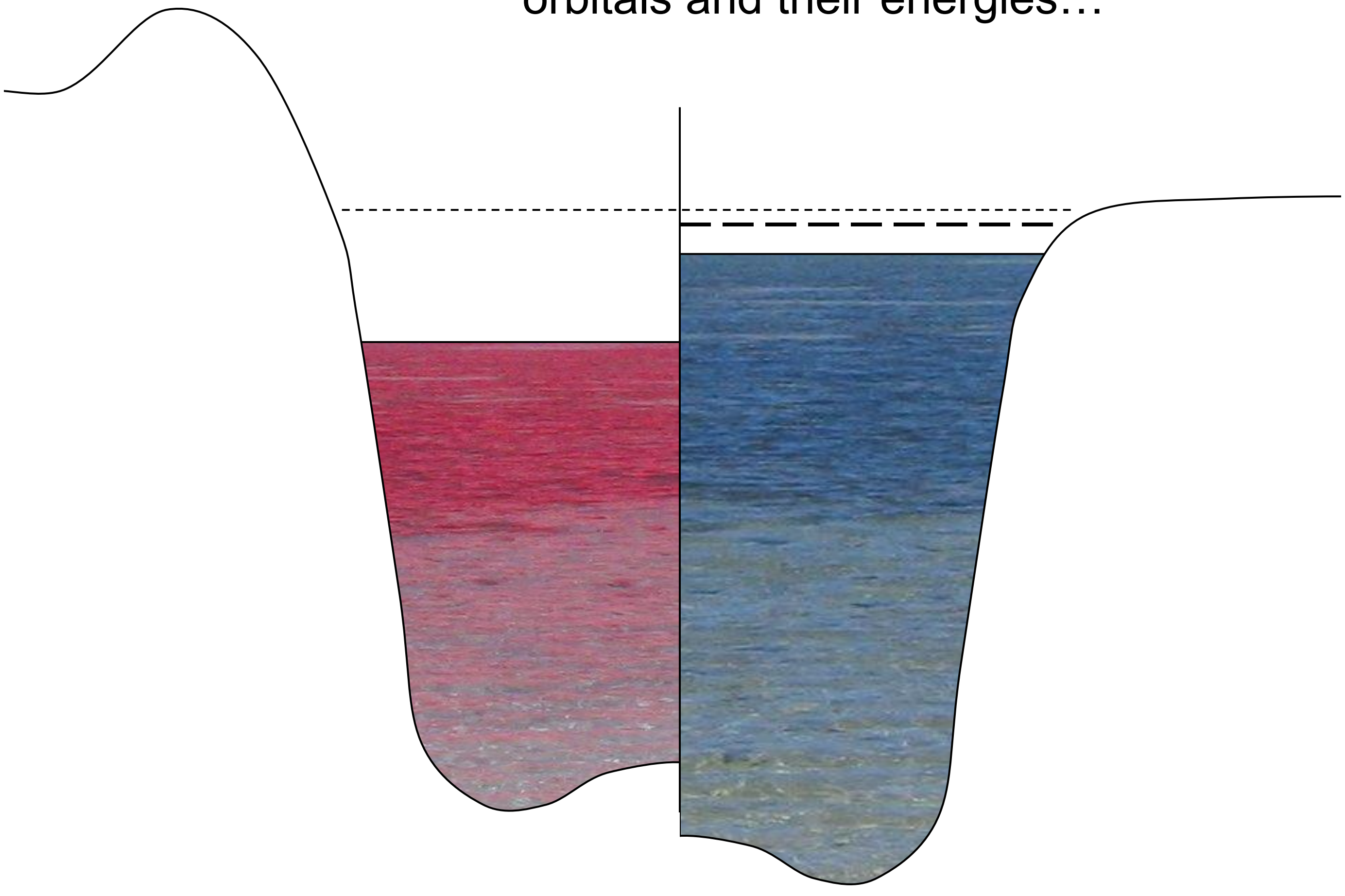

SINGLE PARTICLE STATES in the SHELL MODEL:

As we approach the dripline, we also have to worry about the meaning and theoretical methods for probing resonant orbitals in the continuum…

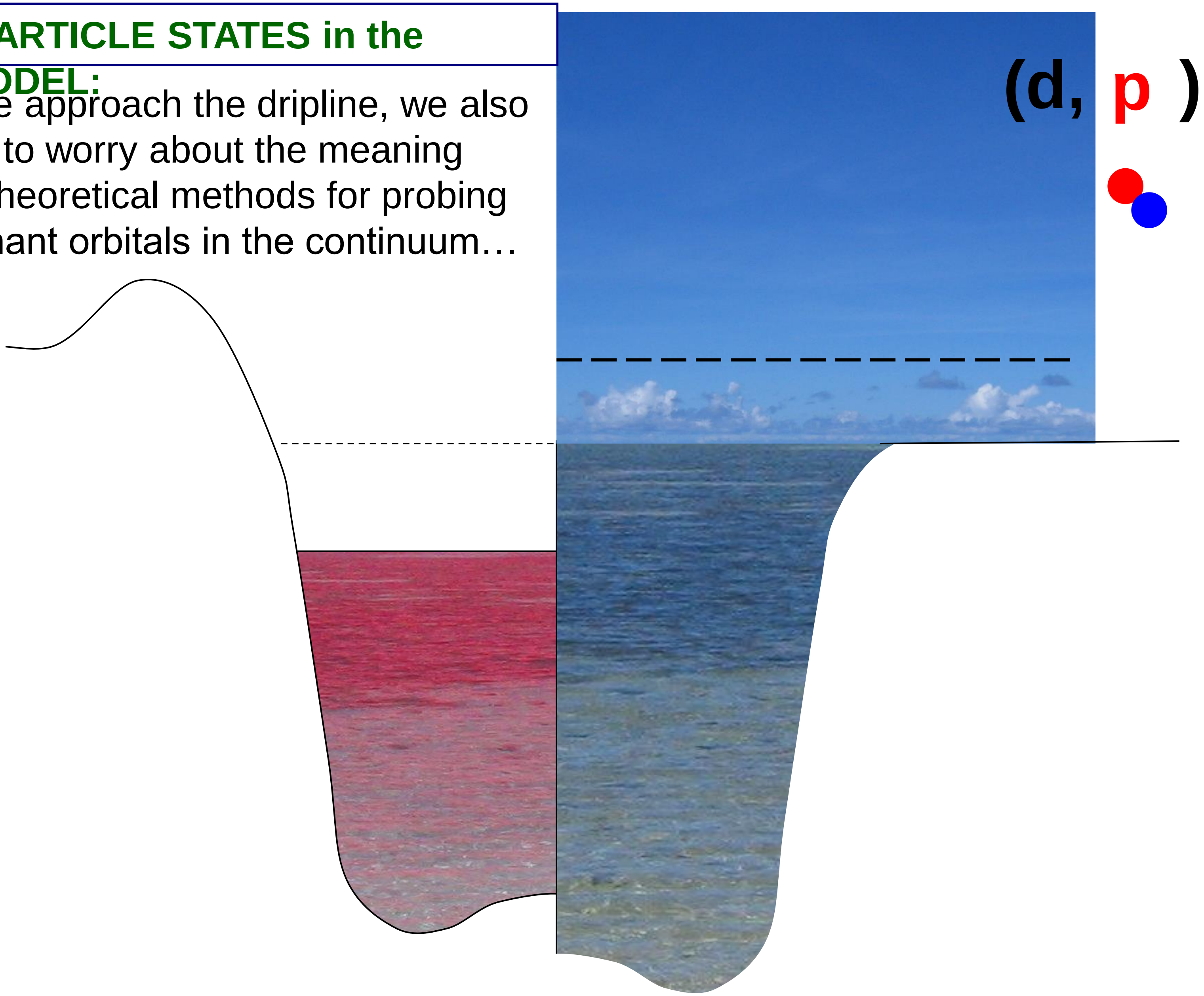

Changing shell structure and collectivity at the drip line

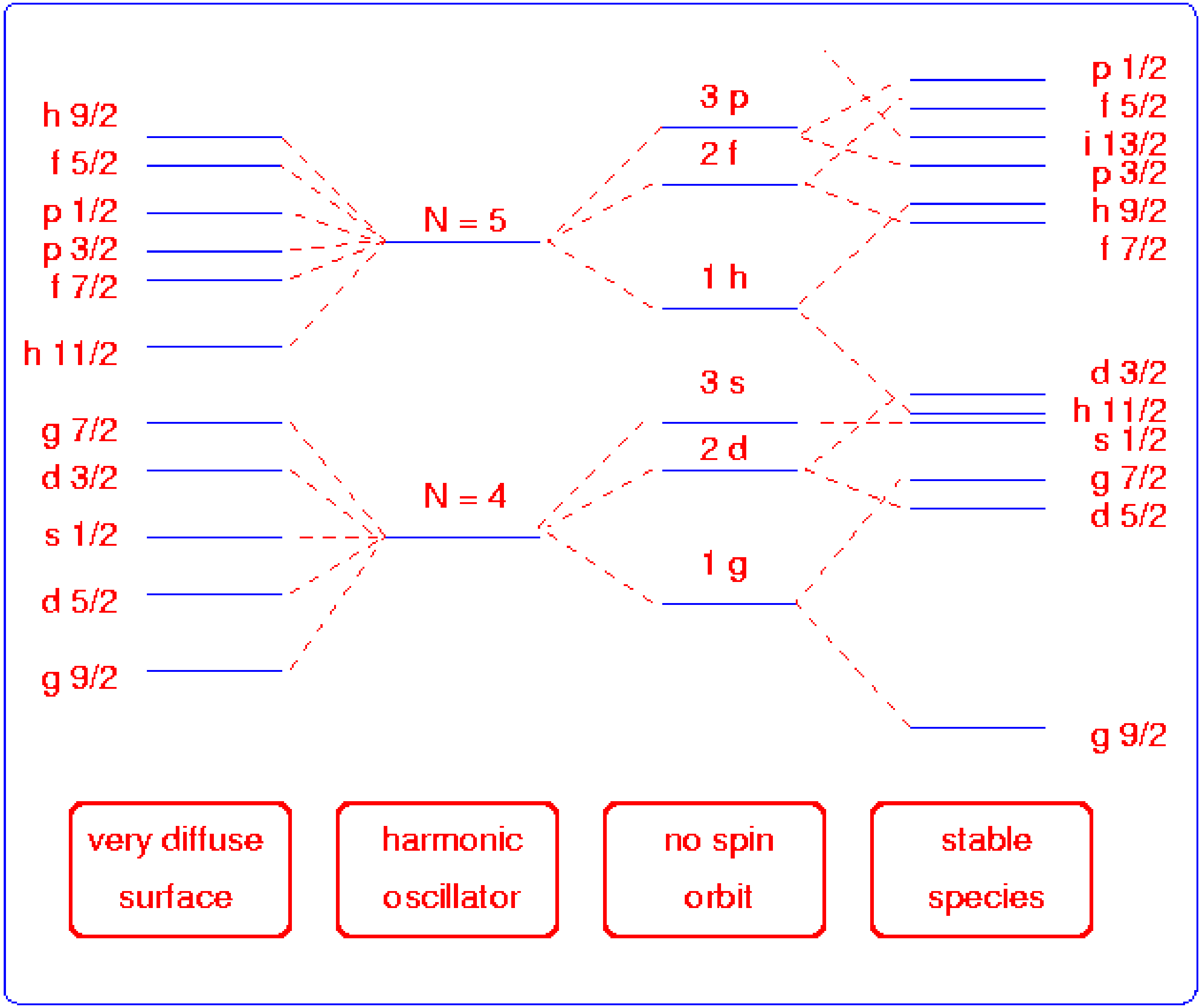

J.Dobaczewski et al., PRC 53 (1996) 2809

N=16 / N=20 / N=28 Development

N=14 (N=15)

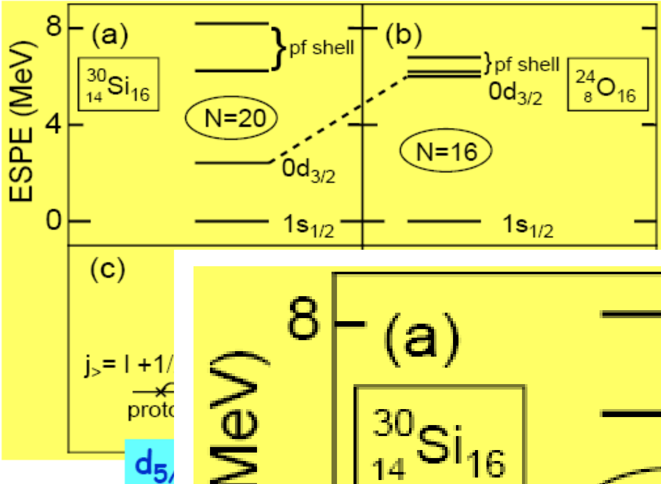

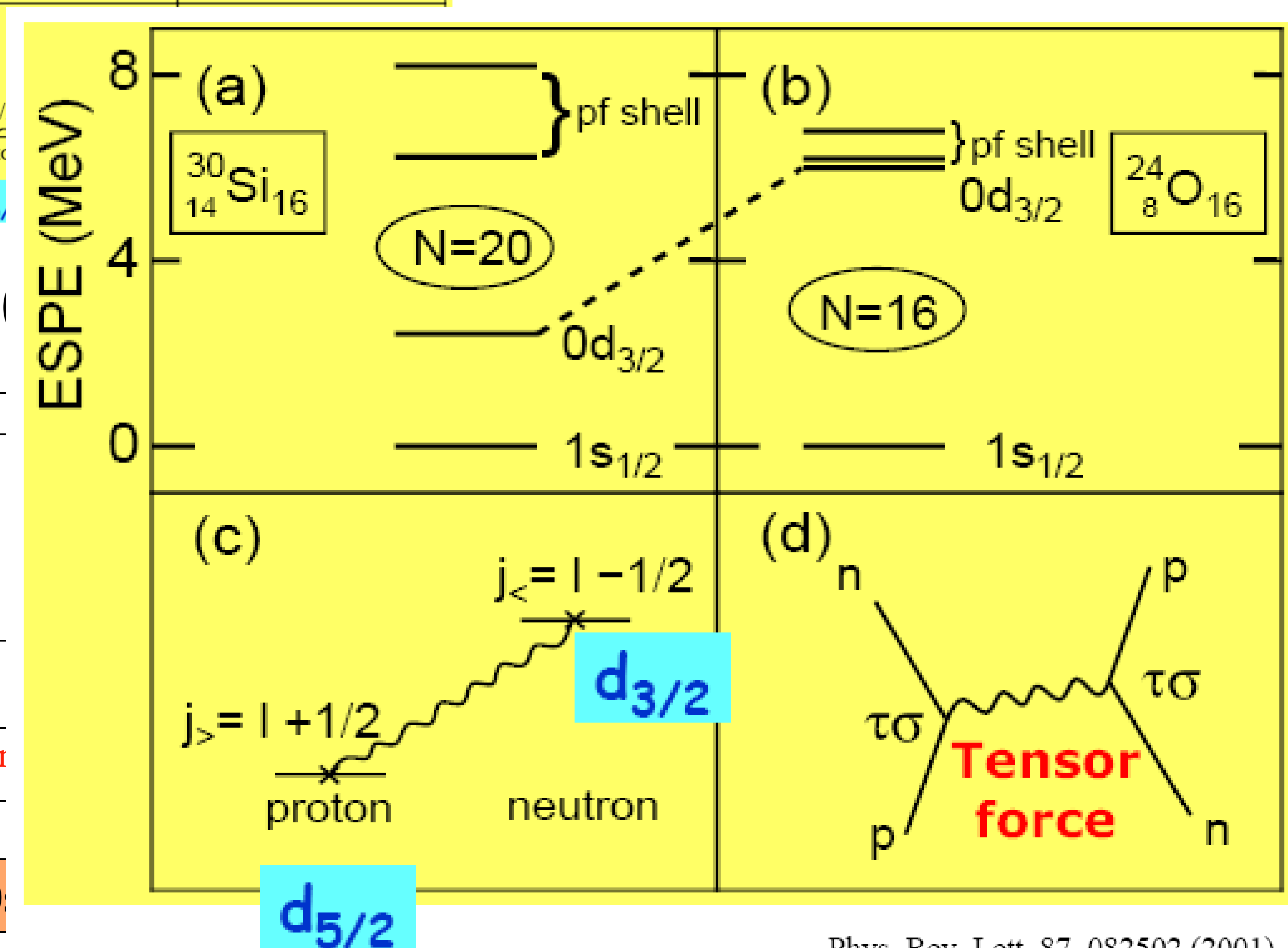

directly
^{24}Ne

22(

(^{29}Si)

$1p_{3/2}$

$0f_{7/2}$

$0d_{3/2}$

$1s_{1/2}$

er

$0d_{5/2}$

0s

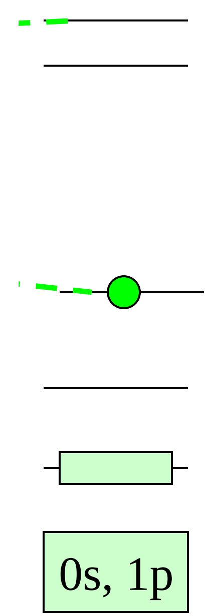

π ν | π ν ν

T. Otsuka et al.

Phys. Rev. Lett. 87, 082502 (2001)
Phys. Rev. Lett. 95, 232502 (2005)

Changing Magic Numbers

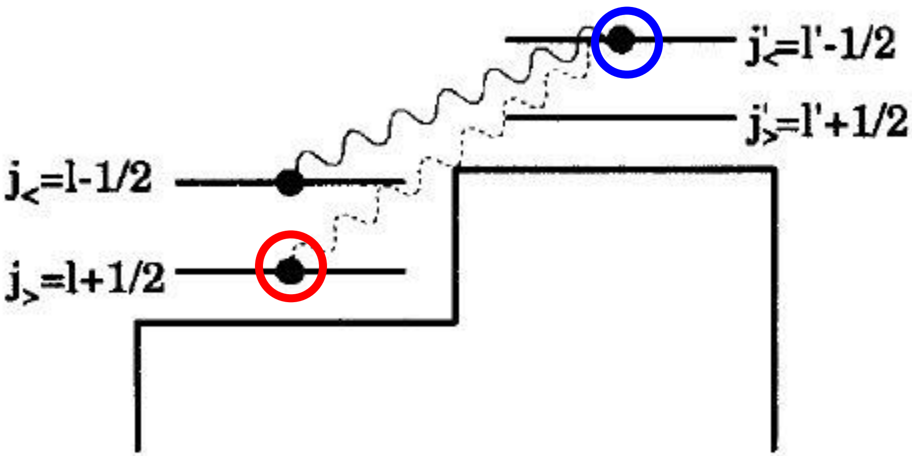

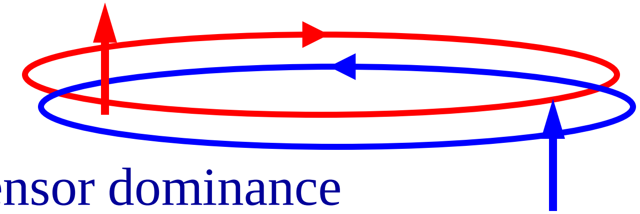

T. Otsuka *et al.*, Phys. Rev. Lett. **97**, 162501 (2006).

T. Otsuka *et al.*, Phys. Rev. Lett. **87**, 082502 (2001).

Nuclei are quantum fluids comprising two distinguishable particle types…

They separately fill their quantum wells…

Shell structure emerges…

Valence nucleons interact…

This can perturb the orbital energies…

The shell magic numbers for p(n) depend on the level of filling for the n(p)

Changing Magic Numbers

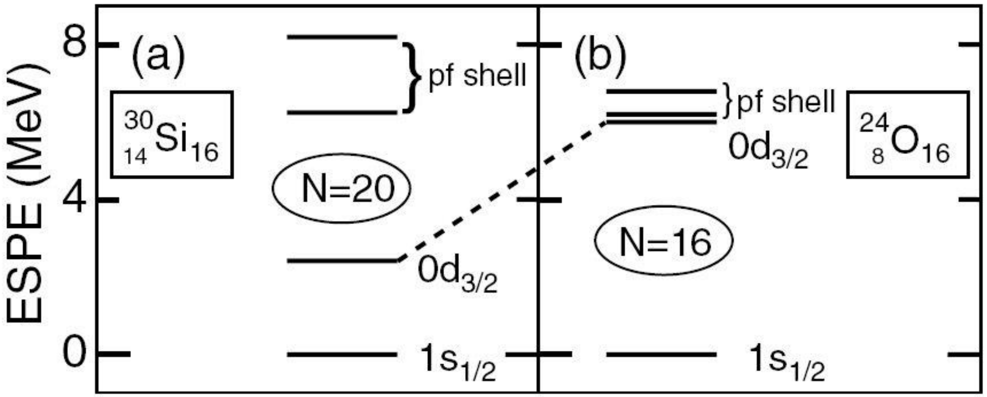

As the occupancy of the $j_>$ orbit $d_{5/2}$ is reduced in going from (a) ^{30}Si to (b) ^{24}O, then the attractive force on $j_<$ $d_{3/2}$ neutrons is reduced, and the orbital rises relatively in energy. This is shown in the final panel by the $s_{1/2}$ to $d_{3/2}$ gap, calculated using various interactions within the Monte-Carlo shell model.

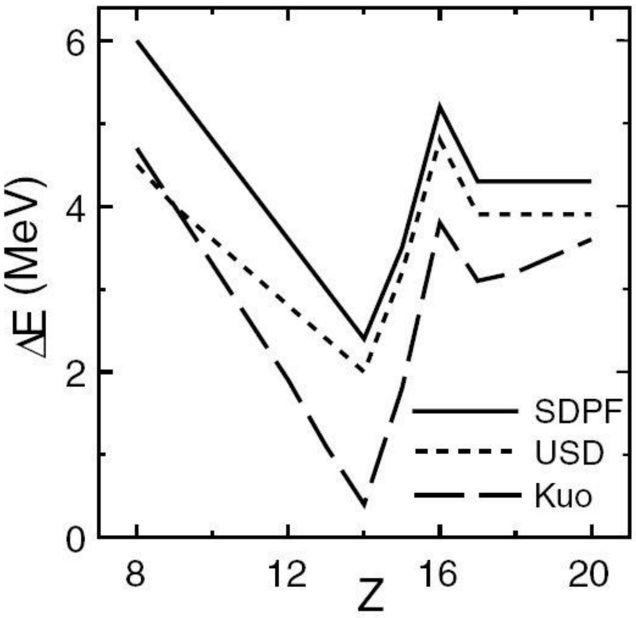

Utsuno et al., PRC,60,054315(1999)
Monte-Carlo Shell Model (SDPF-M)

Exotic — Stable

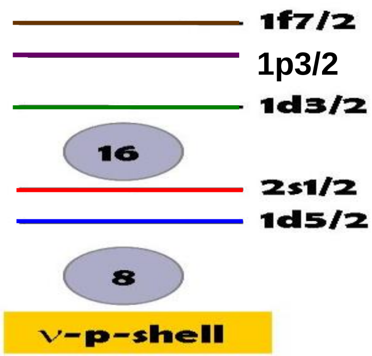

Exotic

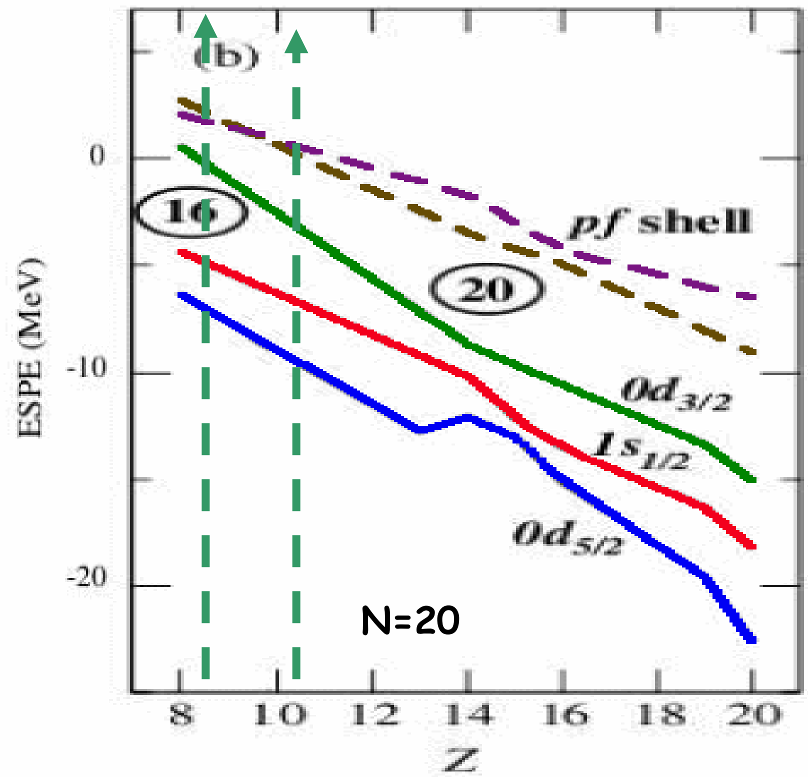

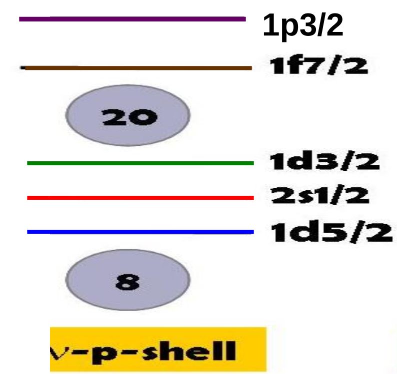

Stable

Removing d5/2 protons (Si →O)

gives relative rise in ν(d3/2)

Note:
This changes collectivity, also…

SINGLE PARTICLE STATES – AN ACTUAL EXAMPLE

Systematics of the 3/2+ for N=15 isotones

removing d5/2 protons raises d3/2 and appears to lower the f7/2

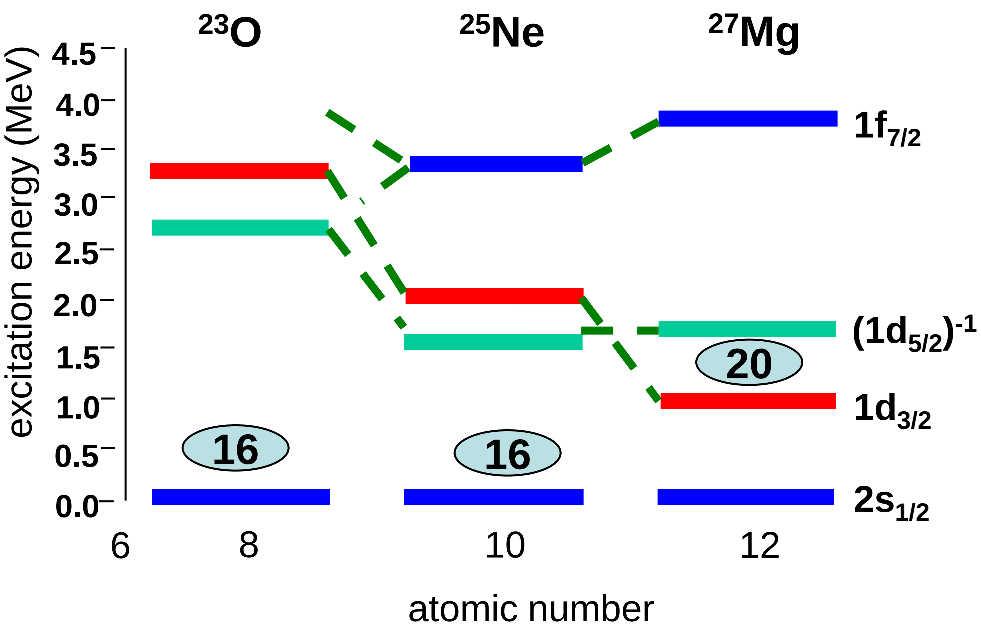

Migration of the 3/2+ state creates N=16 from N=20

^{25}Ne TIARA → USD modified

$^{23,25}O$ raise further challenges

^{21}O has similar 3/2+-1/2+ gap (same d5/2 situation) but poses interesting question of mixing (hence recent $^{20}O(d,p)$@SPIRAL)

- ^{23}O from USD and Stanoiu PRC 69 (2004) 034312 and Elekes PRL 98 (2007) 102502
- ^{25}Ne from TIARA, W.N. Catford et al. Eur. Phys. J. A, 25 S1 251 (2005)

Changing Magic Numbers

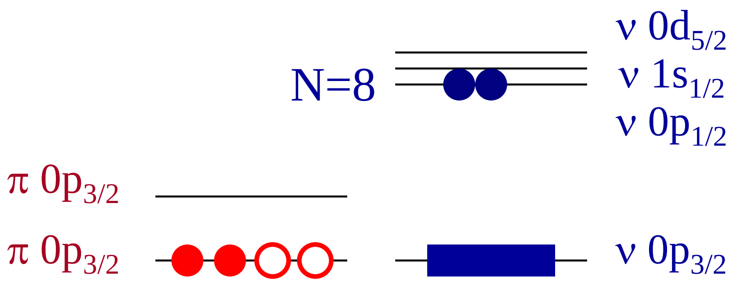

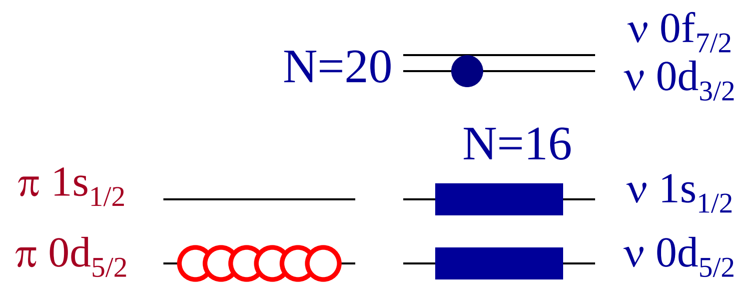

In the lighter nuclei (A<50) a good place to look is near closed proton shells, since a closed shell is followed in energy by a $j_>$ orbital. For example, compared to ^{14}C the nuclei ^{12}Be and ^{11}Li (just above Z=2) have a reduced π ($0p_{3/2}$) occupancy, so the N=8 magic number is lost. Similarly, compared to ^{30}Si, the empty π ($0d_{5/2}$) in ^{24}O (Z=8) leads to the breaking of the N=20 magic number. Another possible extreme is when a particular neutron orbital is much more complete than normal.

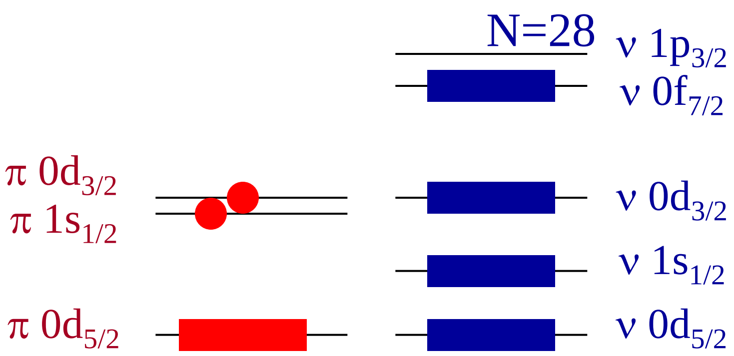

Nuclear states are not in general pure SP states, of course

For nuclear states, we measure the spin and energy
and
the magnitude of the single-particle component for that state
(spectroscopic factor)

Example: (relevant to one of the experiments)… $3/2^+$ in ^{21}O

A. SINGLE PARTICLE STATES – EXAMPLE

Example of population of single particle state: ^{21}O

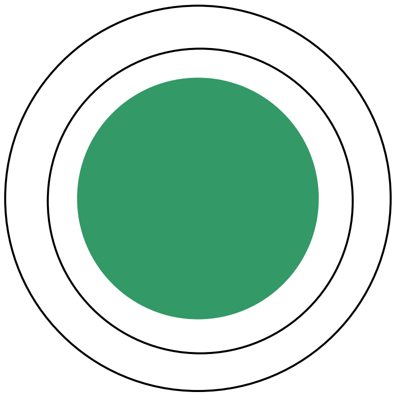

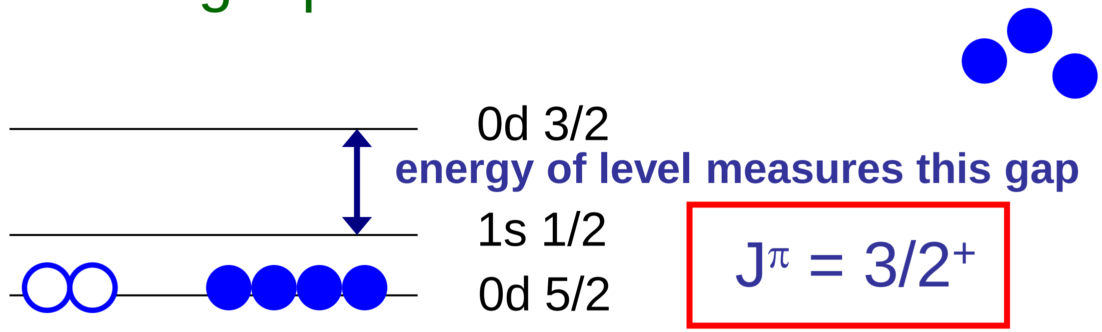

The mean field has orbitals, many of which are filled.
We probe the energies of the orbitals by transferring a nucleon
This nucleon enters a vacant orbital
In principle, we know the orbital wavefunction and the reaction theory

But not all nuclear excited states are single particle states…

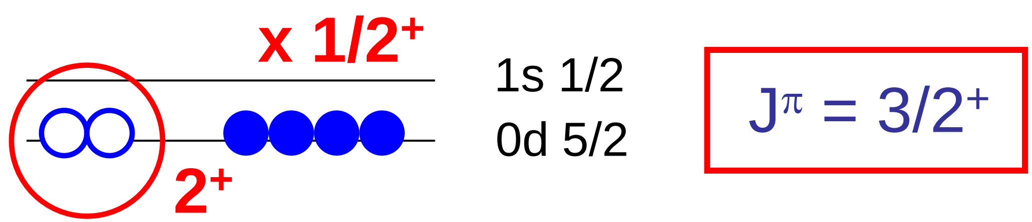

We measure how the two $3/2^{+}$ states share the SP strength when they mix

SINGLE PARTICLE STATES – SPLITTING

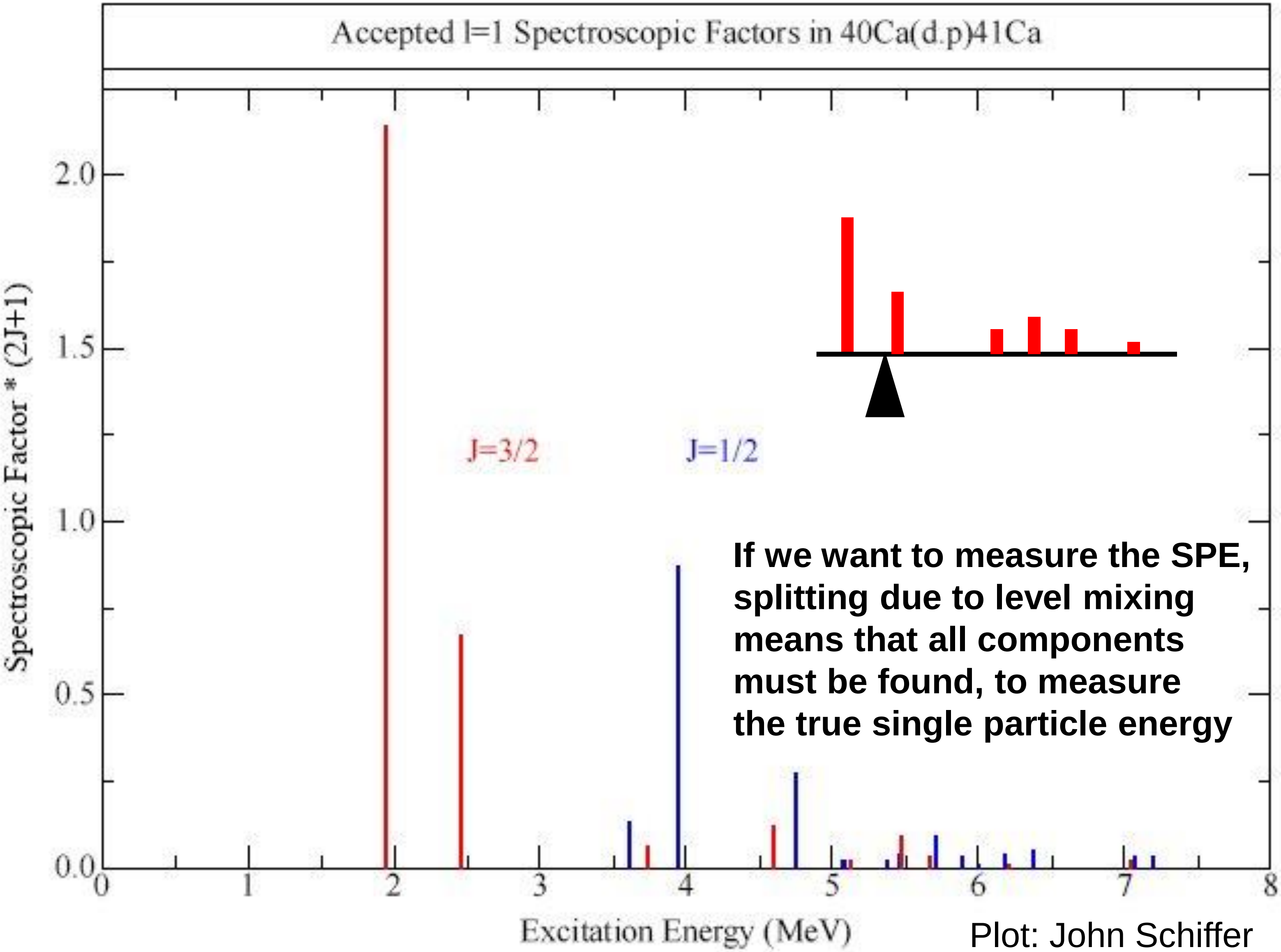

If we want to measure the SPE, splitting due to level mixing means that all components must be found, to measure the true single particle energy

Plot: John Schiffer

Neutron and Proton single-Particle States Built on 208 Pb

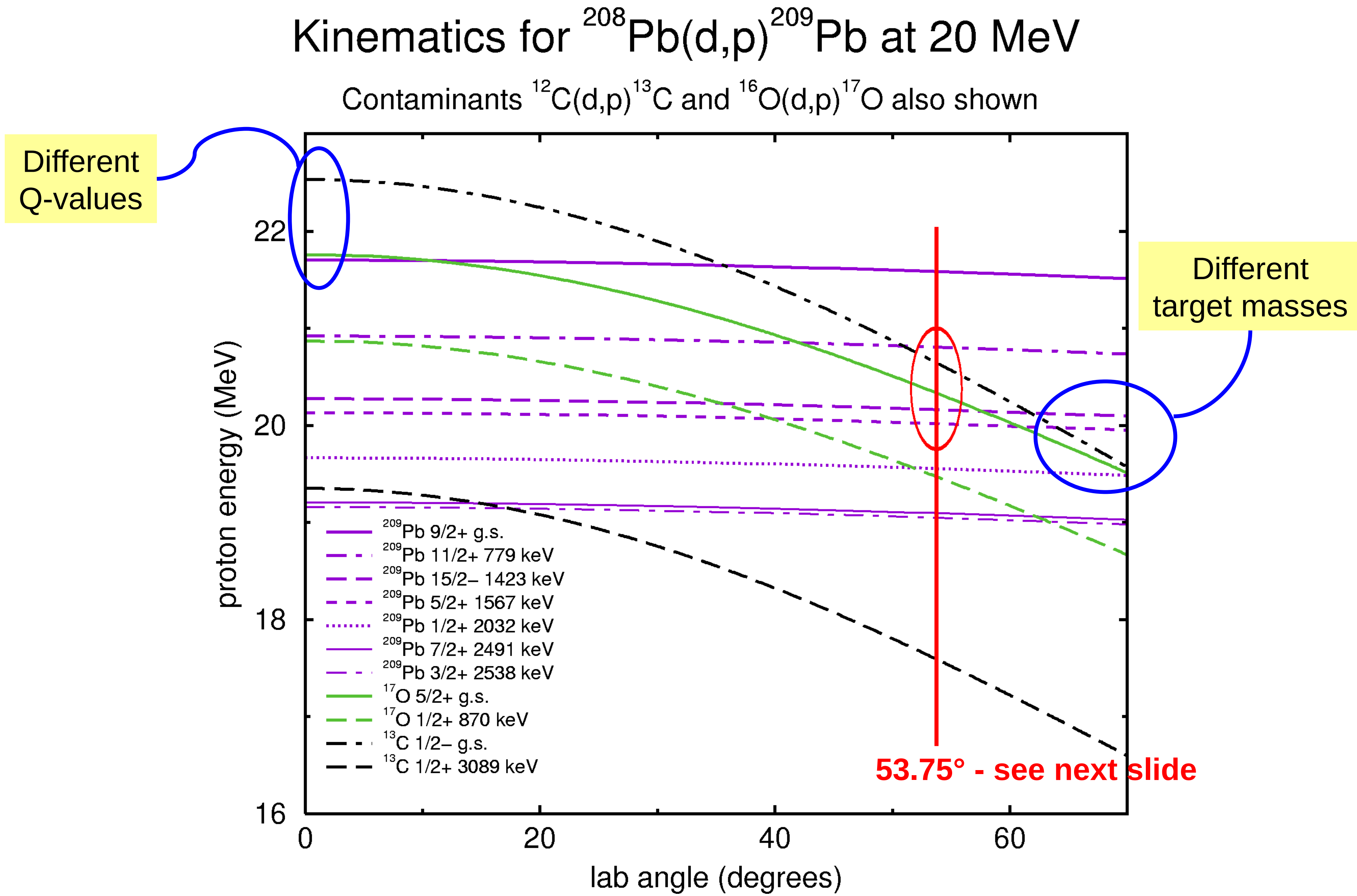

Neutron and Proton Single-Particle States Built on ^{208}Pb

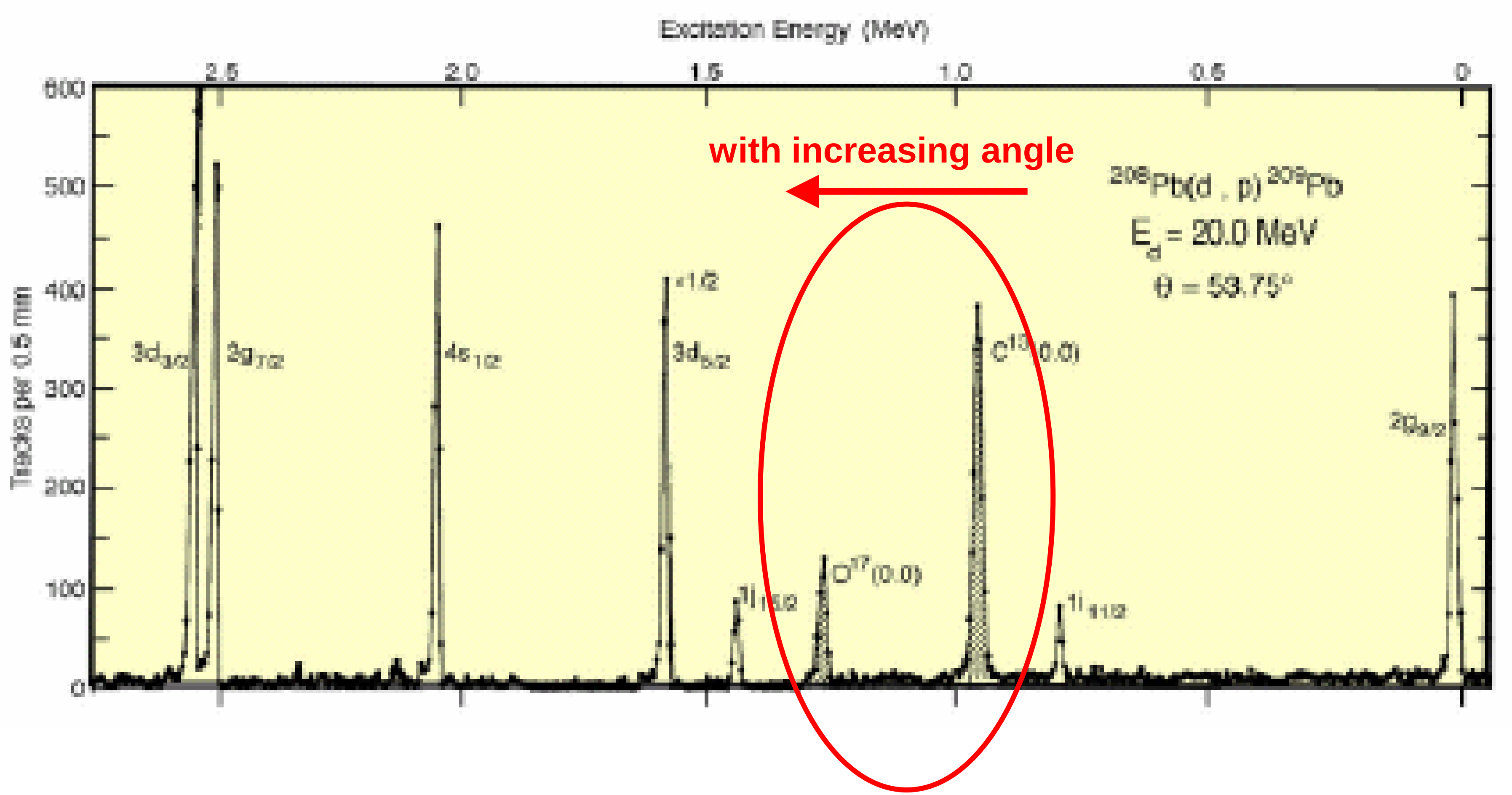

John Schiffer, Argonne

1950’s
1960’s

1967 $^{208}Pb(d,p)^{209}Pb$

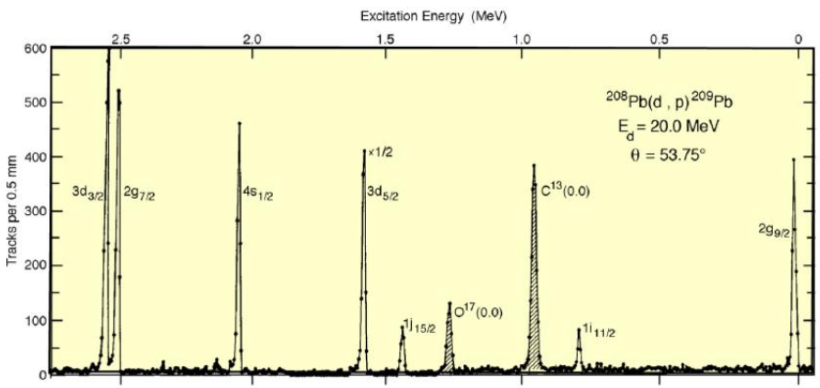

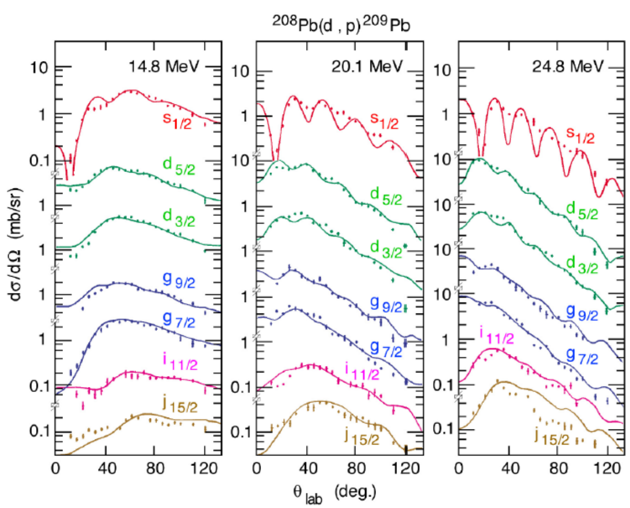

Muehllener et al.
Phys. Rev. 159, 1043 (1967)

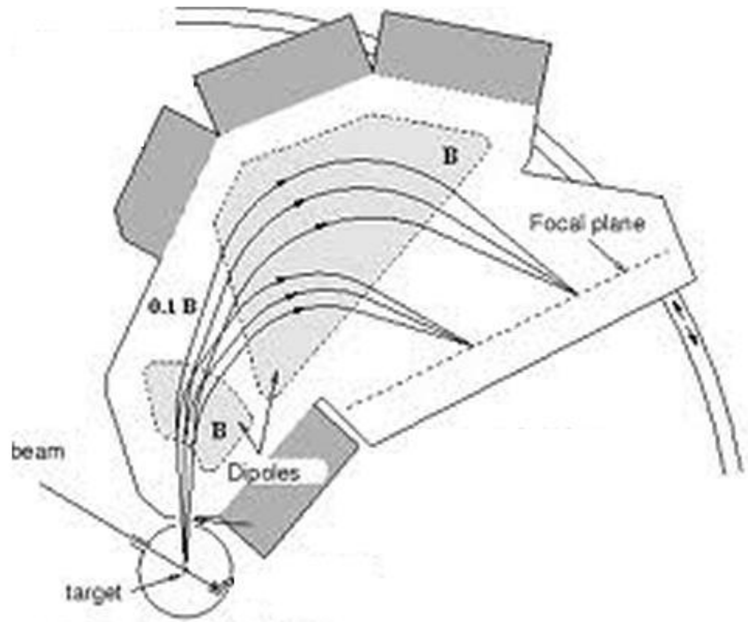

Deuteron beam + target
Tandem + spectrometer
$>10^{10}$ pps (stable) beam
Helpful graduate students

1950's
1960's

STABLE NUCLEI

RADIOACTIVE

1990's
2000's……..

1967 ^{208}Pb(d,p)^{209}Pb

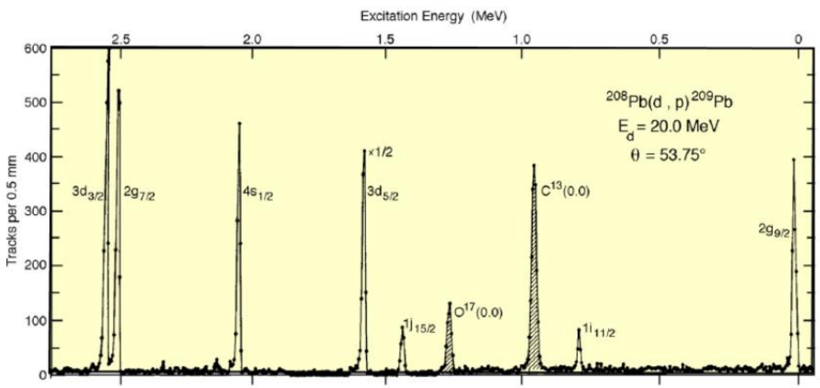

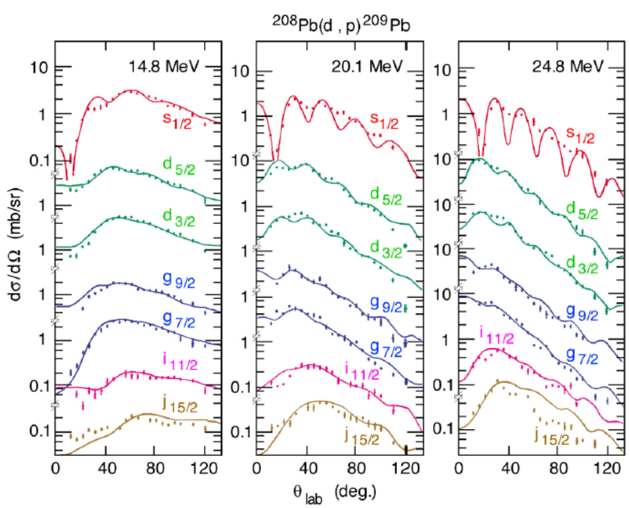

Muehllener et al.
Phys. Rev. 159, 1043 (1967)

1998 d(^{56}Ni,p)^{57}Ni

Rehm ARGONNE

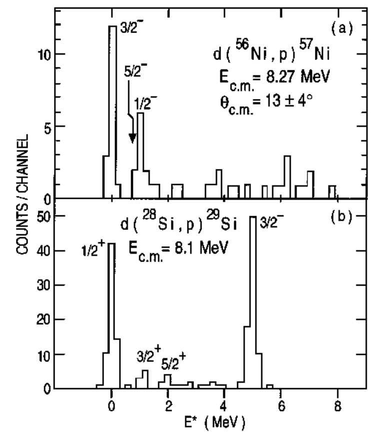

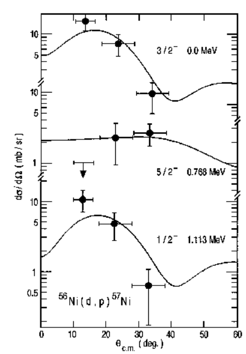

1999 p(^{11}Be,d)^{10}Be

Fortier/Catford GANIL

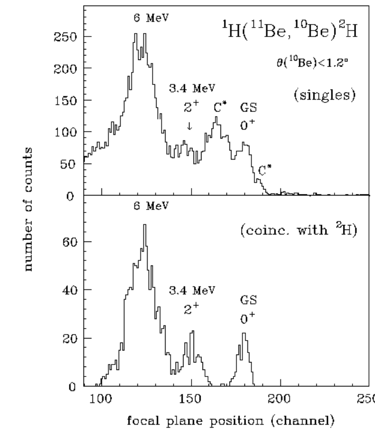

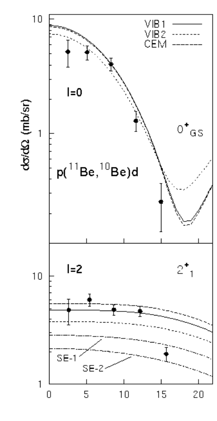

How does the differential cross section vary with beam energy ?

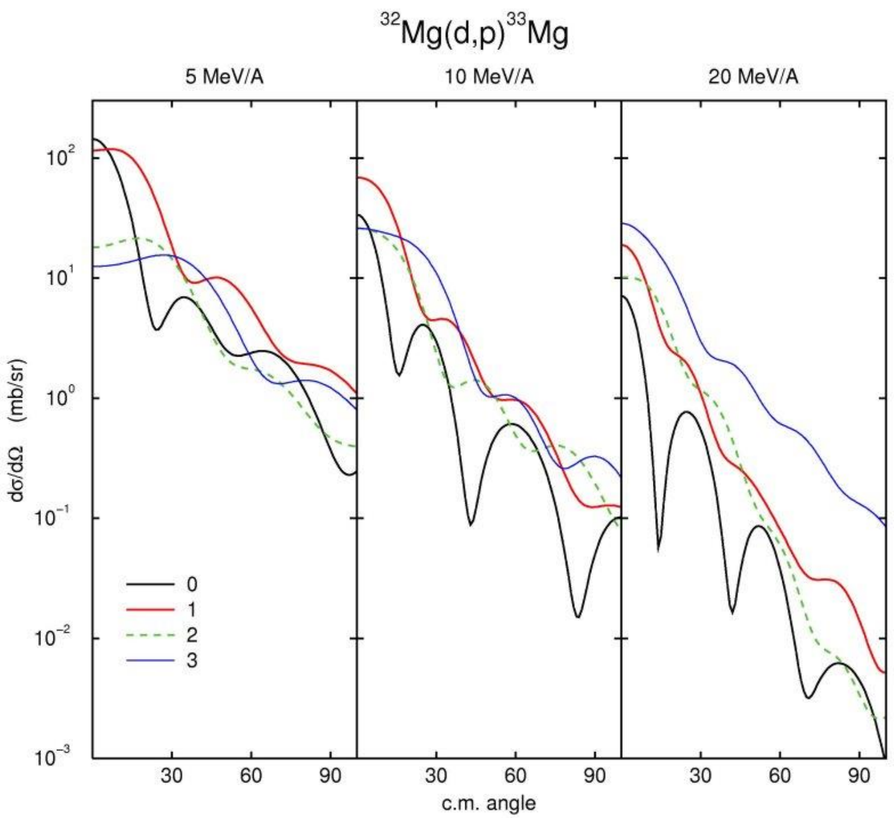

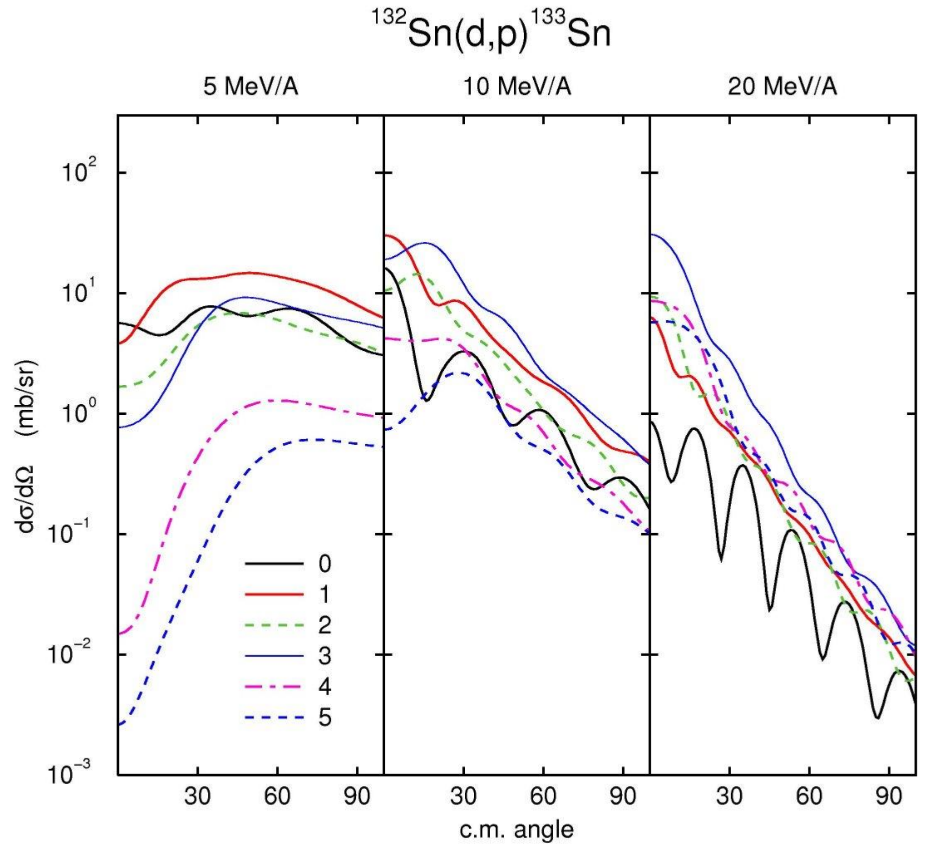

and the total cross section ?

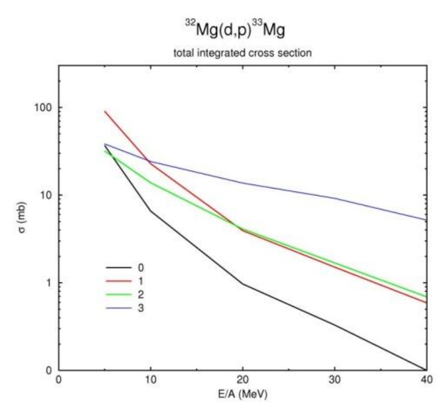

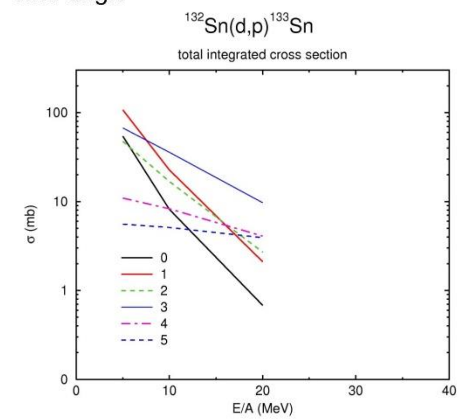

TIARA

W.N. CATFORD SURREY

Angular Momentum transfer

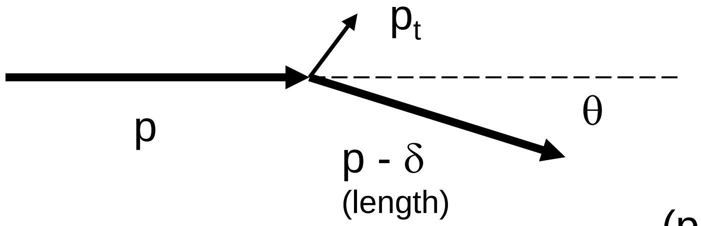

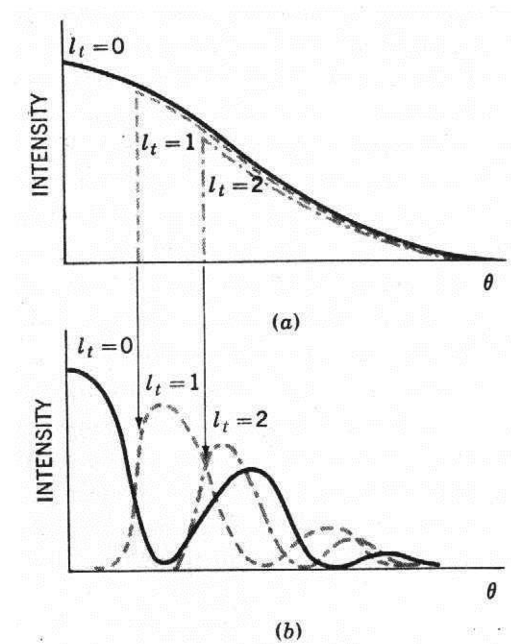

Cosine rule, 2nd order: $$\theta^2 = \frac{(p_t/p)^2 - (\delta/p)^2}{1 - (\delta/p)}$$

But $p_t \times R \geq \sqrt{\ell(\ell+1)}\ \hbar$ (R = max radius)

So $$\theta^2 \geq \frac{\ell(\ell+1)\,\hbar^2 / p^2R^2 - (\delta/p)^2}{1 - (\delta/p)}$$

or $\theta \geq \text{const} \times \sqrt{\ell(\ell+1)}$

$$\theta_{min} \approx \text{const} \times \ell$$

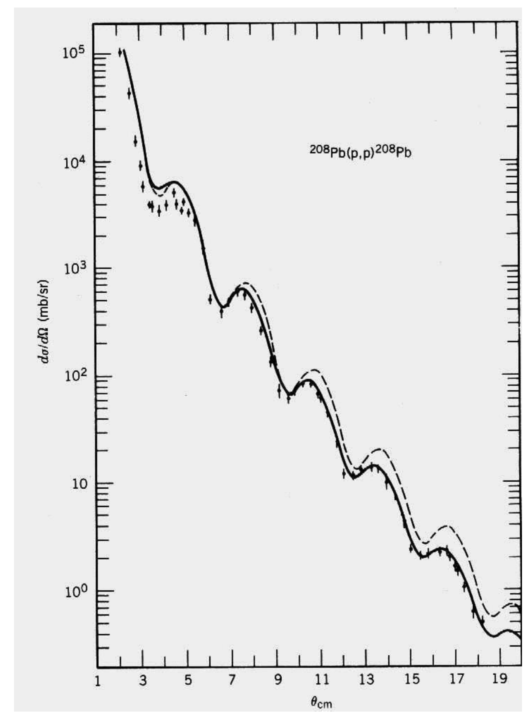

Diffraction structure also expected (cf. Elastics)

PWBA ⇒ spherical Bessel function, $\theta_{peak} \approx 1.4\ \sqrt{\ell(\ell+1)}$

How does the differential cross section vary with beam energy ?

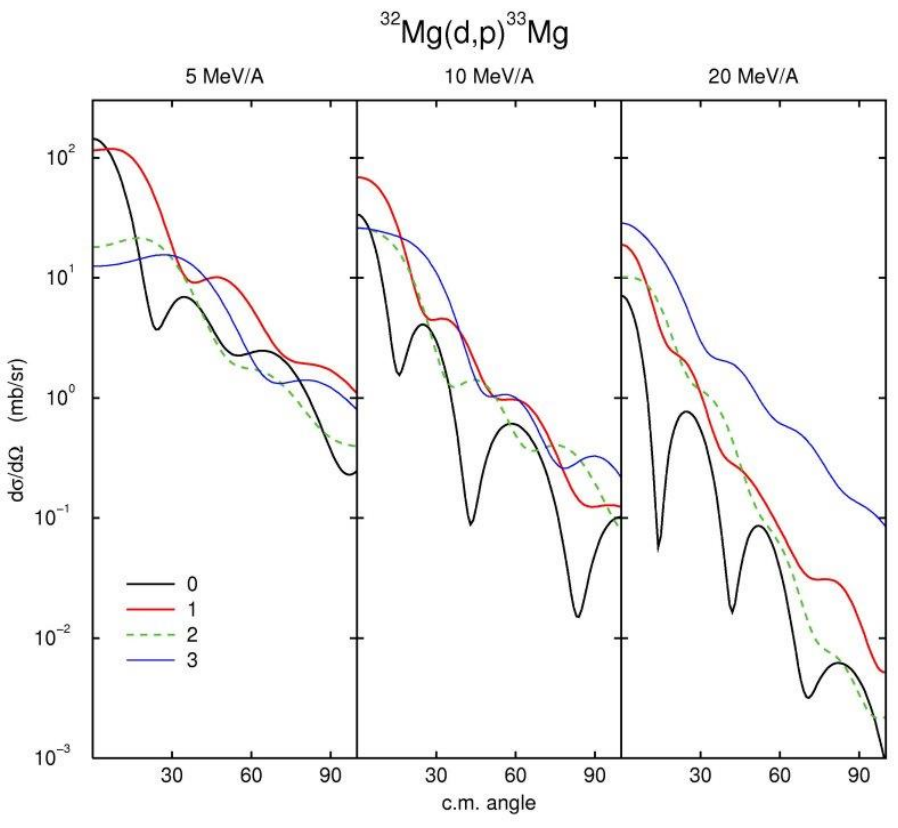

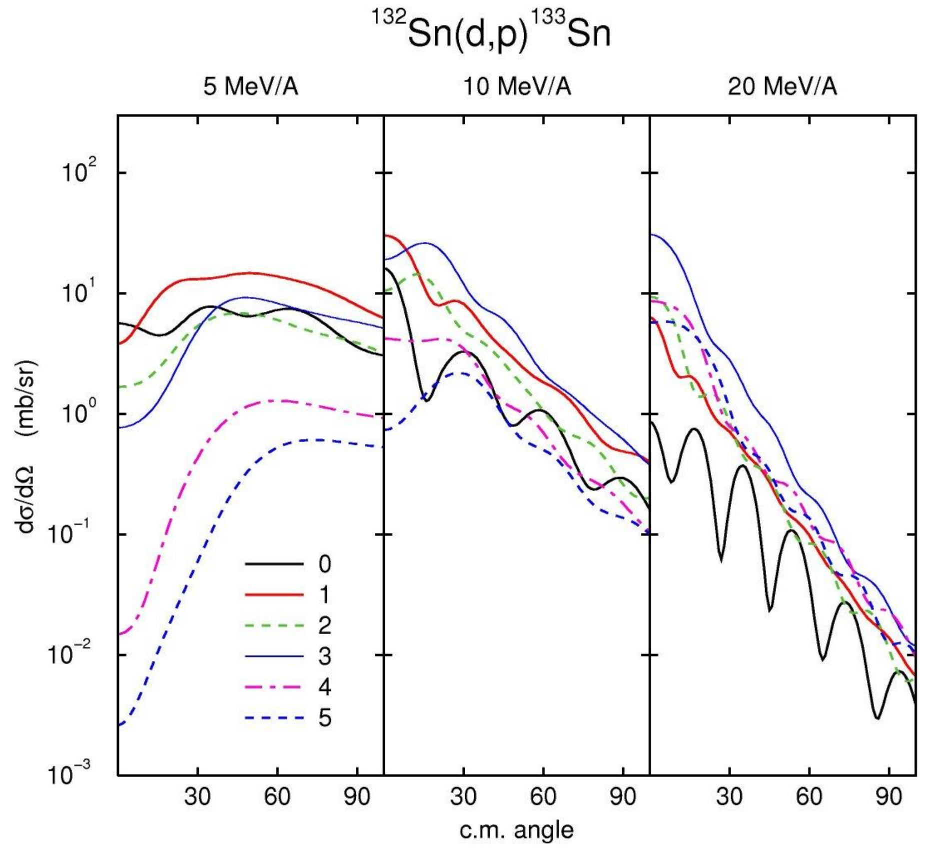

and the total cross section ?

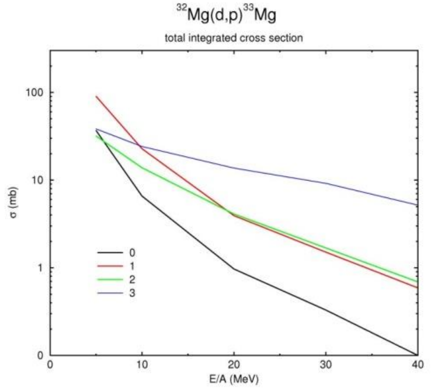

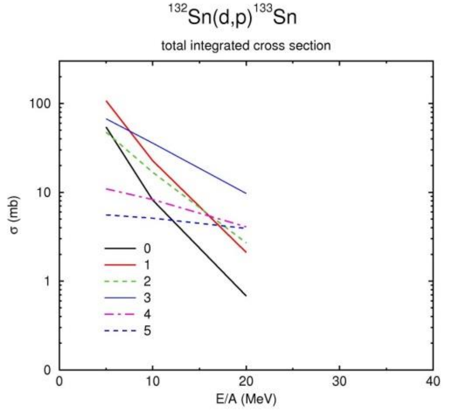

TIARA

W.N. CATFORD SURREY

How does the differential cross section vary with beam energy ?

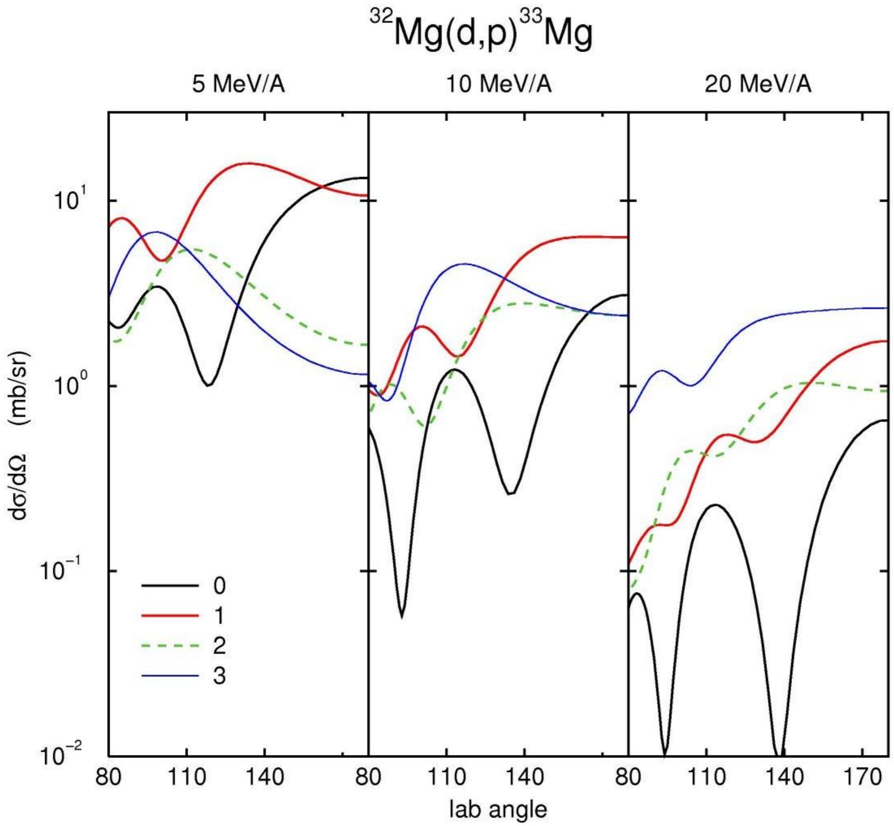

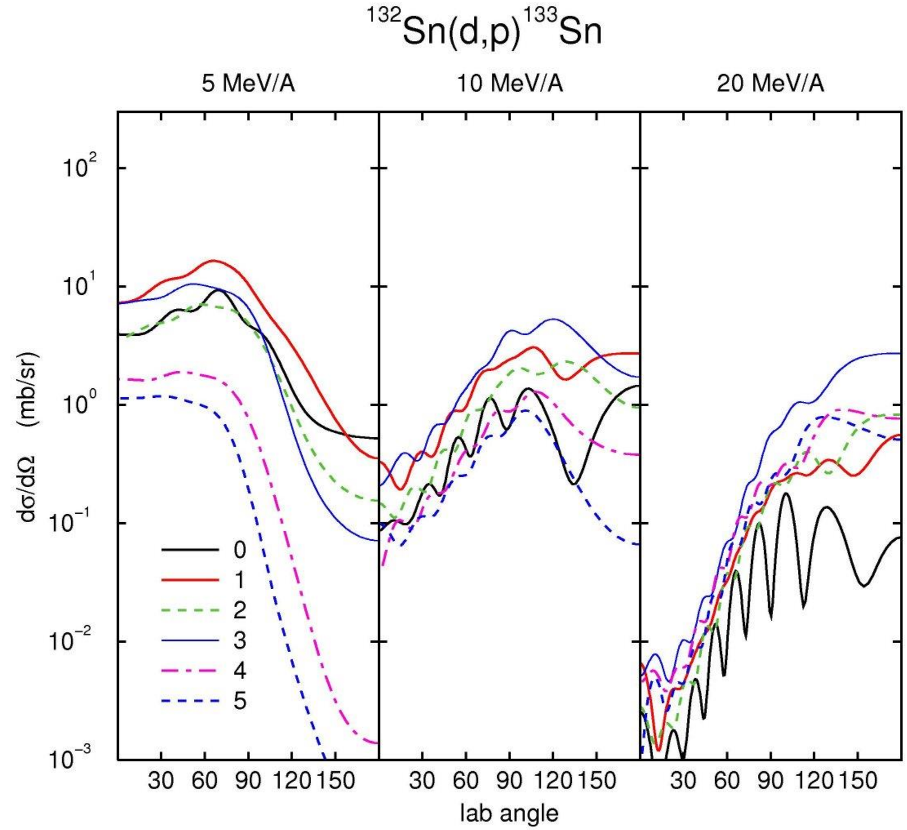

and the total cross section ?

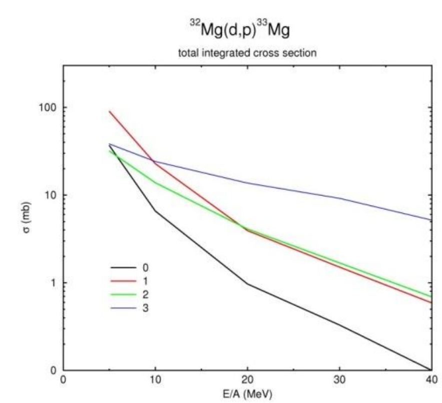

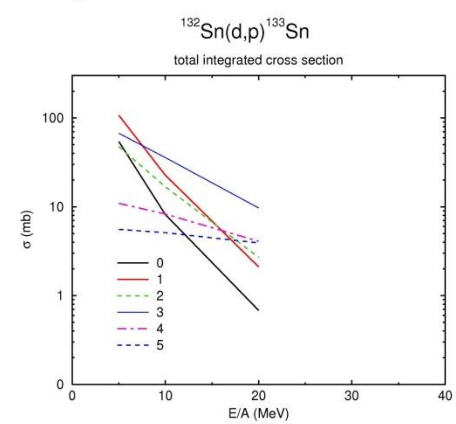

TIARA

W.N. CATFORD SURREY

Distorted Wave Born Approximation - Outline

e.g. (*d*,*p*) with a deuteron beam (following H.A.Enge Chap.13 with ref. also to N.Austern)

$H_{tot} = \Sigma T + \Sigma V$ ... in either entrance/exit ch

Entrance: $H_{tot} = T_{aA} + T_{xb} + V_{xb} + V_{xA} + V_{bA}$

Exit: $H_{tot} = T_{bB} + T_{xA} + V_{xb} + V_{xA} + V_{bA}$

Same in each case

→ But the final scattering state can be written approximately as an outgoing DW using the optical potential for the exit channel:

$$|\psi_f\rangle \approx \underbrace{|\phi_b\rangle\ |\phi_B\rangle}_{\text{Internal wave functions}}\ \underbrace{\chi^-_{bB}}_{\text{outgoing distorted wave}}$$

In the optical model picture, $V_{xb} + V_{bA} \approx U_{bB}$ ($= V^{opt}_{bB} + i\,W^{opt}_{bB}$, the optical potential)

And the final state, we have said, can be approximated by an eigenstate of U_{bB}

Thus, the transition is induced by the interaction $V_{int} = H_{entrance} - H_{exit} = V_{xb} + \underbrace{V_{bA} - U_{bB}}_{\text{Remnant term}}$

Remnant term ≈ 0 if $x << A$

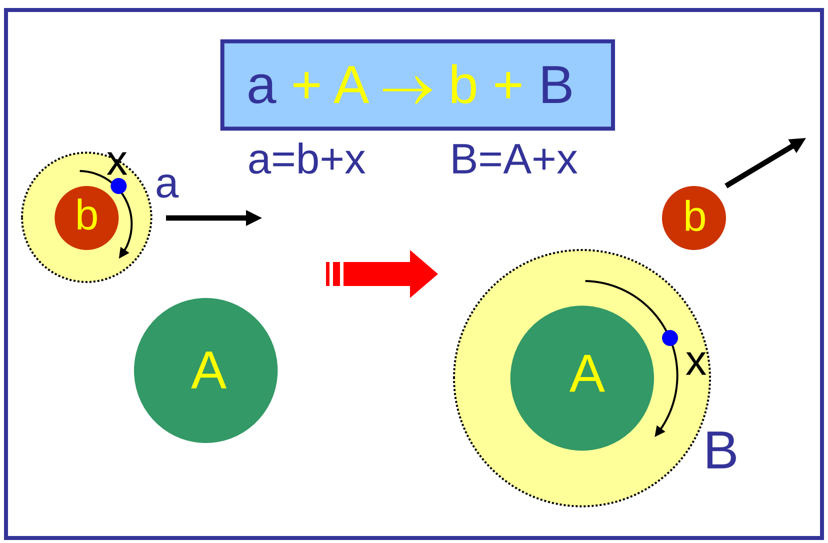

i.e. $V_{int} \approx V_{xb}$ which we can estimate reasonably well

$$T_{i,f}^{DWBA} = \langle\, \phi_b\, \phi_B\, \chi_{bB}^- \,|\, V_{xb} \,|\, \chi_{aA}^+\, \phi_a\, \phi_A \,\rangle$$

$\phi_B\,\ldots = \phi_x\, \phi_A\, \psi_{rel,Ax}$ $\qquad$ $\phi_a = \phi_x\, \phi_b\, \psi_{rel,bx}$

so $T_{i,f}^{DWBA} = \langle\, \underbrace{\psi_{rel,Ax}}\, \chi_{bB}^- \,|\, V_{xb} \,|\, \chi_{aA}^+\, \underbrace{\psi_{rel,bx}} \,\rangle$

known as *radial form factor* for the transferred nucleon $\qquad$ often simple, e.g. if a = *d*

Distorted Wave Born Approximation - Outline 2

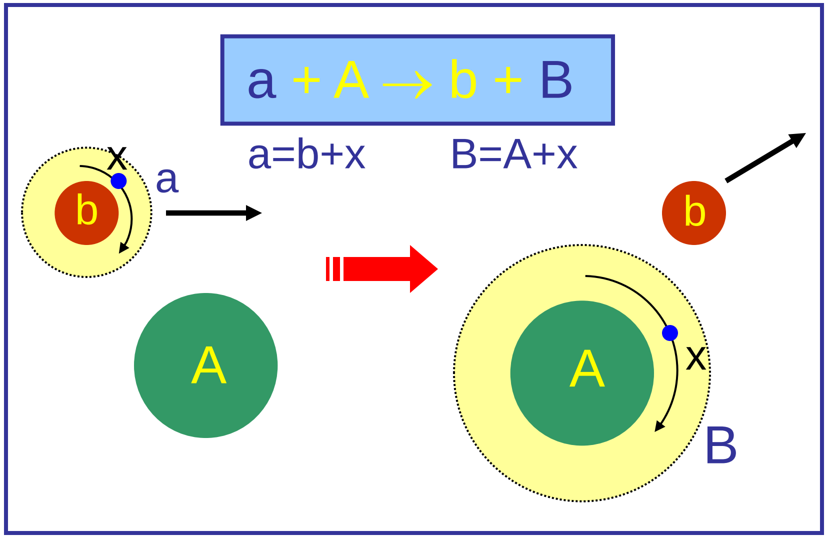

so $T_{i,f}^{DWBA} = \langle \psi_{rel,Ax}\, \chi_{bB}^{-} \mid V_{xb} \mid \chi_{aA}^{+}\, \psi_{rel,bx} \rangle$

(compare Enge eq. 13-60)

The wave function of the transferred nucleon, orbiting A, inside of B

radial wave function u(r) given by $\psi(r) = u(r)/r$

V(r) given by Woods-Saxon; depth determined by known binding energy

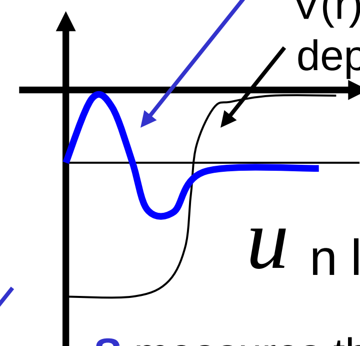

$u_{n\,l\,j} * S^{1/2}_{n\,l\,j}$

S measures the occupancy of the shell model orbital… the ***spectroscopic factor***

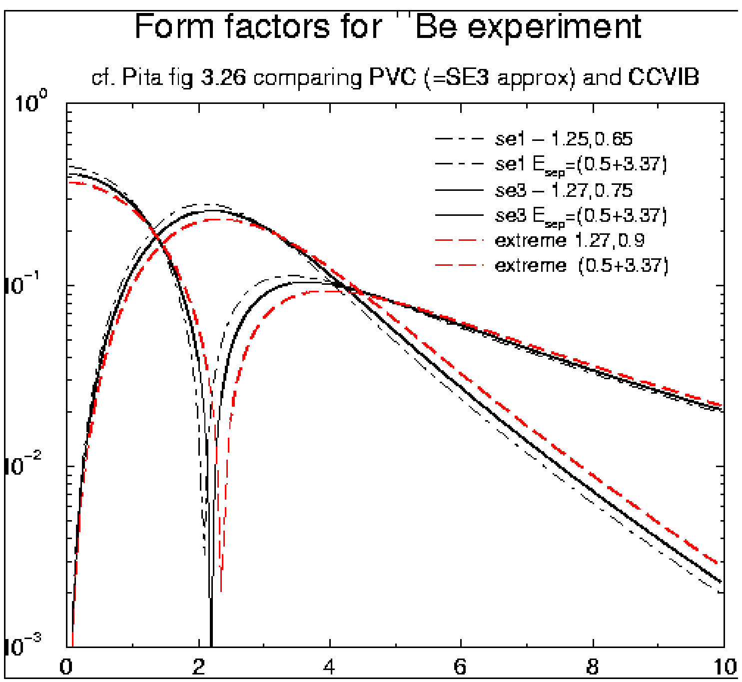

Radial wave functions in Woods-saxon potential with various geometries

Woods-Saxon:

$$V(r) = \frac{-V_0}{1 + e^{(r - r_0 A^{1/3})/a}}$$

Photographs of Distorted Waves

N. Austern
Direct Reactions

Beam of α's on ^{40}Ca
18 MeV from left

Beam of p's on ^{40}Ca
40 MeV from left

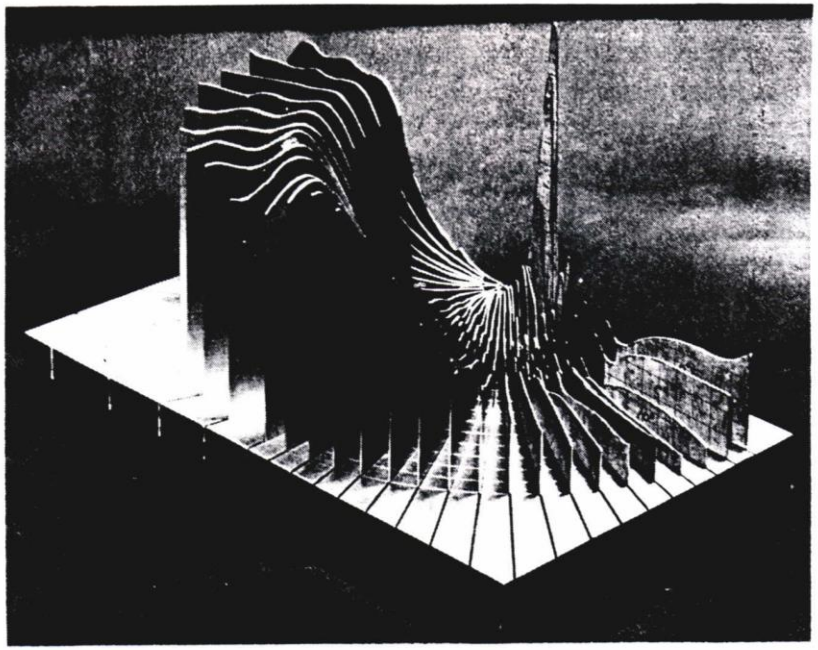

Fig. 7.1 Three-dimensional model of $|\chi^{(+)}|$, the modulus of the optical model wavefunction, for 18 MeV alpha particles bombarding Ca^{40}. The beam is incident from the left. The dark zone is the 10%–90% region of the optical potential. (Computed by R. M. Drisko and N. Austern, unpublished.)

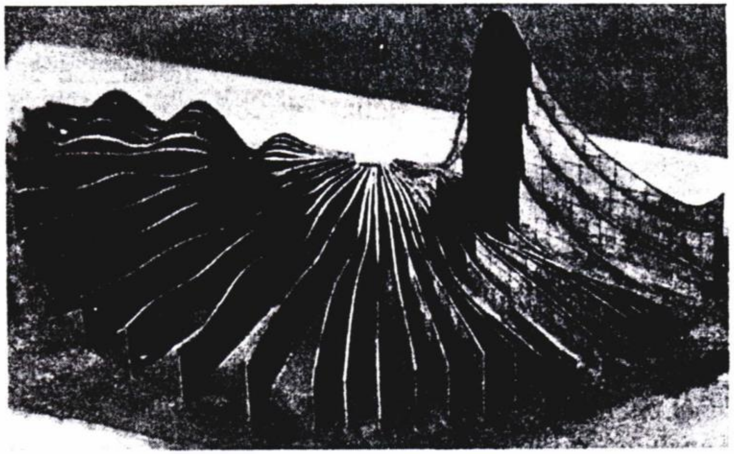

Fig. 7.2 This figure is the same as Fig. 7.1, for 40 MeV protons bombarding Ca^{40}.

SUM RULES FOR 1N TRANSFER

For adding a nucleon to a given j-shell the sum rule gives the vacancy in the shell

$$Number\ of\ Holes = \sum_i \left(\frac{2T_f^i+1}{2T_0+1}\right)\left(\frac{2J_f^i+1}{2J_0+1}\right)S_i$$

for removing a nucleon from a given j-shell it gives the occupancy of the shell, with the sum running over all final states *i*.

$$Number\ of\ Particles = \sum_i \left(\frac{2T_f^i+1}{2T_0+1}\right)S_i$$

Note that only one value of isospin $T_f(=T_0+1/2)$ is allowed for neutron adding or proton removing reactions, and two values $T_f(=T_0 \pm 1/2)$ for neutron removal or proton adding.

John Schiffer, Argonne

Some Illustrations of Complications in Transfer Calculations

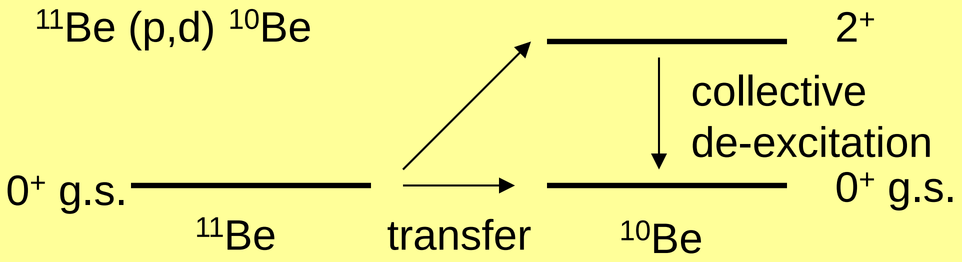

Example of two-step

the two paths will interfere

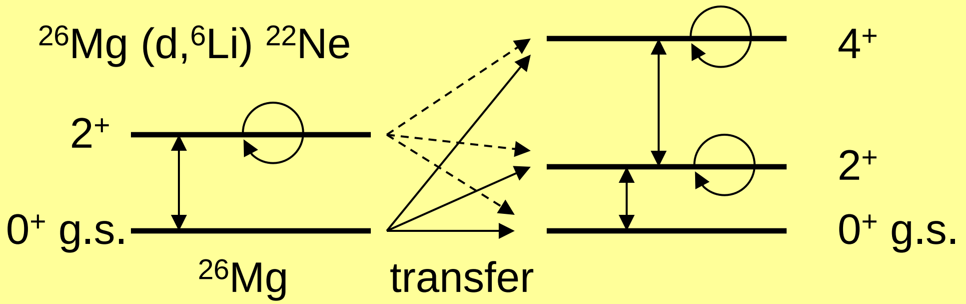

Example of coupled channels

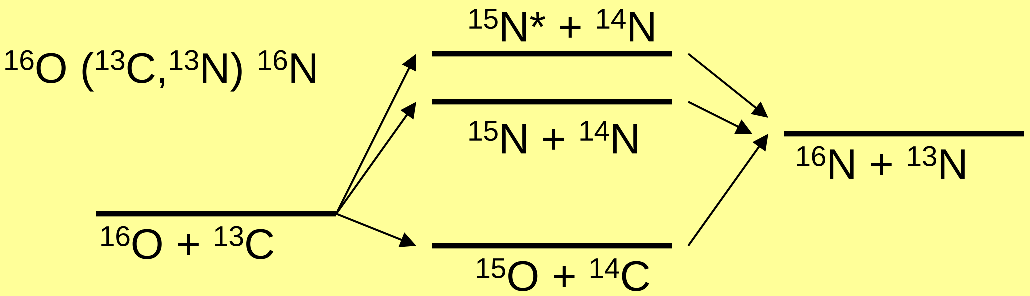

Example of coupled reaction channels

REACTION MODEL FOR (d,p) TRANSFER – the ADWA

<u>**Johnson-Soper** Model:</u> an **alternative to DWBA** that gives a simple prescription for taking into account coherent *entangled* **effects of deuteron break-up** on (d,p) reactions [1,2]

- does not use deuteron optical potential – uses ***nucleon-nucleus optical potentials*** only
- formulated in terms of adiabatic approximation, which is sufficient but not necessary [3]
- uses parameters (overlap functions, **spectroscopic factors**, ANC's) just as in DWBA

[1] Johnson and Soper, PRC 1 (1970) 976
[2] Harvey and Johnson, PRC 3 (1971) 636; Wales and Johnson, NPA 274 (1976) 168
[3] Johnson and Tandy NPA 235 (1974) 56; Laid, Tostevin and Johnson, PRC 48 (1993) 1307

Spectroscopic Factor

Shell Model: overlap of $|\psi(N+1)\rangle$ **with** $|\psi(N)\rangle_{core} \otimes n(\ell j)$

Reaction: the observed yield is not just proportional to this S, because in T the **overlap integral** has a radial-dependent weighting or sampling

Many-body theory of $d + A(N,Z) \rightarrow B(N+1,Z) + p$

Hence the yield, and hence deduced spectroscopic factor, depends on the radial wave function and thus the geometry of the assumed potential well for the transferred nucleon, or details of some other structure model

overlap integral

$$\phi_n^{BA}(\vec{r}_n) = \sqrt{N+1}\int d\xi_A \phi_B^*(\xi_A,\vec{r}_n)\phi_A(\xi_A)$$

spectroscopic factor

$$S^{AB} = \int d\vec{r}_n \mid \phi_n^{AB}(\vec{r}_n) \mid^2$$

$$T_{d,p} = \langle \chi_p^{(-)} \phi_n^{BA} \mid V_{np} \mid \Psi_{\vec{K}_d} \rangle$$

REACTION MODEL FOR (d,p) TRANSFER – the ADWA

A **CONSISTENT** application of ADWA gives 20% agreement with large basis SM

JENNY LEE, M. B. TSANG, AND W. G. LYNCH

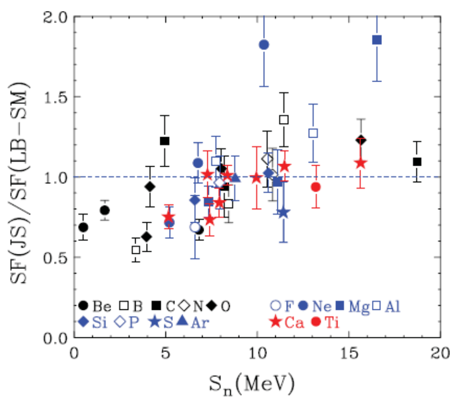

FIG. 12. (Color online) Ratios of SF(JS) values and the LBSM predicted SF values as a function of neutron separation energy (S_n). Open and closed symbols denote elements with odd and even Z, respectively. Only data with an overall uncertainties of less than 25% are included.

PHYSICAL REVIEW C 75, 064320 (2007)

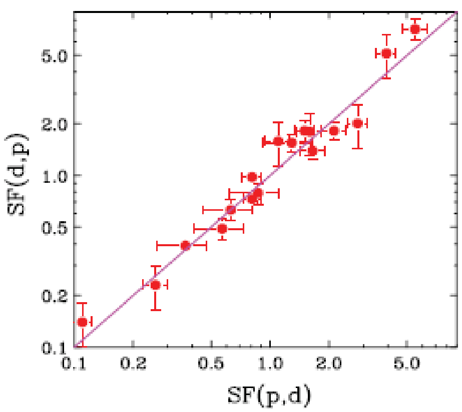

FIG. 8. (Color online) Comparison of spectroscopic factors obtained from (p, d) and (d, p) reactions as listed in Table II. Line indicates perfect agreement between the two values.

80 spectroscopic factors
Z = 3 to 24
Jenny Lee et al.

Tsang et al
PRL 95 (2005) 222501

Lee et al
PRC 75 (2007) 064320

Delaunay at al
PRC 72 (2005) 014610

REACTION MODEL FOR (d,p) TRANSFER

Given what we have seen, **is transfer the BEST way** to isolate and study single particle structure and its evolution in exotic nuclei?

Transfer – decades of (positive) experience

Removal – high cross section, similar outputs, requires full orbitals

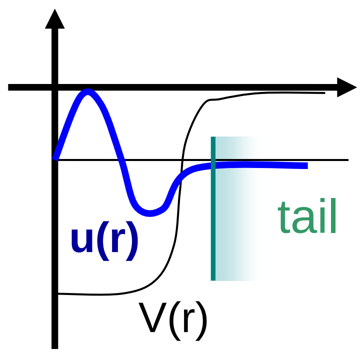

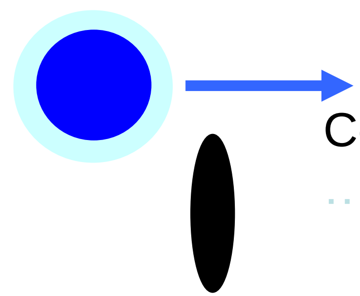

Complementary to (d,p)

…to be validated with (d,t)

(e,e'p) – a bit ambitious for general RIB application

(p,p'p) – more practical than (e,e'p) for RIB now, does have problems

YES

Also:

Heavy Ion transfer (^{9}Be),

^{3,4}He-induced reactions

Some Common Codes in Transfer Reaction Work

DWUCK - can be zero range or finite range

CHUCK - a coupled channels, zero range code

FRESCO - full finite range, non-locality, coupled channels, coupled reaction channels, you-name-it code
(Ian Thompson, University of Surrey)

TWOFNR - includes an implementation of ADWA which is very well suited to (d,p)… plus other options
(J. Tostevin, University of Surrey, on-line version)
(A. Moro, University of Seville, examples in this School)

Summary of single-nucleon transfer and knockout

Each of these processes can probe single-particle structure:
• measure the occupancy of single-particle (shell model) orbitals *(spectroscopic factors)*
• identify the angular momentum of the relevant nucleon.

Knockout has recently been developed specifically for radioactive beams (initially for haloes) and the nucleus being studied is the projectile. The removed nucleon may go anywhere.

Transfer was developed in the 1950's for stable beams (initially for p, d, t, ^{3}He, …) and the nucleus being studied was the target. The removed nucleon must transfer and "stick". With radioactive beams, the p, d, …etc., becomes the target, known as *inverse kinematics*

With knockout we can probe:
• occupancy of single-particle (shell model) orbitals in the projectile ground state
• identify the angular momentum of the removed nucleon
• hence, identify the s.p. level energies in odd-A nuclei produced from even-even projectiles
and the projectile-like particle is detected essentially at zero degrees

With transfer we can probe:
• occupancy of single-particle (shell model) orbitals in the original nucleus A ground state
    or distribution of s.p. strength in all final states of A–1 or A+1 nucleus
    that is, can add a nucleon to the original nucleus, e.g. by (d,p)
• identify the angular momentum of the transferred nucleon
• hence, identify the s.p. level energies in A–1 or A+1 nuclei produced from even-even nuclei
• identify the s.p. purity of coupled states in A–1 or A+1 nuclei produced from odd nuclei
and the scattered particle is detected, with most yield being at small centre-of-mass angles

Energy regimes of single-nucleon transfer and knockout

Energy	Facility
< 10 MeV/A	HIE-ISOLDE
10-50 MeV/A	GANIL/SPIRAL
>100 MeV/A	GSI / FRS

example European facility for this energy

transfer (< 10 MeV/A to 10-50 MeV/A)

- Lenske & Schrieder
  Eur. J. Phys. A2(1998)41
- Winfield et al
  Nucl. Phys. A683(2001)48

knockout (10-50 MeV/A to >100 MeV/A)

- Sauvan et al
  Phys. Lett. B175(2000)1
- Hansen & Sherrill
  Nucl. Phys. A693(2001)133

example useful papers in these energy regimes

Intensity regimes of single-nucleon transfer and knockout

knockout

$>$ 1 pps near drip-lines; $>10^3$ pps for more-bound projectiles
~ 100 mb near drip-lines, closer to 1 mb for more-bound

transfer

$>10^4$ pps is essentially the minimum possible
~ 1 mb cross sections typical

Some general observations for transfer reactions

The nucleon having to "stick" places kinematic restrictions on the population of states:
- the reaction Q-value is important (for Q large and negative, higher ℓ values are favoured)
- the degree (ℓ-dependent) to which the kinematics favour a transfer is known as ***matching***

Various types of transfer are employed typically, and using different mass probe-particles:
- **light-ion transfer reactions**: (probe$\leq \alpha$ say) … (d,p) (p,d) (d,t) (d,^{3}He) also (^{3}He,α) etc.
- **heavy-ion transfer reactions**: e.g. (^{13}C,^{12}C) (^{13}C,^{14}C) (^{17}O,^{16}O) (^{9}Be,^{8}Be)
- **two-nucleon transfer**: e.g. (p,t) (t,p) (^{9}Be,^{7}Be) (^{12}C,^{14}C) (d,α)
- **alpha-particle transfer** (or α-transfer): e.g. (^{6}Li,d), (^{7}Li,t), (d,^{6}Li), (^{12}C,^{8}Be)

Light-ion transfer reactions with Radioactive Beams

Light-ion induced reactions give the clearest measure of the transferred ℓ,
and have a long history of application in experiment and refinement of the theory

Thus, they are attractive to employ as an essentially reliable tool, as soon as radioactive beams of sufficient intensity become available (i.e. NOW)

To the **theorist**, there are some new aspects to address, near the drip lines.

To the **experimentalist**, the transformation of reference frames is a much bigger problem!

The new experiments need a hydrogen (or He) nucleus as target the beam is much heavier.
This is inverse kinematics, and the energy-angle systematics are completely different.

A PLAN for how to STUDY STRUCTURE

- Use **transfer reactions** to identify strong single-particle states, measuring their spins and strengths

- Use the energies of these states to compare with theory

- Refine the theory

- Improve the extrapolation to very exotic nuclei

- **Hence learn the structure of very exotic nuclei**

N.B. The **shell model** is arguably the best theoretical approach for us to confront with our results, but it's **not the only one**. The experiments are needed, no matter which theory we use.

N.B. Transfer (as opposed to knockout) allows us to study orbitals that are empty, so **we don't need** quite such exotic beams.

USING RADIOACTIVE BEAMS in INVERSE KINEMATICS

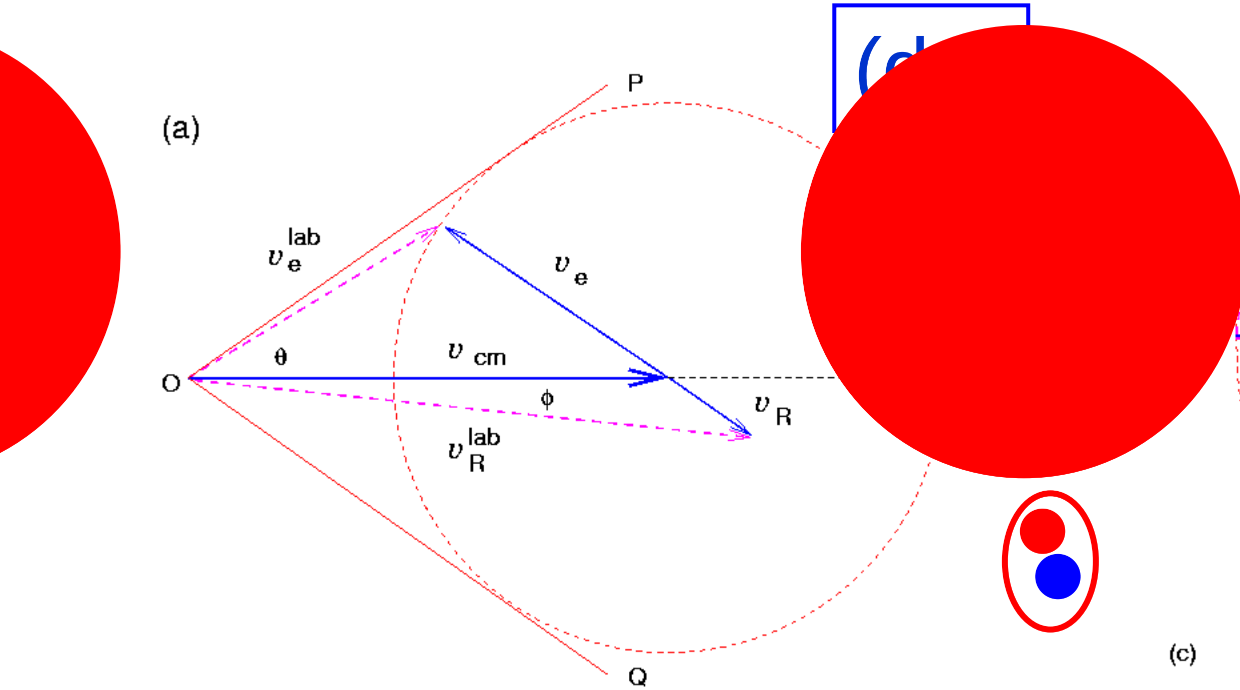

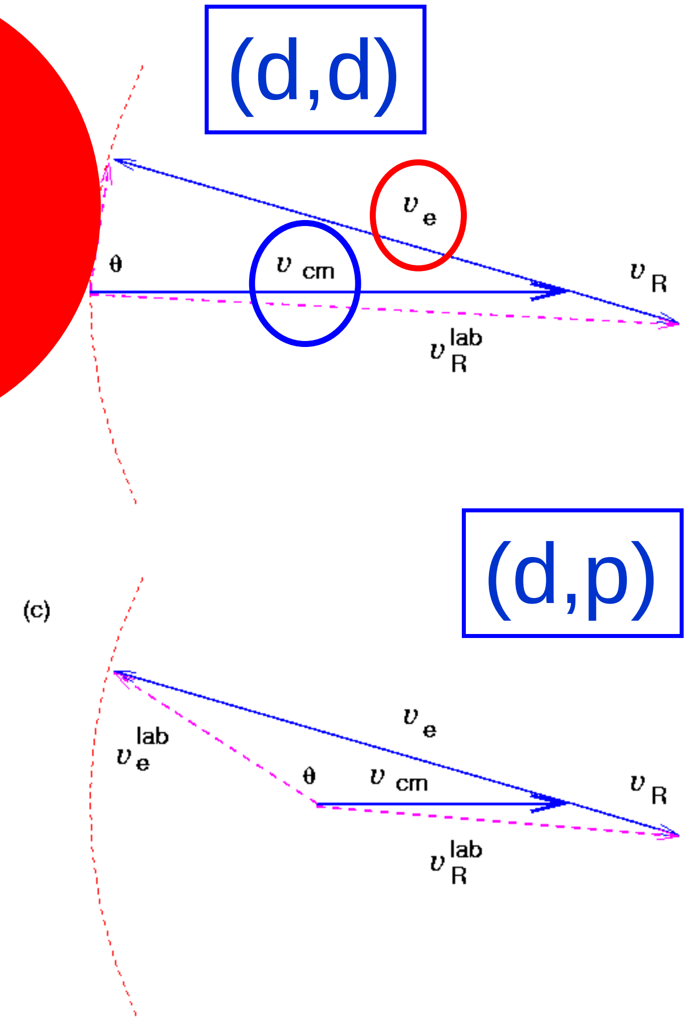

$$\frac{v_e}{v_{cm}} = \left(q\, f \frac{M_R}{M_P} \right)^{1/2} \cong \sqrt{q\, f}$$

$$\theta_{max} = \sin^{-1}\sqrt{f}$$

f = 1/2 for (p,d), 2/3 for (d,t)

$q \cong 1 + Q_{tot} / (E/A)_{beam}$

Velocity vector addition diagram

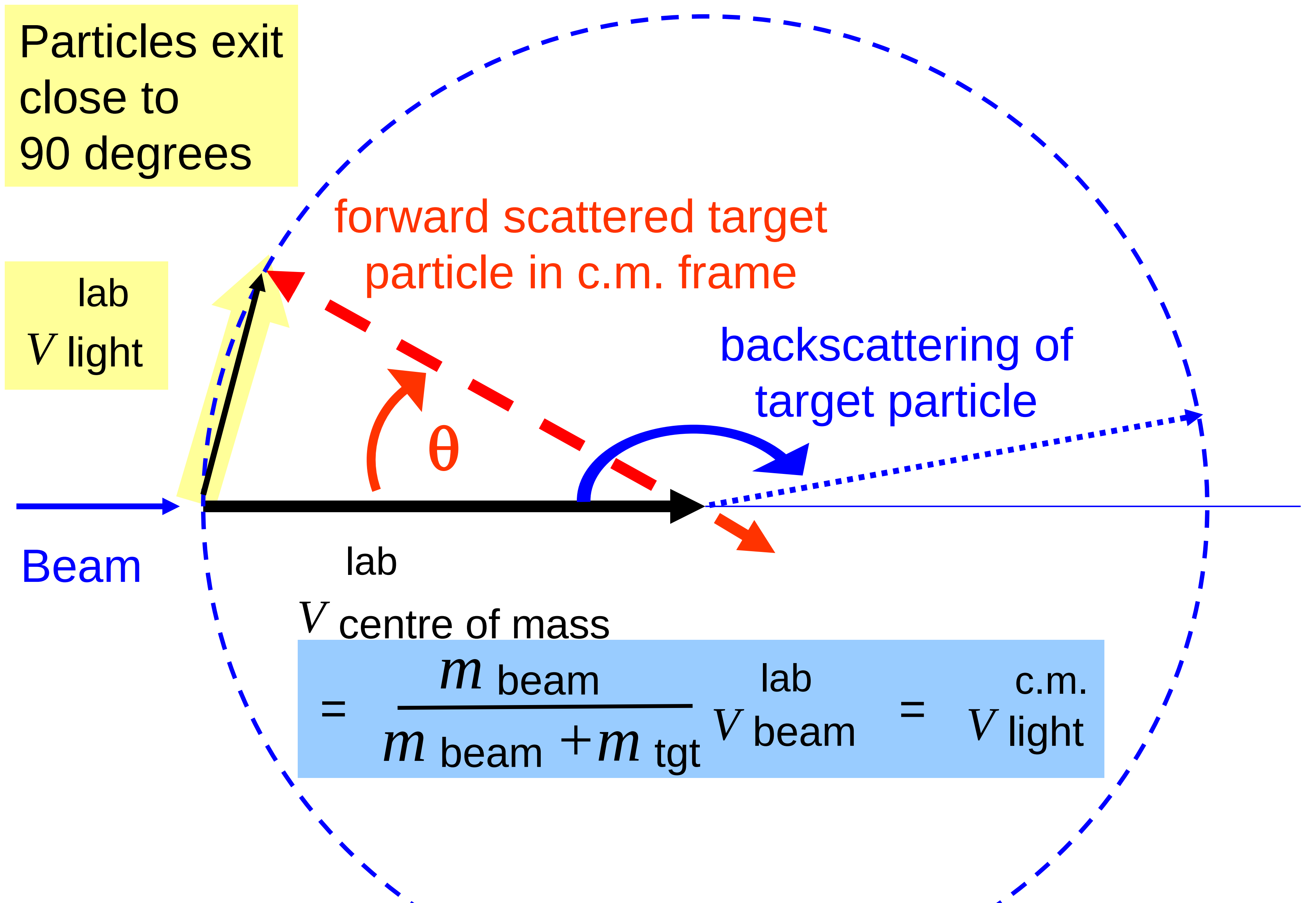

$$V_{\text{centre of mass}}^{\text{lab}} = \frac{m_{\text{beam}}}{m_{\text{beam}} + m_{\text{tgt}}} V_{\text{beam}}^{\text{lab}} = V_{\text{light}}^{\text{c.m.}}$$

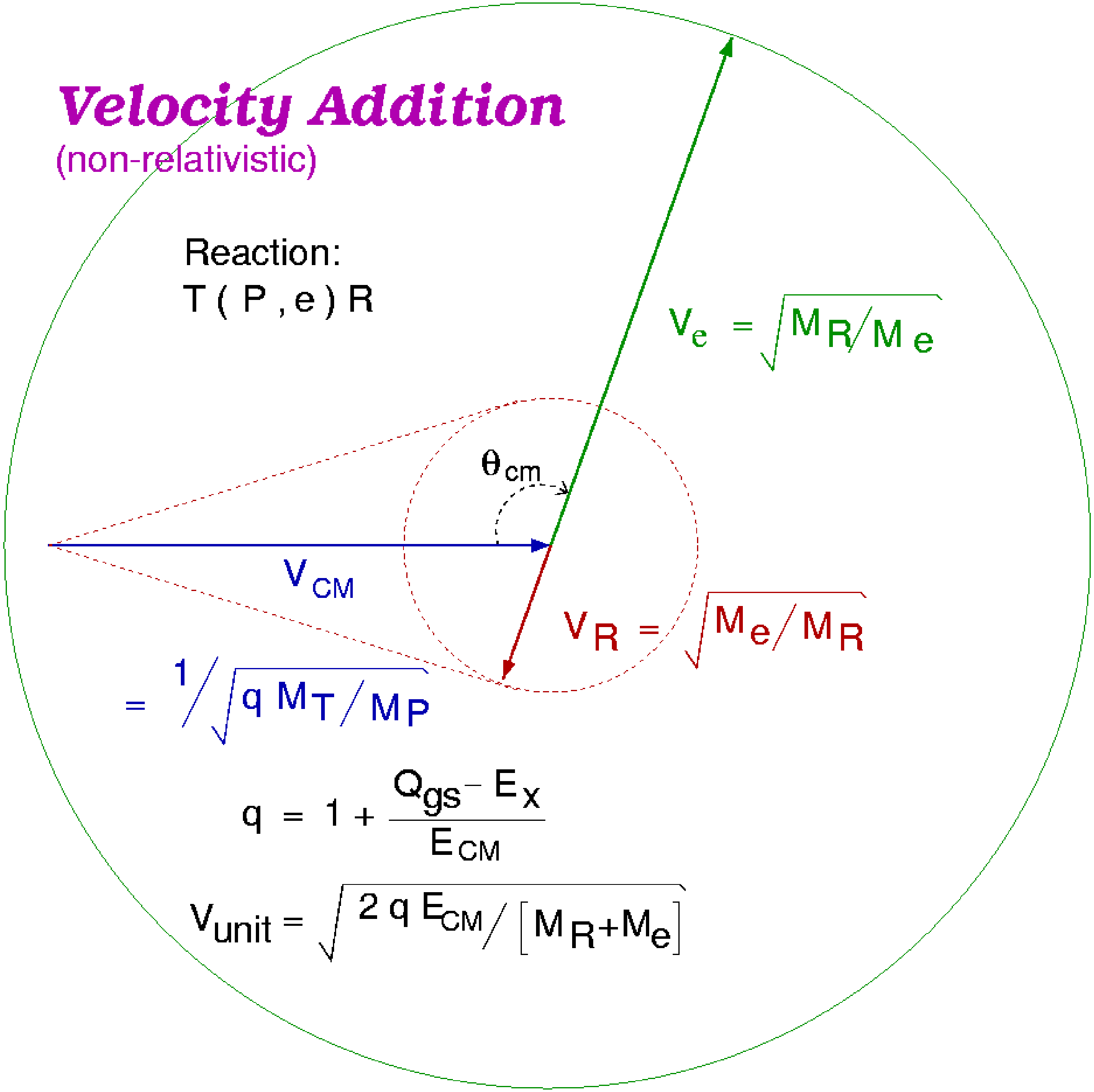
Velocity Addition
(non-relativistic)
Reaction:
T (P , e) R
$V_e = \sqrt{M_R / M_e}$
θ_{cm}
V_{CM}
$= 1 / \sqrt{q \, M_T / M_P}$
$V_R = \sqrt{M_e / M_R}$
$q = 1 + \frac{Q_{gs} - E_x}{E_{CM}}$
$V_{unit} = \sqrt{2 \, q \, E_{CM} / [M_R + M_e]}$

Inverse Kinematics

$q \cong 1 + Q_{tot} / (E/A)_{beam}$
$f = 1/2$ for (p,d), $2/3$ for (d,t)

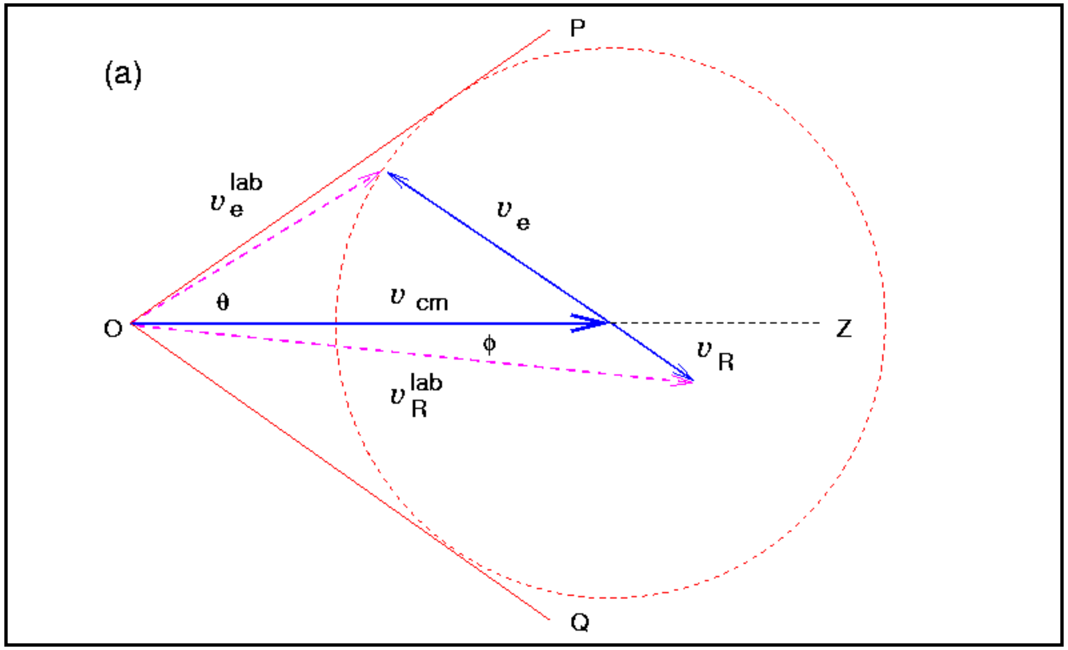

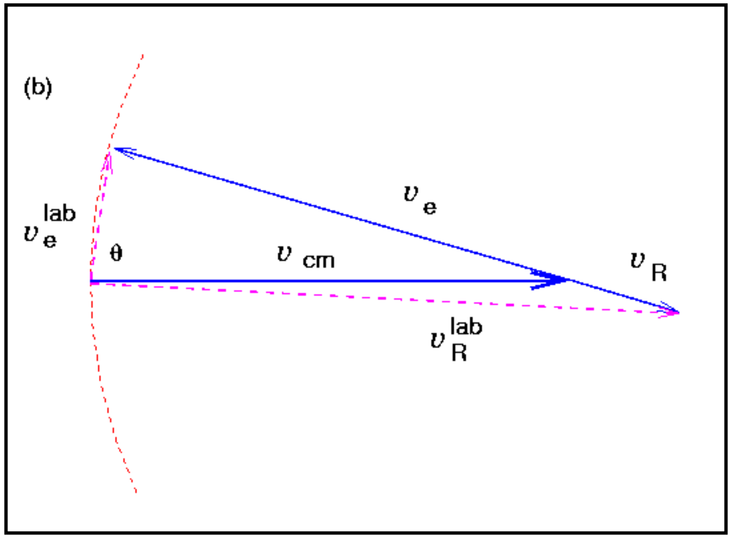

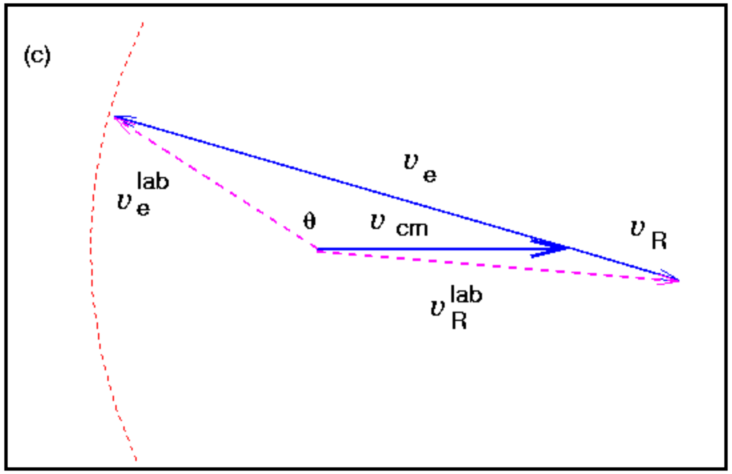

$$\frac{v_e}{v_{cm}} = \left(q\, f \frac{M_R}{M_P} \right)^{1/2} \cong \sqrt{q\, f}$$

$$\theta_{max} = \sin^{-1} \sqrt{f}$$

v_{cm} is the velocity of the centre of mass, in the laboratory frame

Reaction Q-values in MeV

Z

Ne				14	15	16: -77.6	17: -13.4	18: -17.0	19: -9.4	**20: -14.6**	21: -4.5	**22: -8.1**	23: -3.0	24: -6.6	25: -2.0	26: -3.3	27: 0.1	28: -1.5	29: 2.5	30: -2.1
F				13	14: -81.1	15: -22.7	16: -11.9	17: -14.6	18: -6.9	**19: -8.2**	20: -4.4	21: -5.9	22: -3.0	23: -5.3	24: -1.4	25: -2.7	26: 0.9	27: 2.5	28: 1.8	↑ N=20
O				12	13: -14.8	14: -21.0	15: -11.0	**16: -13.4**	**17: -1.9**	**18: -5.8**	19: -1.7	20: -5.4	21: -1.6	22: -4.5	23: -0.7					
N				11: -20.7	12: -13.4	13: -17.8	**14: -8.3**	**15: -8.6**	16: -0.3	17: -3.7	18: -0.6	19: -3.1	20: 0.2	21: -2.6						
C		8	9: -12.0	10: -19.1	11: -10.9	**12: -16.5**	**13: -2.7**	14: -6.0	15: 1.0	16: -2.0	17: 1.5	18: -2.0	19: 1.9	20: -1.4						
B		7	8: -10.8	9: -16.4	**10: -6.2**	**11: -9.2**	12: -1.1	13: -2.7	14: 1.3	15: -0.5				↑ N=14						
Be		6	7: -8.5	8: -16.7	**9: 0.6**	10: -4.6	11: 1.7	12: -0.9	13: 4.1	14: -0.7										
Li	4	5: -19.3	**6: -3.4**	**7: -5.0**	8: 0.2	9: -1.8	10: 3.0	↑ N=8												

□ = stable

Reaction Q-value in MeV

(p , d) : refer to cell of TARGET

(d , p) : (-1) x (Cell of PRODUCT)

(d , t) : Cell of TARGET + 4.0 MeV

Ne					15: 60.3	16: 5.4	17: 4.0	18: 1.6	19: -0.9	**20: -7.4**	21: -7.5	**22: -9.8**	23: -9.8	24: -11.1	25: -11.6	26: -12.3	27: -13.1	28: -17.1	29: -16.4	30: -18.4
F				13: 75.0	14: 8.7	15: 7.0	16: 6.0	17: 4.9	18: -0.1	**19: -2.5**	20: -5.1	21: -5.6	22: -7.0	23: -7.9	24: -8.6	25: -9.6	26: -16.7	27: -14.1	28: -15.6	↑ N=20
O				12: 5.4	13: 4.0	14: 0.9	15: -1.8	**16: -6.6**	**17: -8.3**	**18: -10.4**	19: -11.6	20: -13.9	21: -15.6	22: -17.5	23: -19.0					
N				11: 7.3	12: 4.9	13: 3.6	**14: -2.1**	**15: -4.7**	16: -6.0	17: -7.6	18: -9.7	19: -10.8	20: -12.5	21: -13.7						
C		8: 5.4	9: 4.2	10: 1.5	11: -3.1	**12: -10.5**	**13: -12.0**	14: -15.3	15: -15.6	16: -17.1	17: -17.9	18: -20.2	19: -21.4	20: -24.1						
B		7: 7.7	8: 5.4	9: 5.7	**10: -1.1**	**11: -5.7**	12: -8.6	13: -10.3	14: -13.1	15: -12.9				↑ N=14						
Be		6: 4.9	7: -0.1	8: -11.8	**9: -11.4**	10: -14.1	11: -15.5	12: -17.6												
Li	4: 8.4	5: 7.5	**6: 0.9**	**7: -4.5**	8: -7.0	9: -8.4	10: -8.7	↑ N=8												

N

□ = stable

Reaction Q-value in MeV

(d , ^{3}He) : refer to cell of TARGET

The general form of the kinematic diagrams is determined by the light particle masses, and has little dependence on the beam mass or velocity

^{16}C incident on ^{2}H at 35 MeV/u

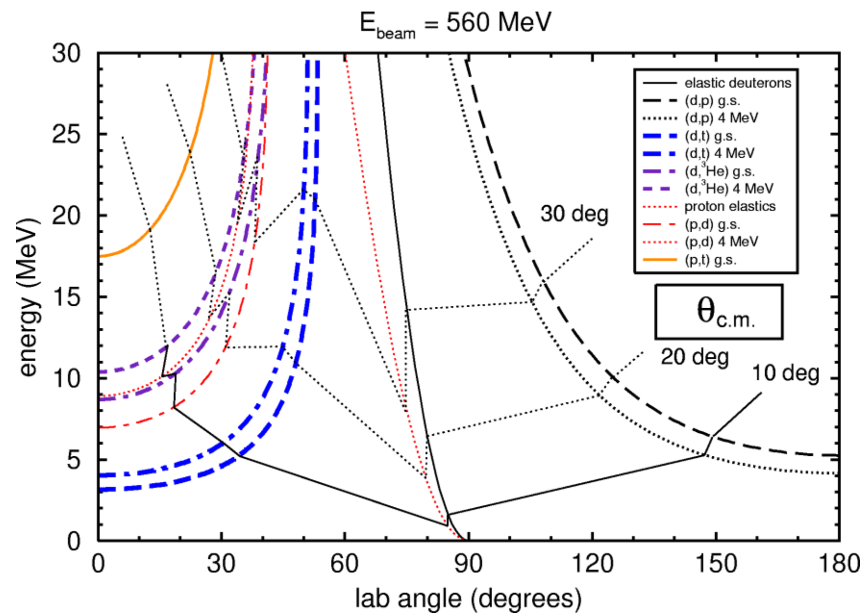

(p,d) and (d,t) and (d,p) on ^{74}Kr in inverse kinematics

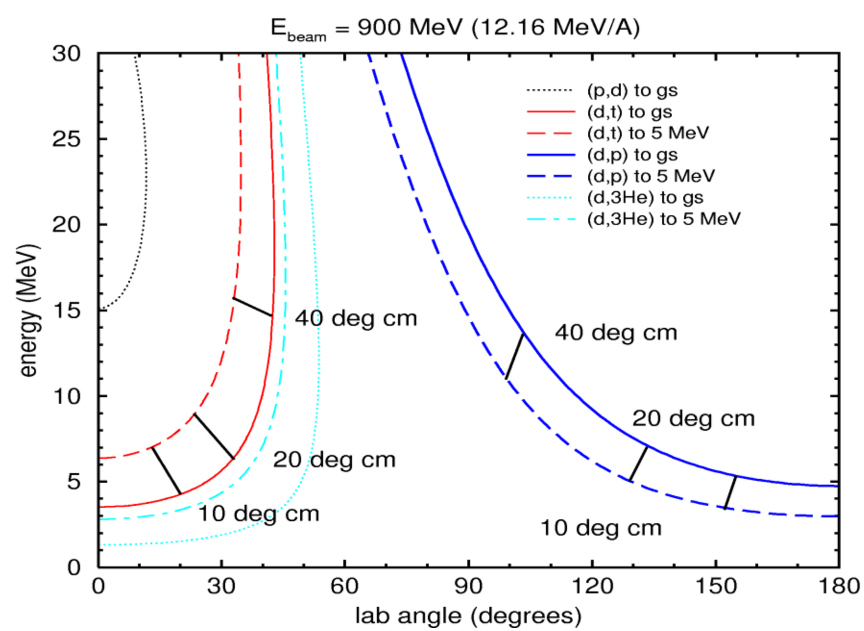

^{94}Sr (d,p) ^{95}Sr

4.0 MeV/A
(~24MV 15+)
376 MeV

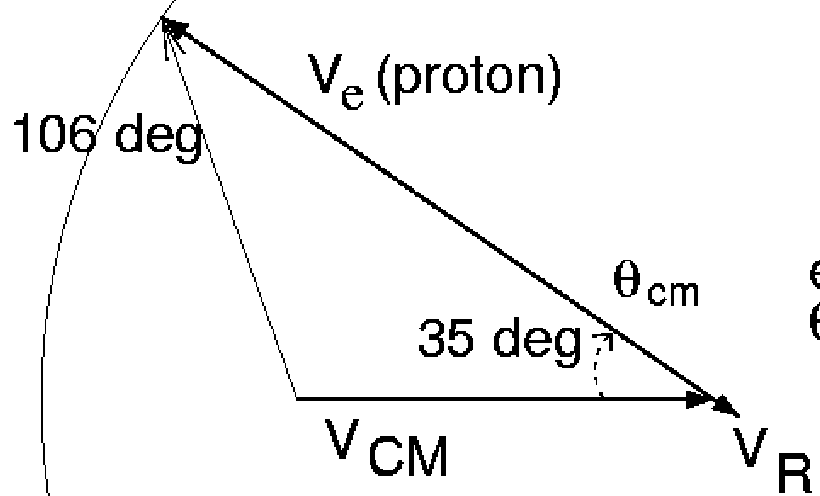

experiment to study
θ_{cm} between 10, 32 deg

θ_{lab}	θ_{cm}	E_{proton}	0.2 deg $\Delta\theta$	35 keV E_{res}	ENRGY STRAG	MULT/ SCATT	DIFF'L DE/DX TARG	TOTAL IN QUAD	DE(Ex) /DE(Ep)
112	32	3.33	23	50	19	56	393	401	-1.43
154	10	1.58	7	87	21	23	389	400	-2.53

Solid Angle Transformation Jacobian

typical (d,p) reaction

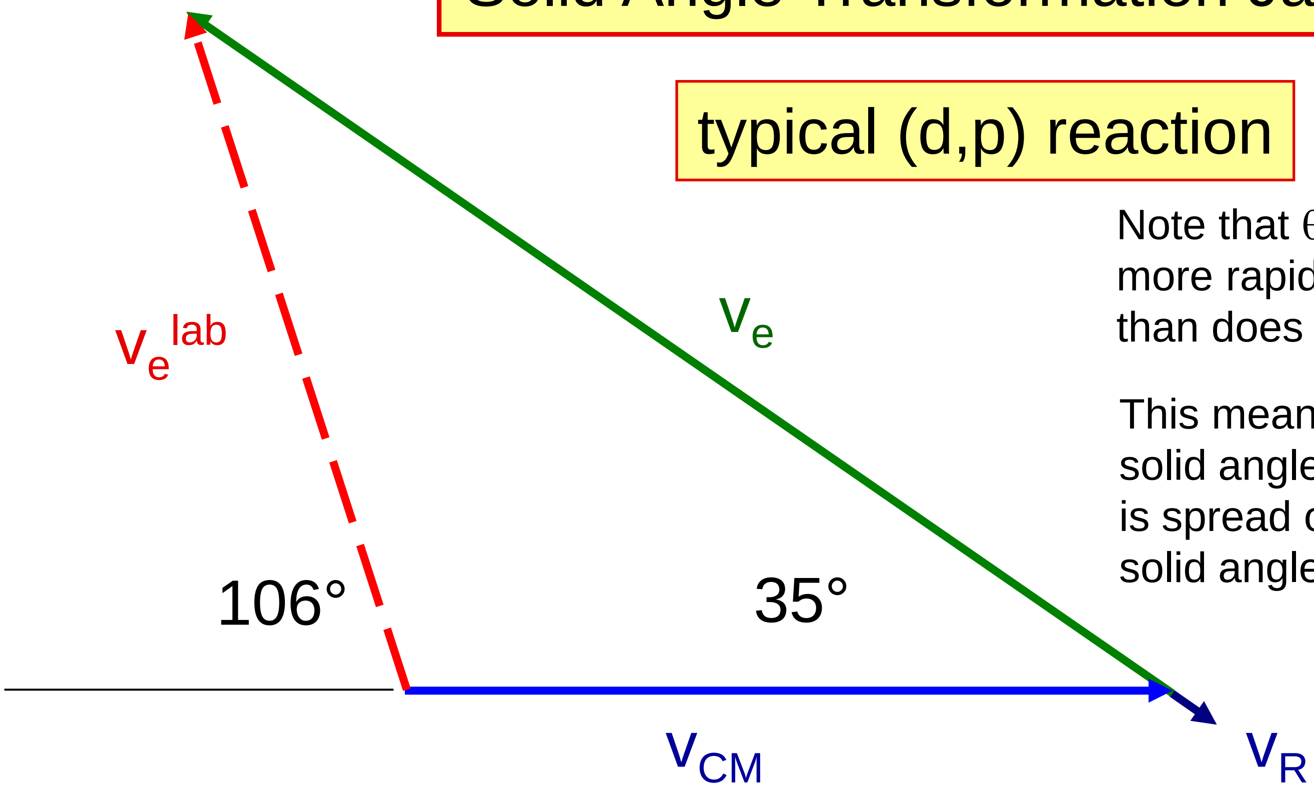

Note that θ_{lab} changes much more rapidly (at back angles) than does θ_{CM}

This means that a small solid angle in the CM, $d\Omega_{CM}$ is spread over a rather large solid angle $d\Omega_{lab}$ in the lab

This means that although $d\sigma / d\Omega_{CM}$ is largest at small θ_{CM} or near 180° in the lab, the effect of the Jacobian is that $d\sigma / d\Omega_{lab}$ near 180° is reduced relative to less backward angles

Defining: $\gamma = v_{CM} / v_e$

$$\frac{d\sigma}{d\Omega_{lab}} = \frac{(1 + \gamma^2 + 2\gamma \cos\theta)^{3/2}}{|1 + \gamma \cos\theta|} \frac{d\sigma}{d\Omega_{CM}}$$

e.g. L.I. Schiff, *Quantum Mechanics*, 3rd Ed., p.113

DWBA ZR: $^{94}Sr(d,p)^{95}Sr^*(1.0 MeV; s_{1/2})$ at 4.894 MeV/u

Adiabatic deuteron potential (B–G) and Perey proton potential

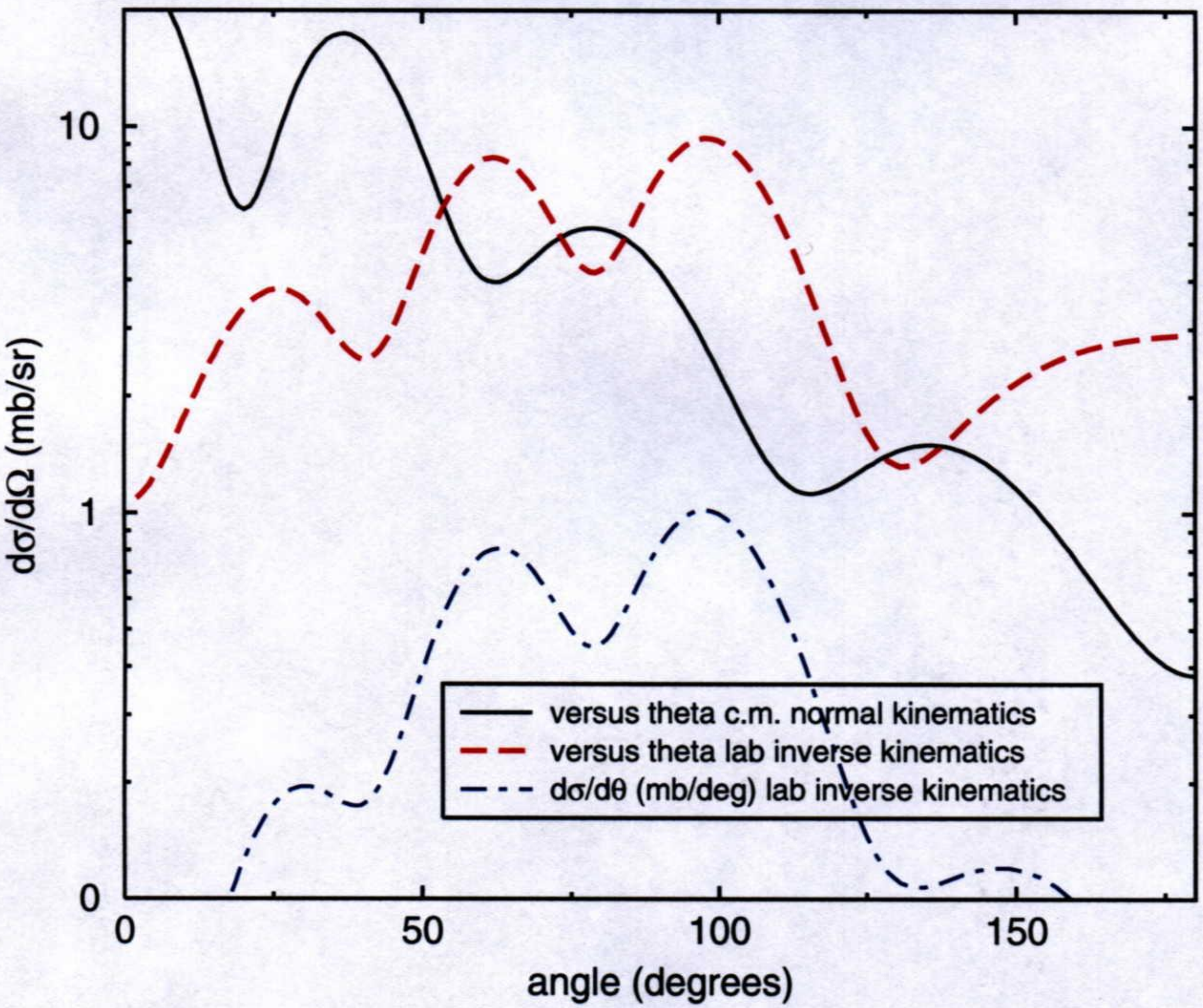

USING RADIOACTIVE BEAMS in INVERSE KINEMATICS

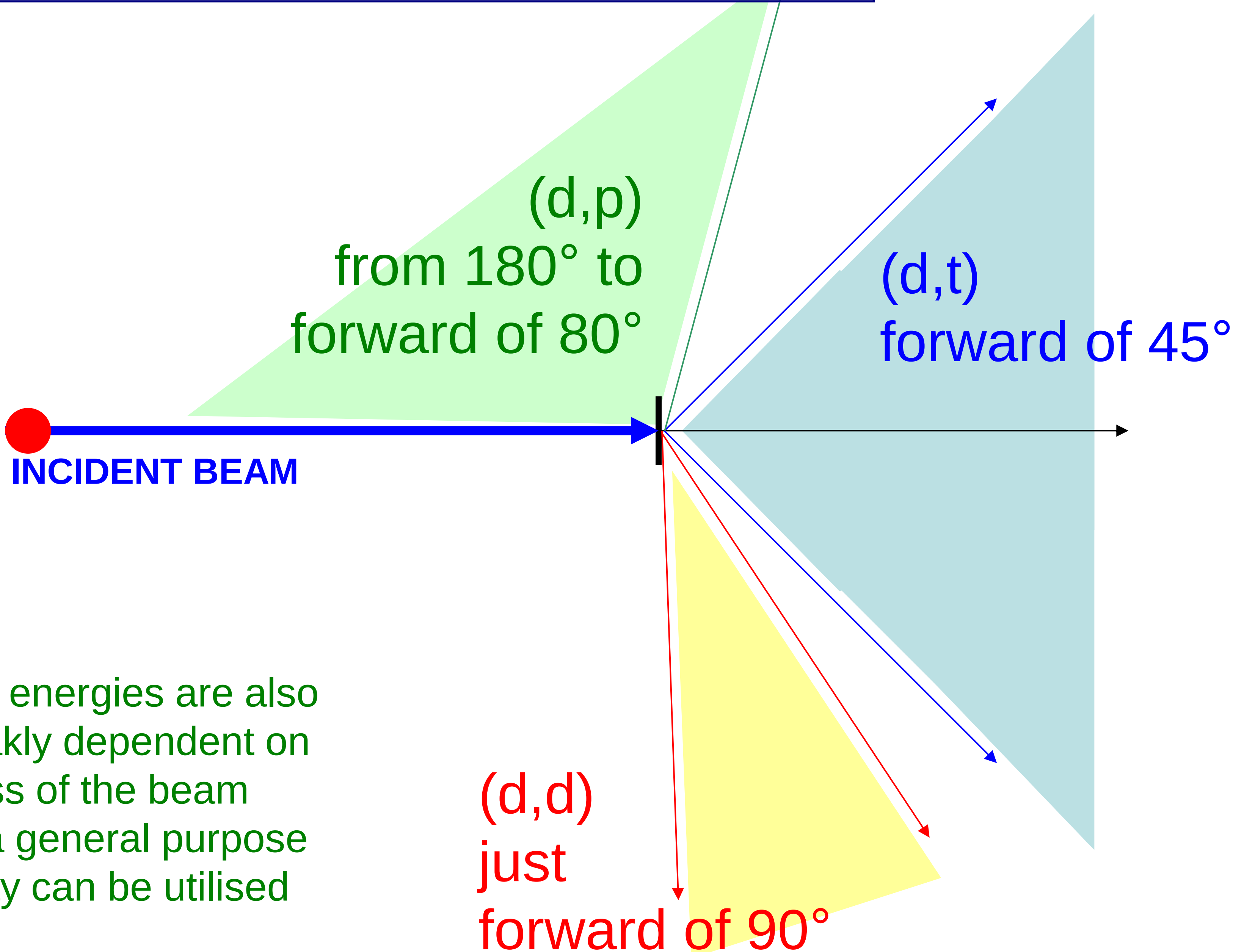

The energies are also weakly dependent on mass of the beam so a general purpose array can be utilised

Calculations of E_x resolution from particle detection

beamlike particle detected

Table 2
Major contributions in keV to the resolution of the excitation energy spectra of single neutron stripping and pickup reactions in inverse kinematics, where the heavy ion is detected in a spectrometer. The detection angle corresponds to 10°_{cm}. The last column is an approximate estimate as a sum in quadrature of the net effect of five non-Gaussian contributions. Other symbols are explained in the text

Reaction	E_i/A (MeV)	θ_{lab}	Origin of contribution					Σ_{quad}
			$\Delta\theta$	Δp	E_{stragg}	$\Theta_{1/2}$	dE/dx	
p(^{12}Be, ^{11}Be)d	30	1.07°	172	147	101	74	23	259
p(^{12}Be, ^{11}Be)d	15	1.06°	84	71	99	74	37	169
p(^{77}Kr, ^{76}Kr)d	30	0.16°	1404	811	808	723	56	1952
p(^{77}Kr, ^{76}Kr)d	10	0.10°	334	143	502	570	268	883
d(^{76}Kr, ^{77}Kr)p	10	0.21°	1140	614	2177	1859	1321	3408

light particle detected

Table 3
Major contributions in keV to the resolution of the excitation energy spectra of single neutron pickup and stripping reactions in inverse kinematics, where the light particle is detected in a silicon detector. Symbols as described in text and Table 2

Reaction	E_i/A (MeV)	θ_{lab}	Origin of contribution					Σ_{quad}
			$\Delta\theta$	ΔE_f	ΔE_i	$\Theta_{1/2}$	dE/dx	
p(^{12}Be, d)^{11}Be	30	19.0°	136	74	114	96	649	685
p(^{12}Be, d)^{11}Be	15	17.8°	66	72	55	89	984	995
p(^{77}Kr, d)^{76}Kr	30	15.0°	124	55	64	63	186	249
p(^{77}Kr, d)^{76}Kr	10	6.0°	26	24	23	19	775	777
d(^{76}Kr, p)^{77}Kr	10	155.3°	52	93	37	60	1309	1316

Lighter projectiles

Some advantages to detect beam-like particle

(gets difficult at higher energies)

Heavier projectiles

Better to detect light particle

(target thickness lilmits resolution)

Possible Experimental Approaches to Nucleon Transfer

1) Rely on detecting the beam-like ejectile in a spectrometer

- Kinematically favourable unless beam mass (and focussing) ***too*** great
- Spread in beam energy (several MeV) translates to E_X measurement
- Hence, need energy tagging, or a dispersion matching spectrometer
- Spectrometer is subject to broadening from gamma-decay in flight

2) Rely on detecting the target-like ejectile in a Si detector

- Kinematically less favourable for angular coverage
- Spread in beam energy generally gives little effect on E_X measurement
- Resolution limited by difference [dE/dx(beam) - dE/dx(ejectile)]
- Target thickness limited to 0.5-1.0 mg/cm^2 to maintain resolution

3) Detect decay gamma-rays in addition to particles

- Need exceptionally high efficiency, of order > 25%
- Resolution limited by Doppler shift and/or broadening
- Target thickness increased up to factor 10 (detection cutoff, mult scatt'g)

J.S. Winfield, W.N. Catford and N.A. Orr, NIM A396 (1997) 147

- Motivation: nuclear structure reasons for transfer
- Choices of reactions and beam energies
- Inverse Kinematics
- Implications for Experimental approaches
- **Early Experiments: examples**
- **Why do people make the choices they do?**
- **Some recent examples: TIARA, MUST2, SHARC**
- **Brief mention of Heavy Ion transfer reactions**

CERN REACTIONS SCHOOL

CERN, Geneva ** 22-24 April 2014

LAKE GENEVA

Possible Experimental Approaches to Nucleon Transfer

1) Rely on detecting the beam-like ejectile in a spectrometer

- Kinematically favourable unless beam mass (and focussing) ***too*** great
- Spread in beam energy (several MeV) translates to E_X measurement
- Hence, need energy tagging, or a dispersion matching spectrometer
- Spectrometer is subject to broadening from gamma-decay in flight

2) Rely on detecting the target-like ejectile in a Si detector

- Kinematically less favourable for angular coverage
- Spread in beam energy generally gives little effect on E_X measurement
- Resolution limited by difference [dE/dx(beam) - dE/dx(ejectile)]
- Target thickness limited to 0.5-1.0 mg/cm^2 to maintain resolution

3) Detect decay gamma-rays in addition to particles

- Need exceptionally high efficiency, of order > 25%
- Resolution limited by Doppler shift and/or broadening
- Target thickness increased up to factor 10 (detection cutoff, mult scatt'g)

J.S. Winfield, W.N. Catford and N.A. Orr, NIM A396 (1997) 147

$^{11}Be(p,d)^{10}Be$

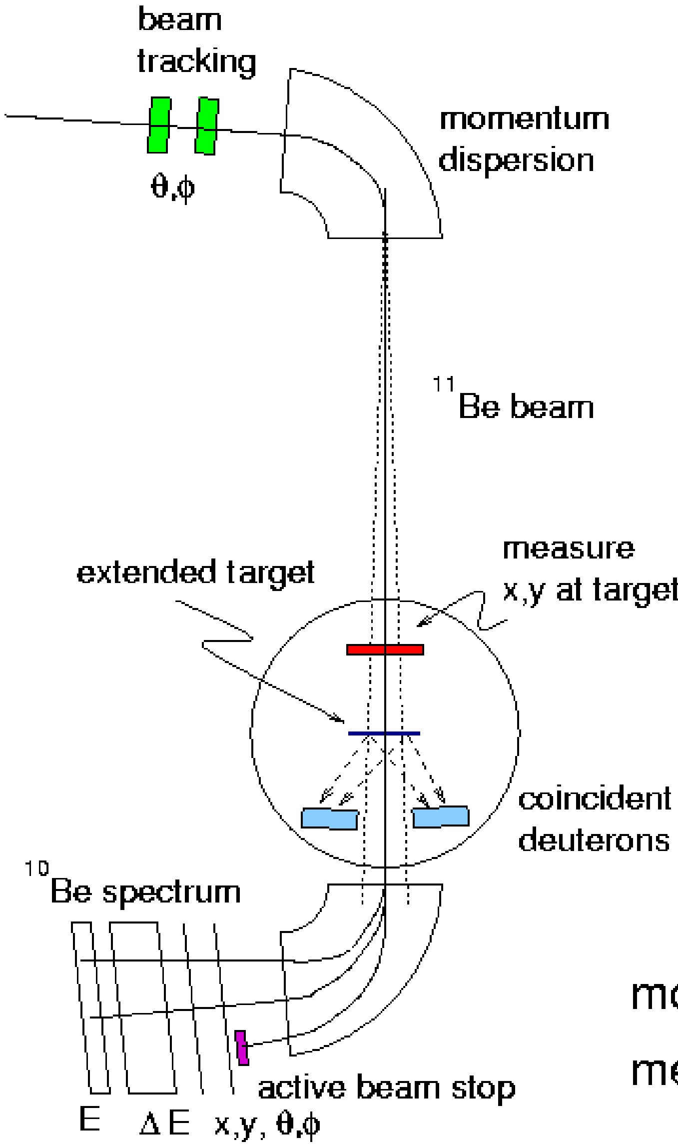

beam energy resolution 2.0-3.0 MeV

angular spread ±1 °

dispersion-matched spectrometer "SPEG"

(Spectromètre à Perte d'Energie du Ganil)

microchannel plate

polythene target

ten Silicon PSD's

momentum analysis

measure reaction angle

Inverse kinematics $^{11}Be\,(p,d)^{10}Be$

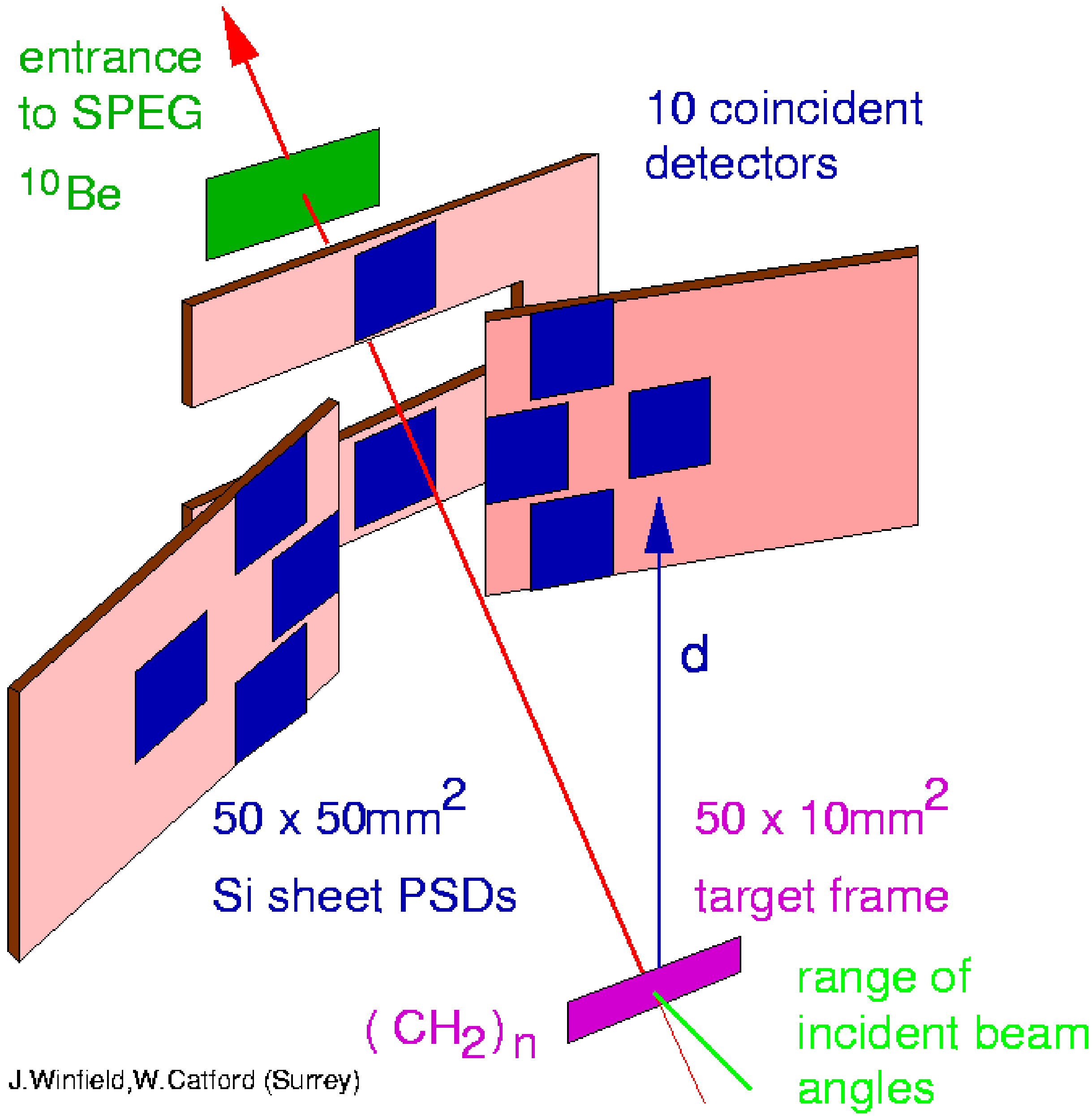

Focal plane spectrum from SPEG magnetic spectrometer

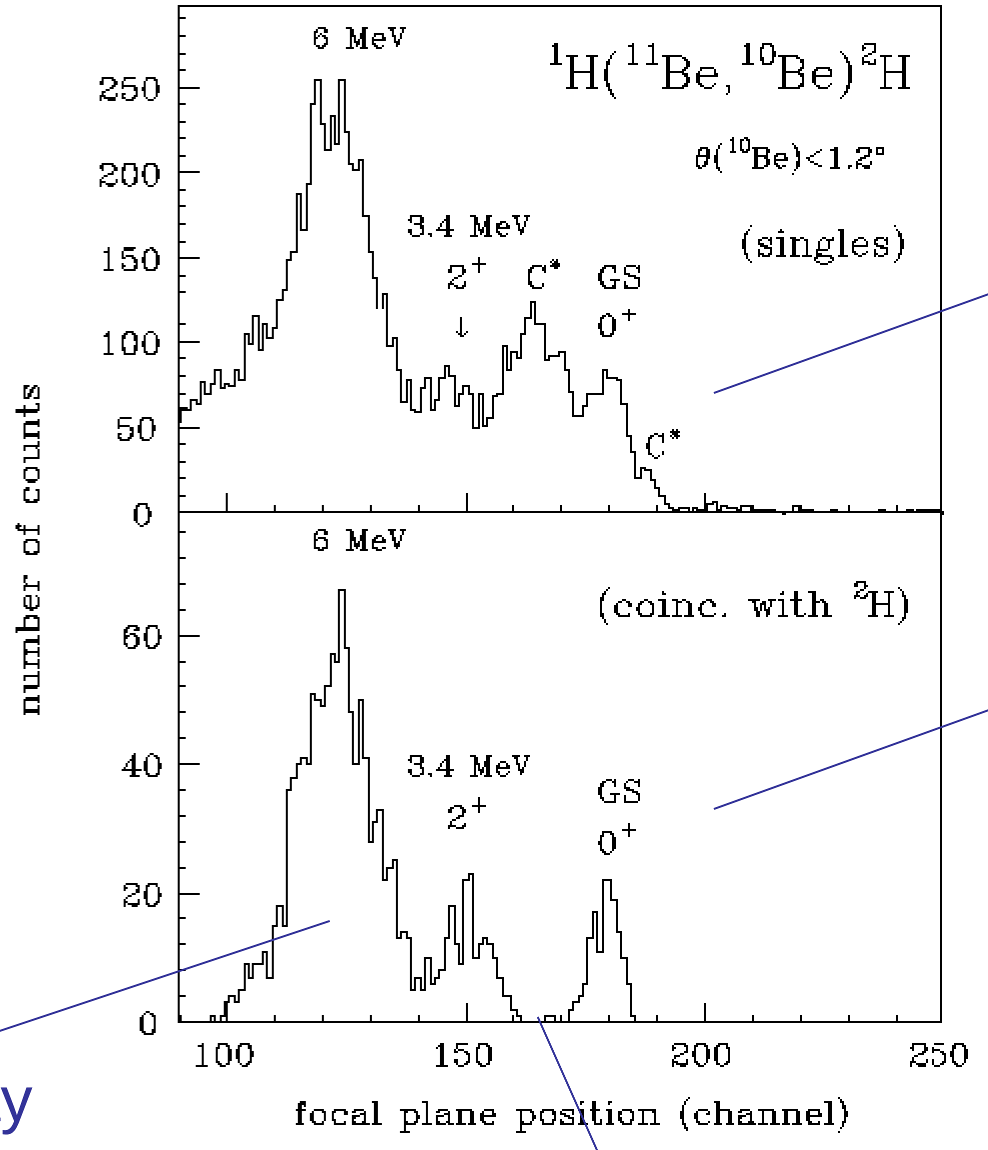

singles

coincidence

gamma-ray broadening

carbon background removed

Separation Energy form factor

Vibrational form factor

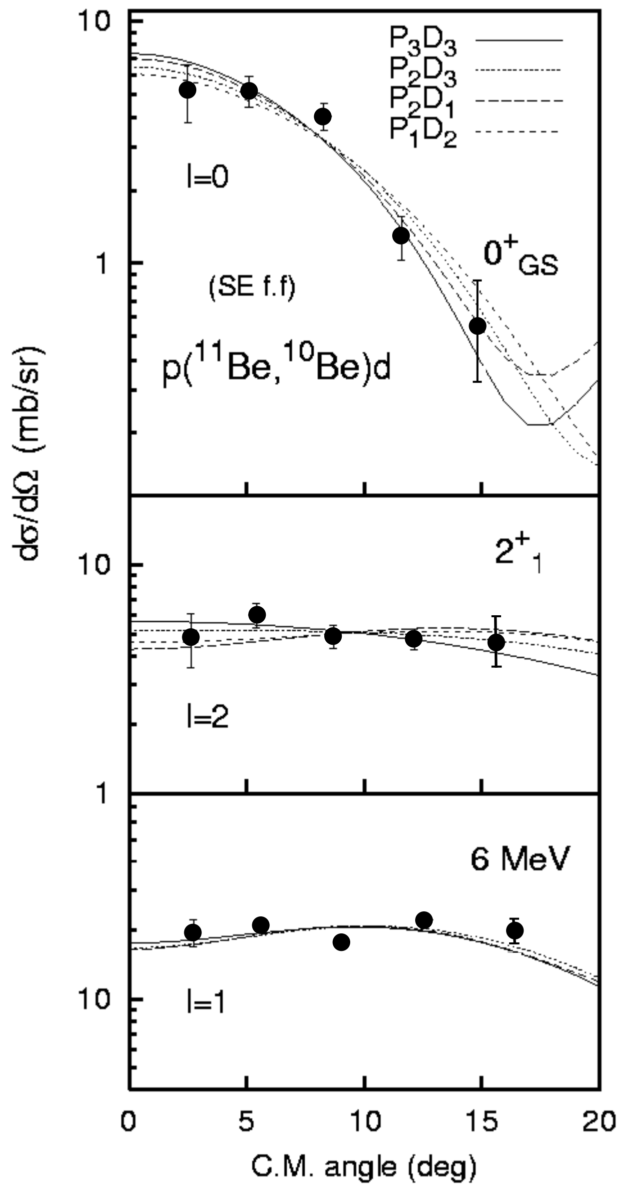

0^+ 2^+

α^2 β^2

~~0.49 0.51~~

- poor form factor
- no core coupling
- no ^{11}Be/d breakup

0.84 0.16

- vibrational model
- core-excited model
- realistic form factor

{ 0.74 0.19 Shell model }

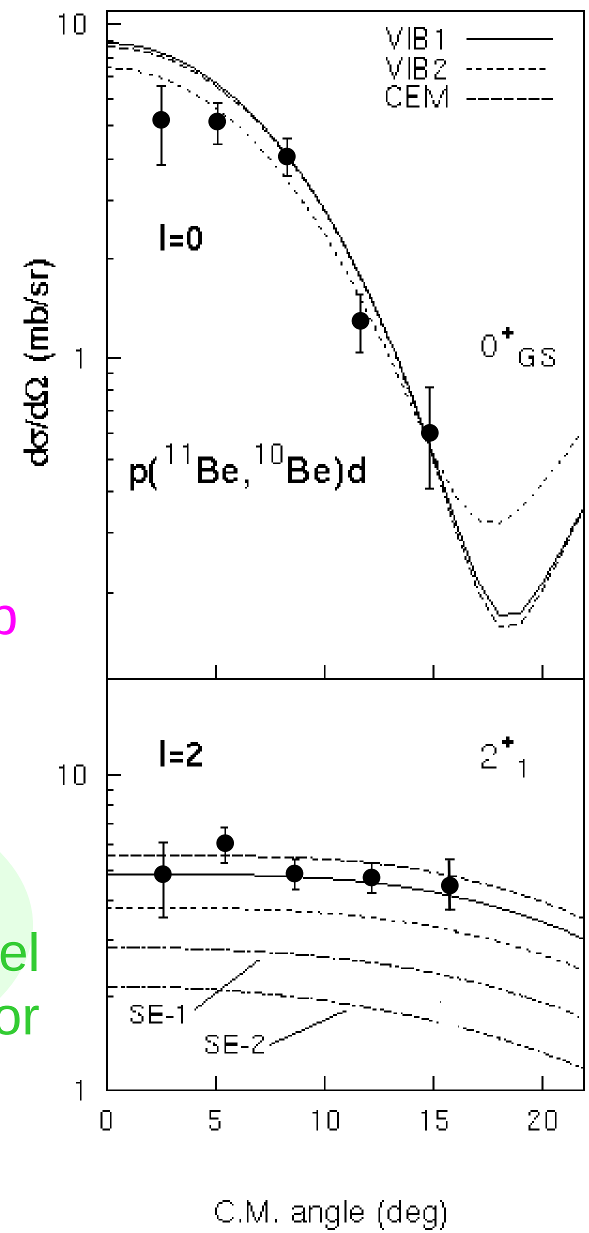

Study of the $^{56}Ni(d,p)^{57}Ni$ Reaction and the Astrophysical $^{56}Ni(p,\gamma)^{57}Cu$ Reaction Rate

K. E. Rehm,[1] F. Borasi,[1] C. L. Jiang,[1] D. Ackermann,[1] I. Ahmad,[1] B. A. Brown,[2] F. Brumwell,[1] C. N. Davids,[1] P. Decrock,[1] S. M. Fischer,[1] J. Görres,[3] J. Greene,[1] G. Hackmann,[1] B. Harss,[1] D. Henderson,[1] W. Henning,[1] R. V. F. Janssens,[1] G. McMichael,[1] V. Nanal,[1] D. Nisius,[1] J. Nolen,[1] R. C. Pardo,[1] M. Paul,[4] P. Reiter,[1] J. P. Schiffer,[1] D. Seweryniak,[1] R. E. Segel,[5] M. Wiescher,[3] and A. H. Wuosmaa[1]

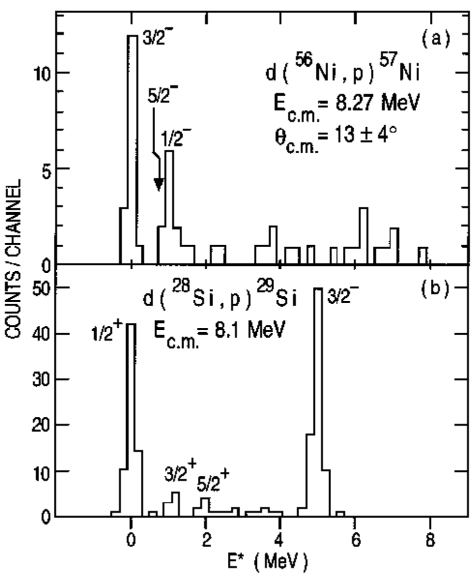

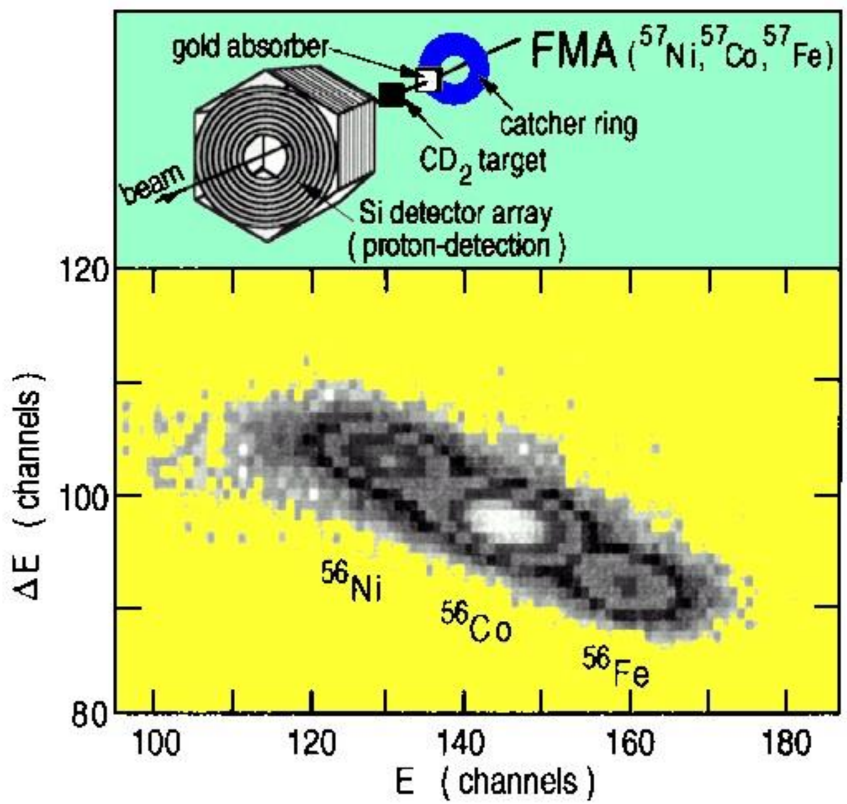

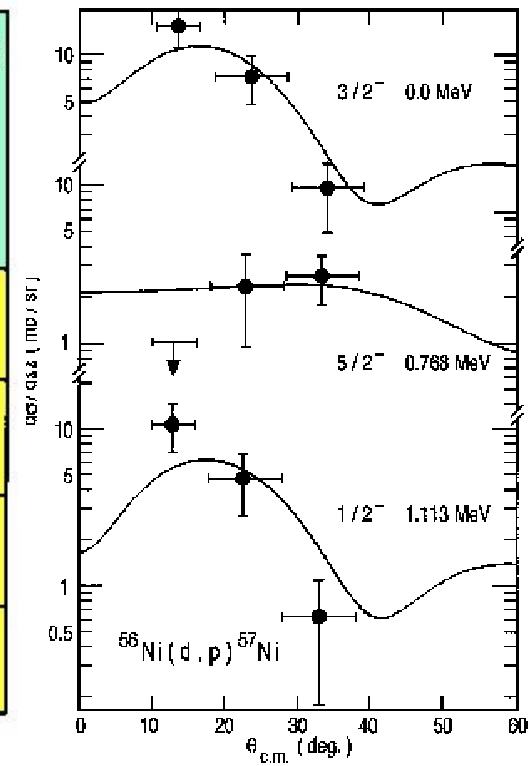

Inverse kinematics $^{11}Be(d,^{3}He)^{10}Li$

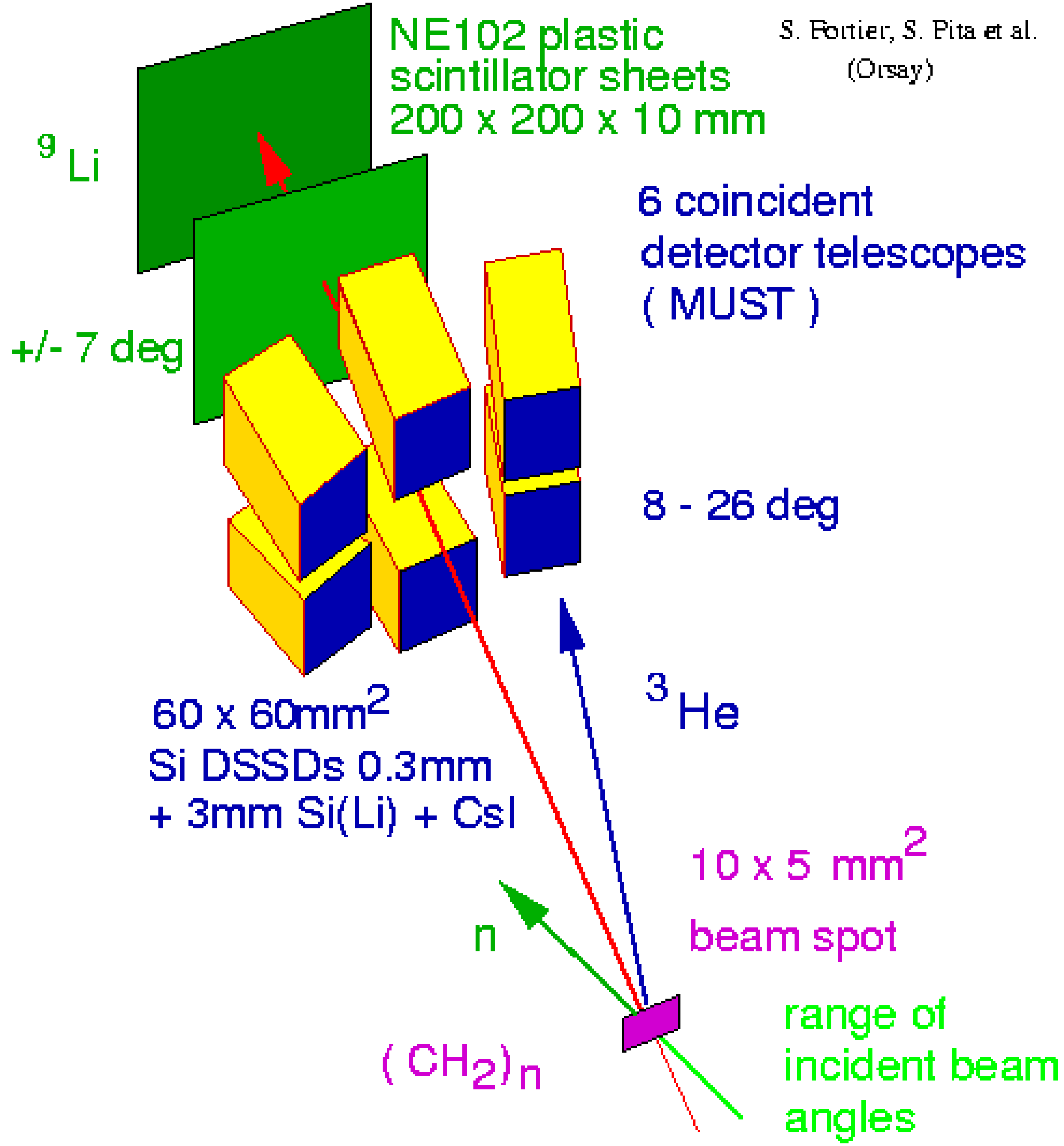

WHAT IS THE BEST IMPLEMENTATION FOR OPTIONS 2 AND 3 ?

It turns out that the target thickness is a real limitation on the energy resolution…

Several hundred keV is implicit, when tens would be required,
So the targets should be as thin as possible…

But RIBs, as well as being heavy compared to the deuteron target, are:
(a) Radioactive
(b) Weak

Issues arising:
(a) Gamma detection useful for improving resolution
(b) Active target (TPC) to minimize loss of resolution
(c) Need MAXIMUM efficiency for detection

Experimental solutions can be classed roughly as:
(a) For beams < 10^3 pps   ACTIVE TARGET
(b) 10^3 < beam < 10^6 pps   Si BOX in a γ-ARRAY
(c) For beams > 10^6 pps   MANAGE RADIOACTIVITY

SOLUTIONS FOR BEAMS IN RANGE 10^2 to 10^4 pps USING TPC's

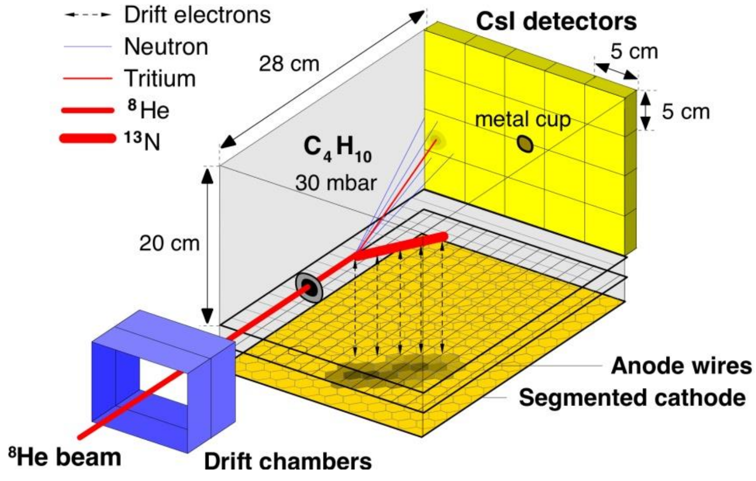

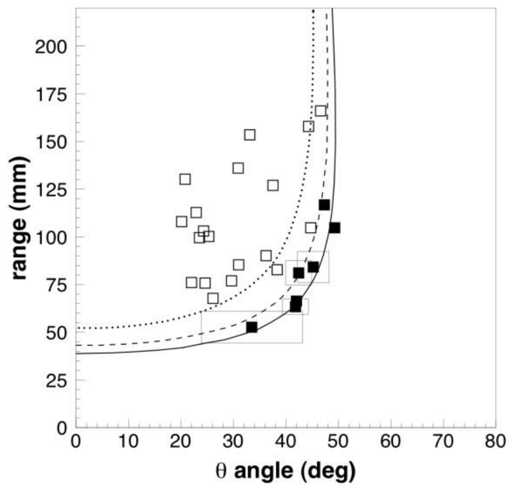

MAYA

Now in use at
GANIL/SPIRAL
TRIUMF

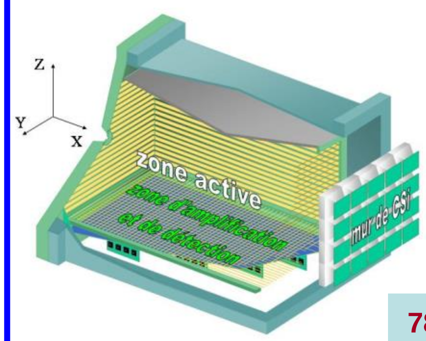

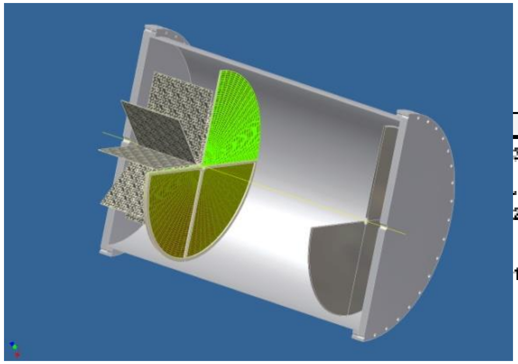

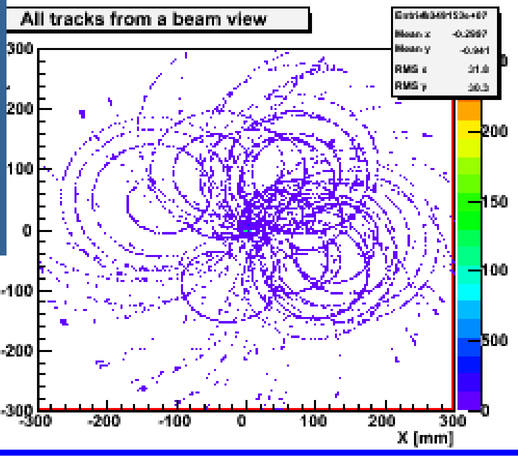

^{78}Ni(d,p)^{79}Ni at 10 A MeV

ACTAR

being designed
for future
SPIRAL2

SOLUTIONS FOR BEAMS IN RANGE 10^4 to 10^6 pps USING GAMMAS

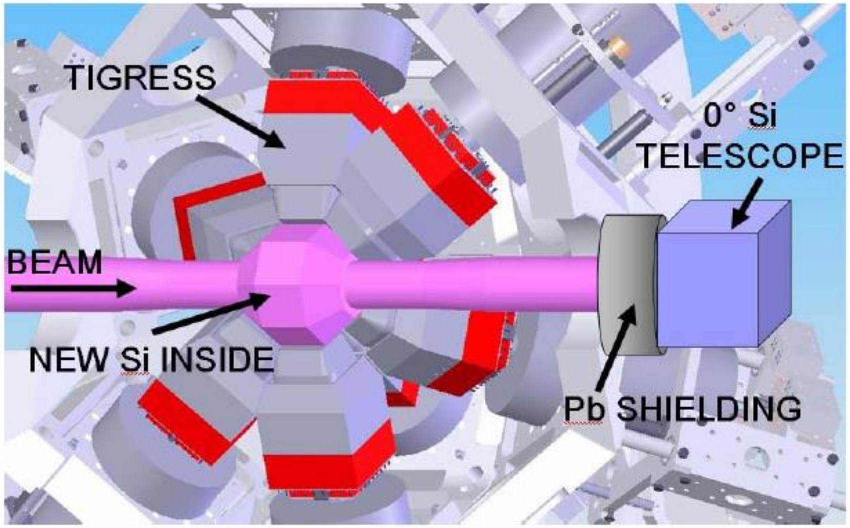

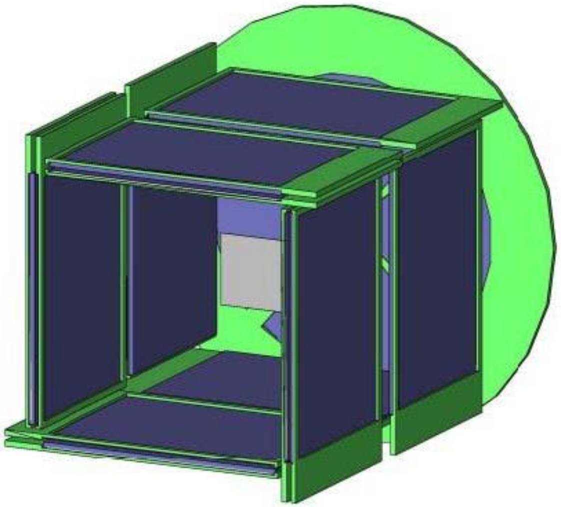

SHARC

TIGRESS
TRIUMF

TIGRESS COLLABORATION
York
Surrey

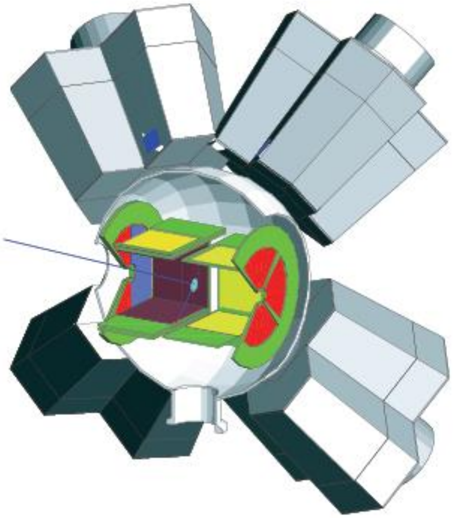

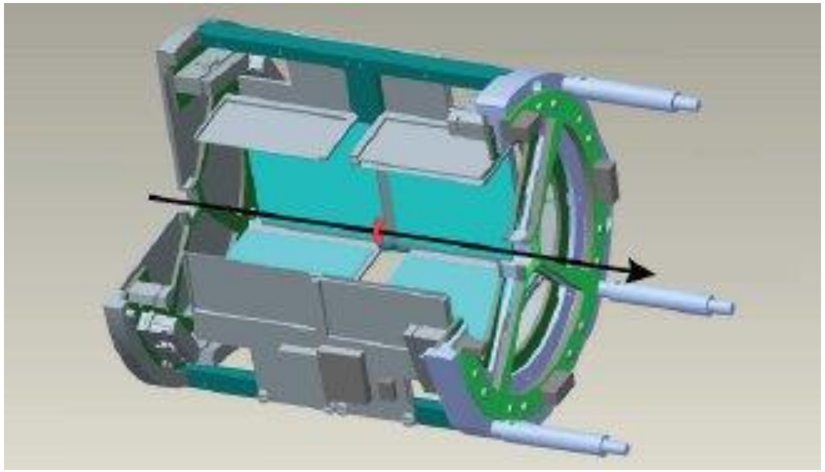

T-REX

MINIBALL
REX-ISOLDE

MINIBALL COLLABORATION
Munich
Leuven

ORRUBA OAK RIDGE

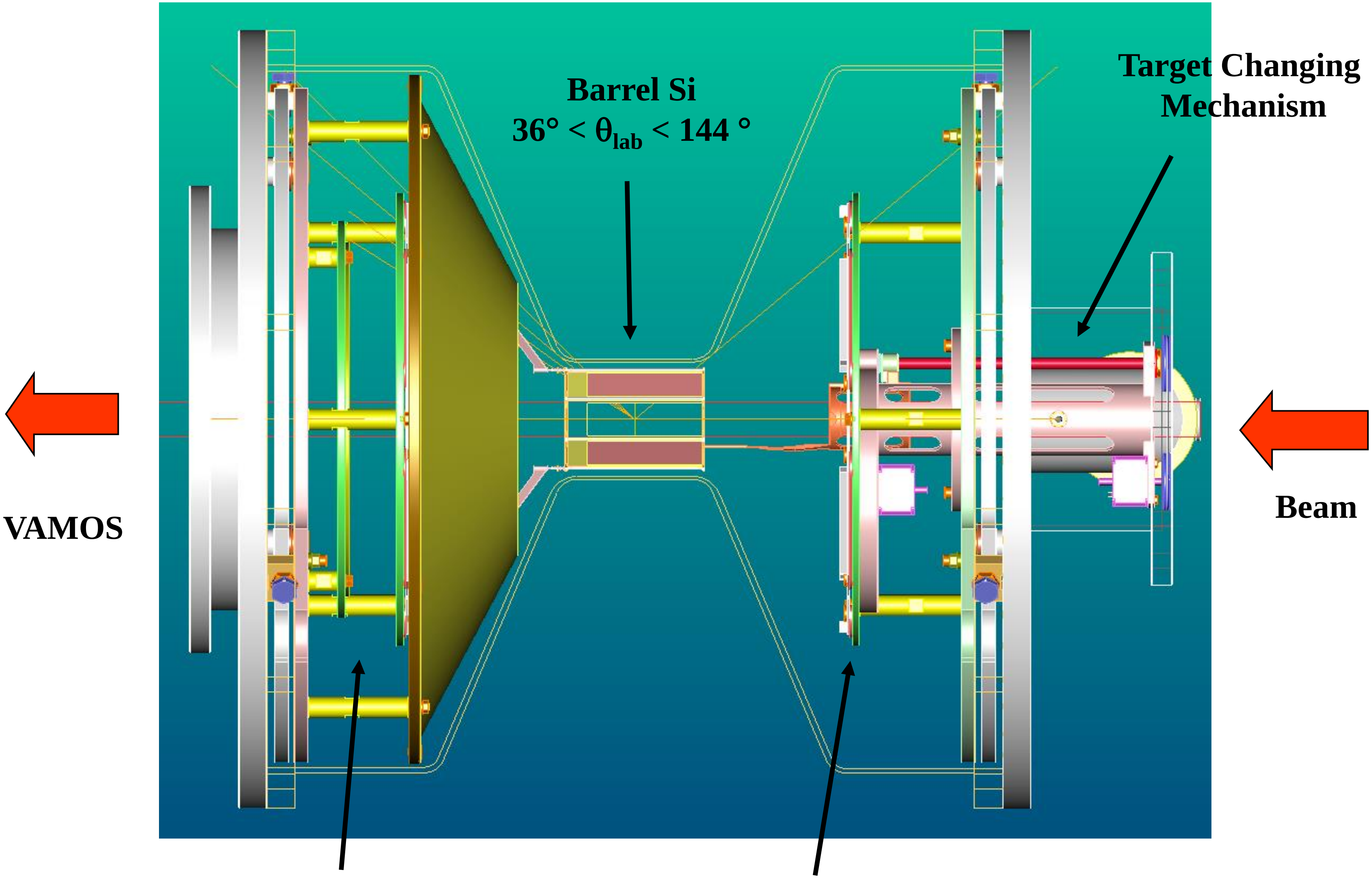

UniS
University of Surrey

SOLUTIONS FOR BEAMS IN RANGE 10^6 to 10^9 pps USING GAMMAS

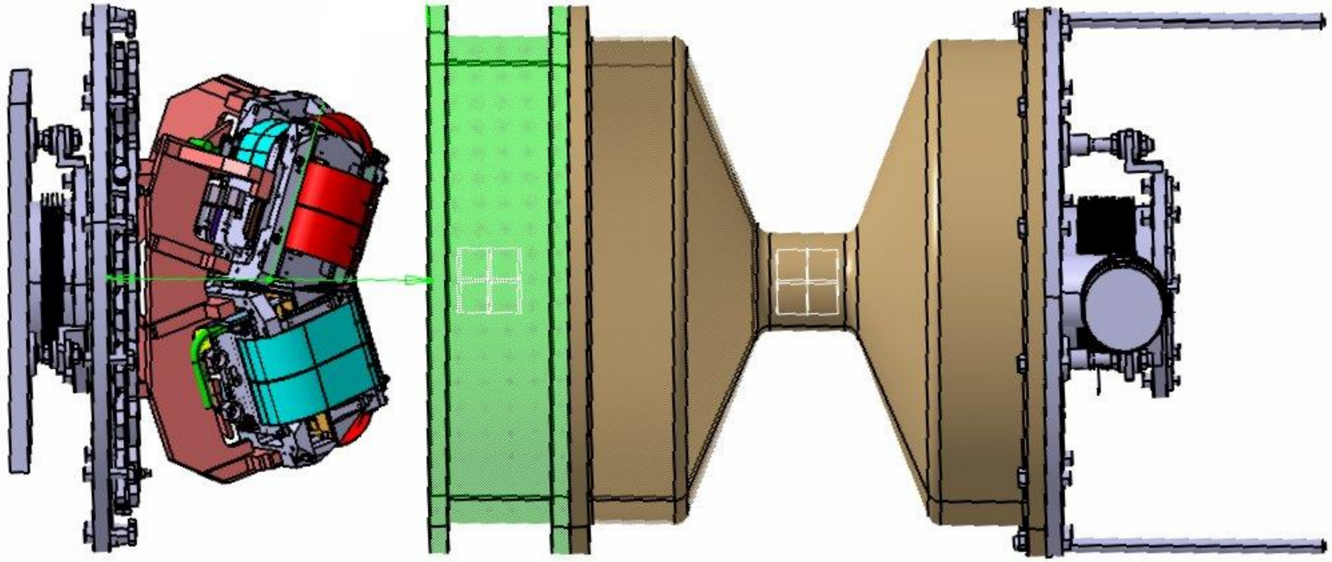

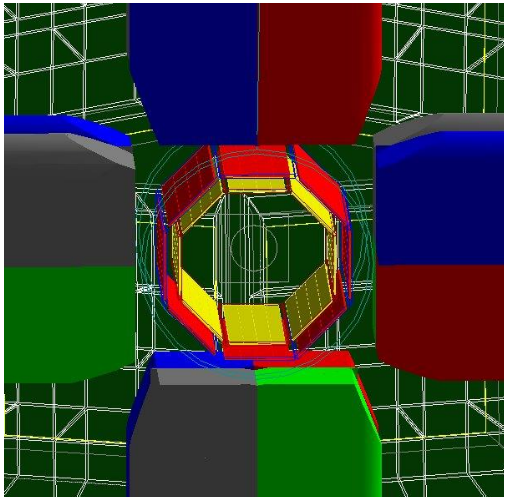

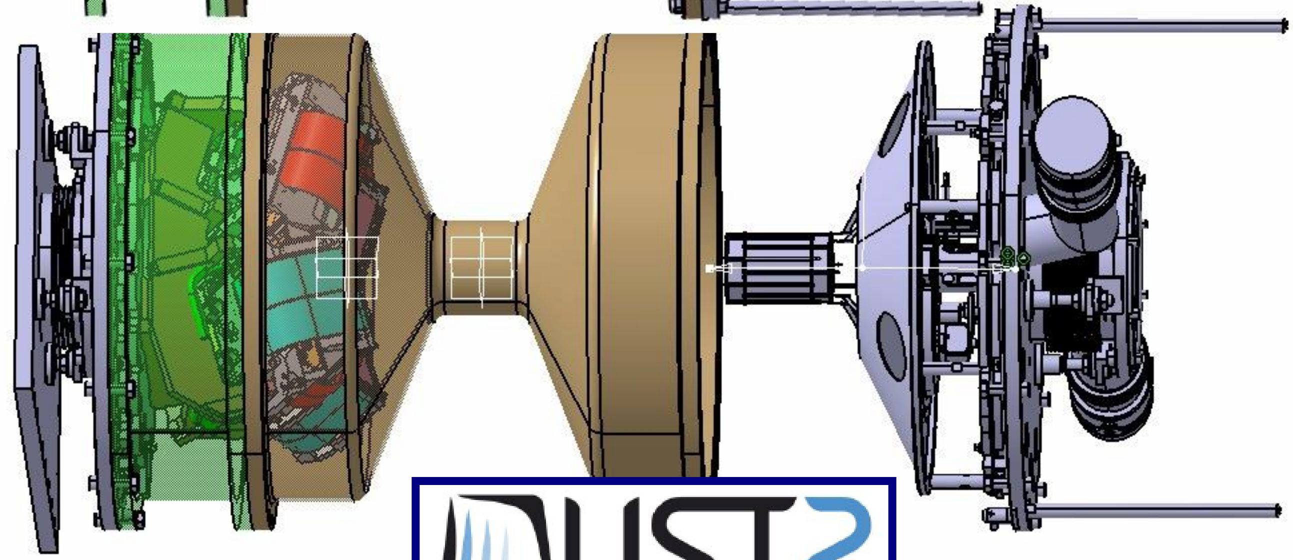

MUST2

TIARA

TIARA SETUP

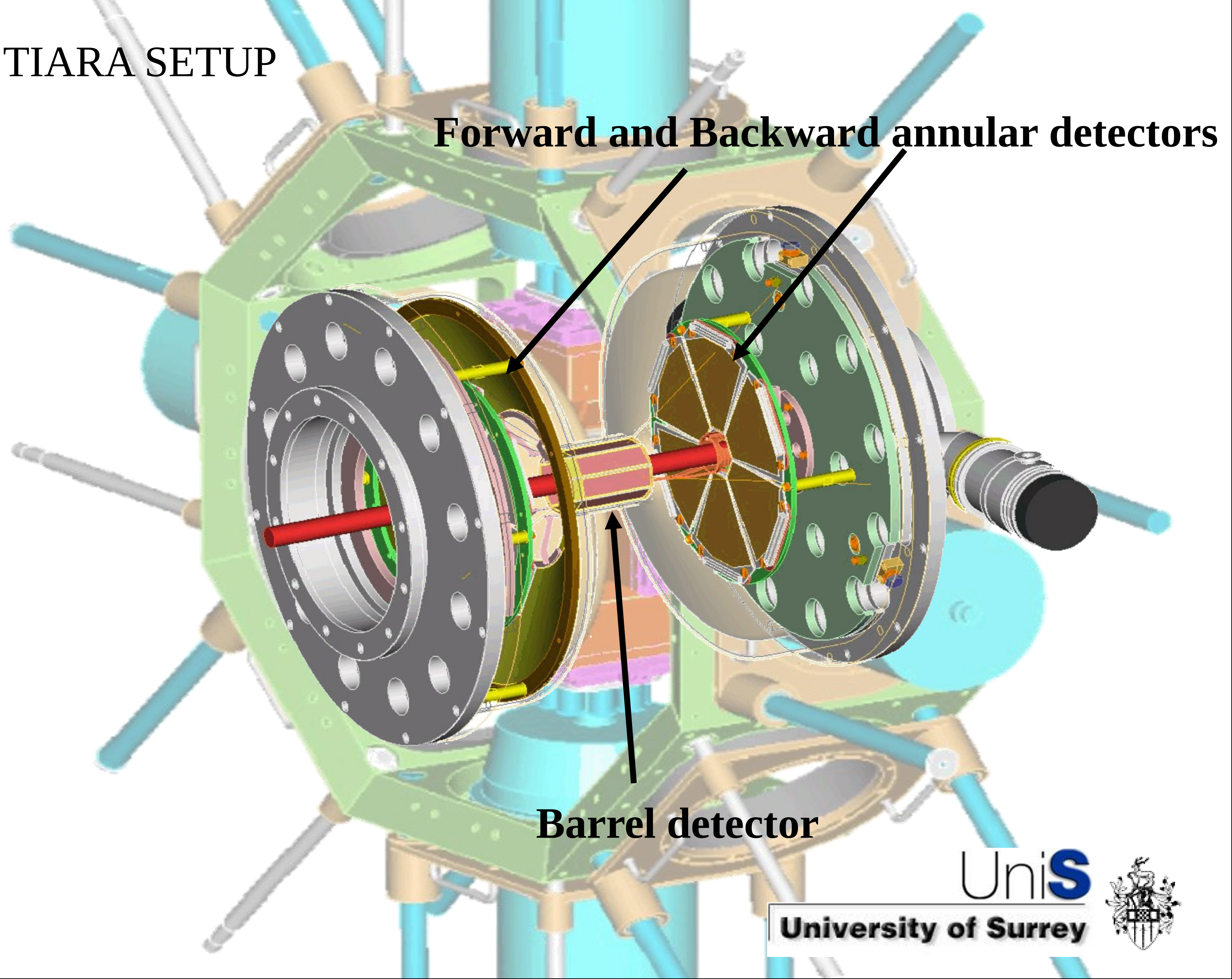

Forward and Backward annular detectors
Barrel detector
UniS
University of Surrey

NOVEL SOLENOID FOR 4π DETECTION to DECOMPRESS KINEMATICS

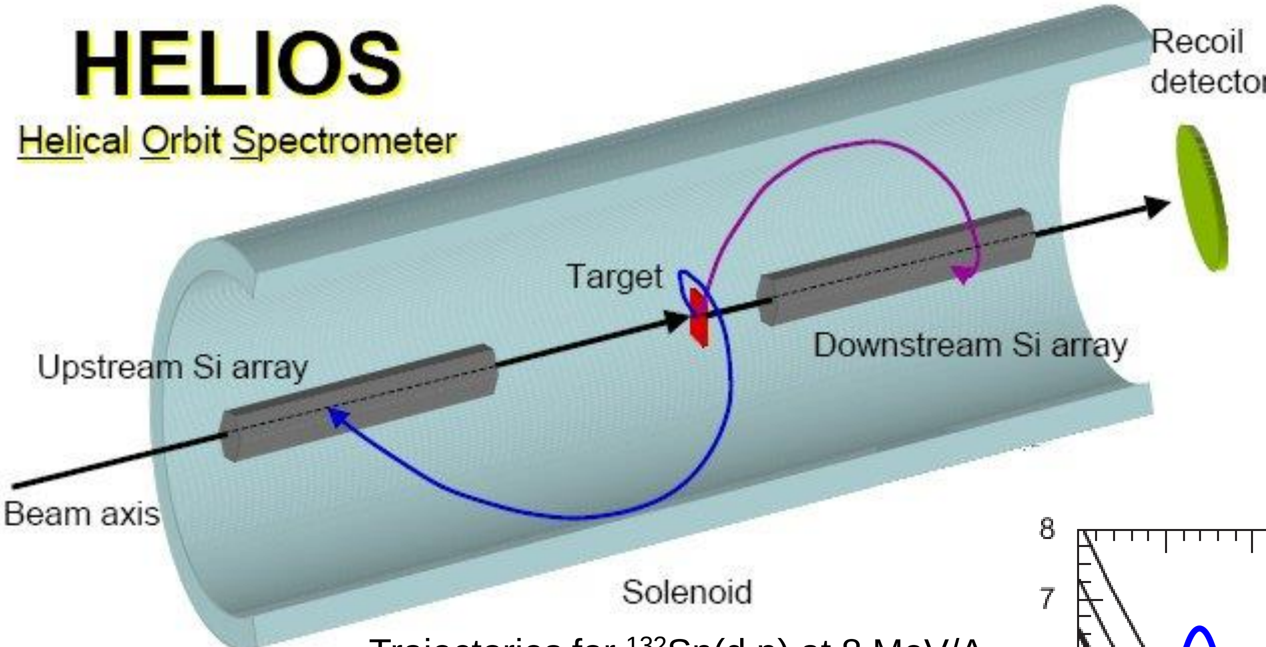

Actual solenoid – from MRI

Trajectories for $^{132}Sn(d,p)$ at 8 MeV/A
HELIOS: Wuosmaa, Schiffer et al.

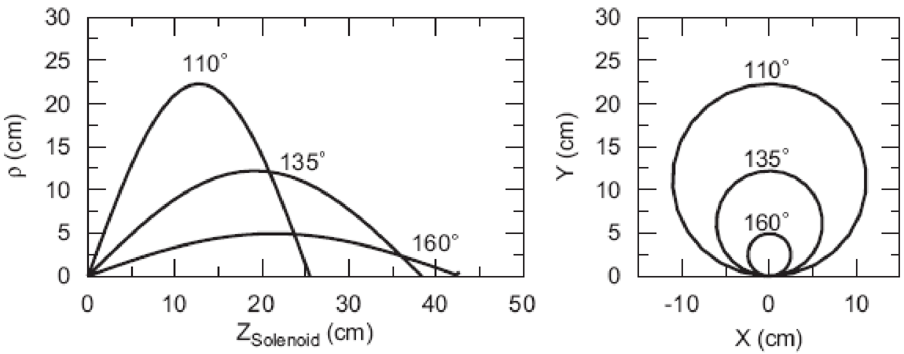

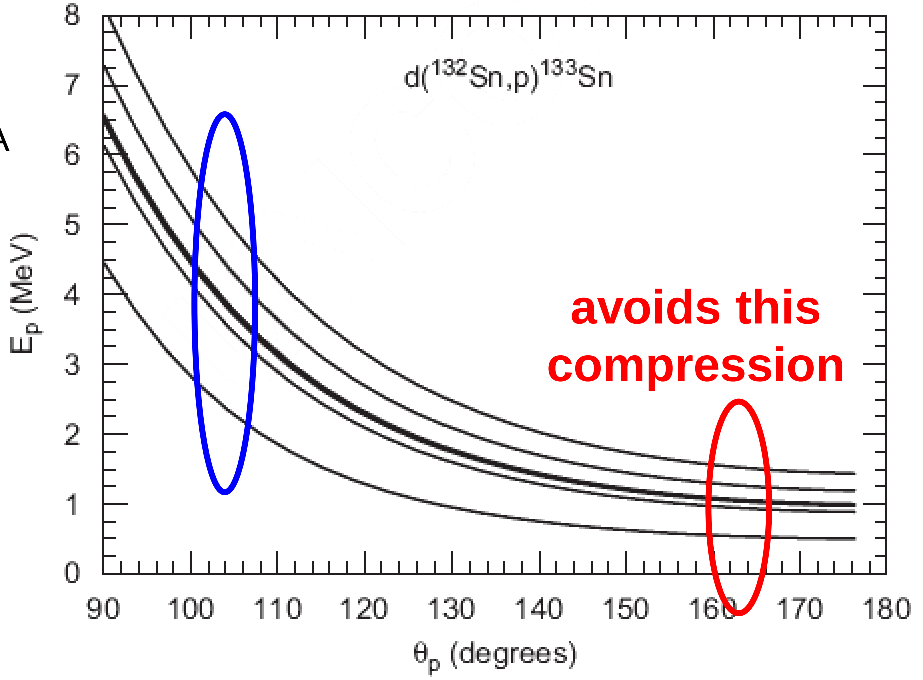

FROZEN TARGETS and not detecting the LIGHT PARTICLE

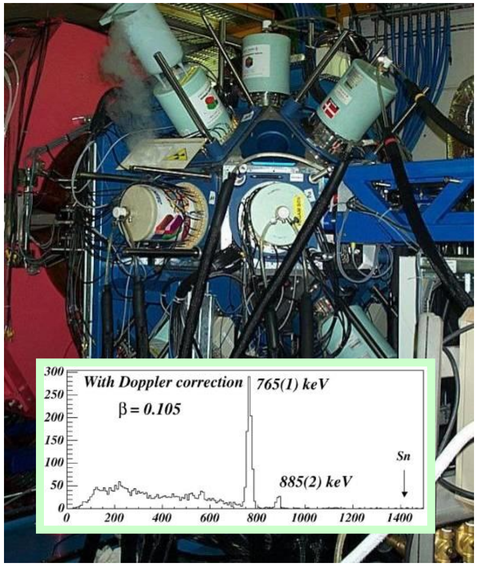

A. Obertelli *et al.*, Phys. Lett. **B633**, 33 (2006).

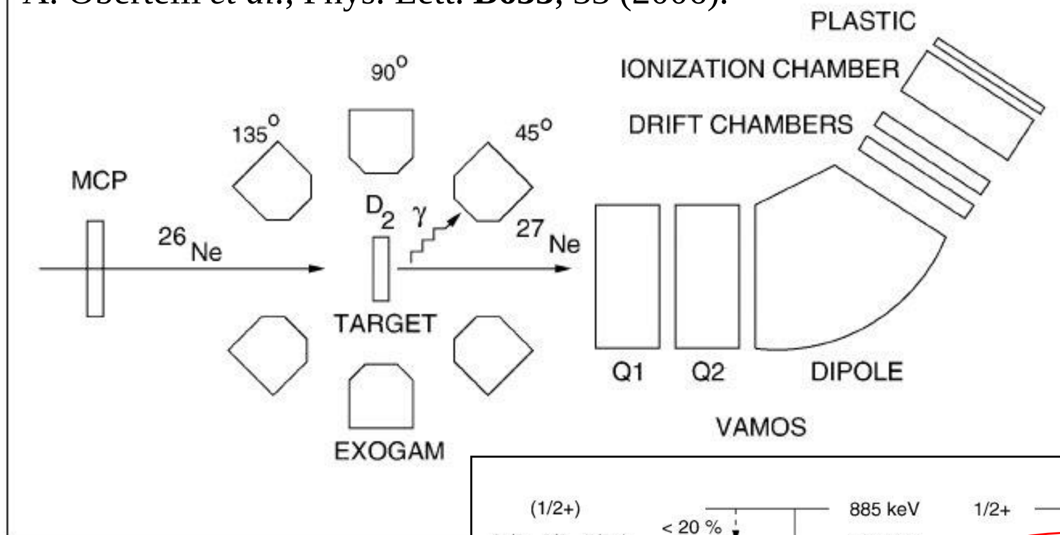

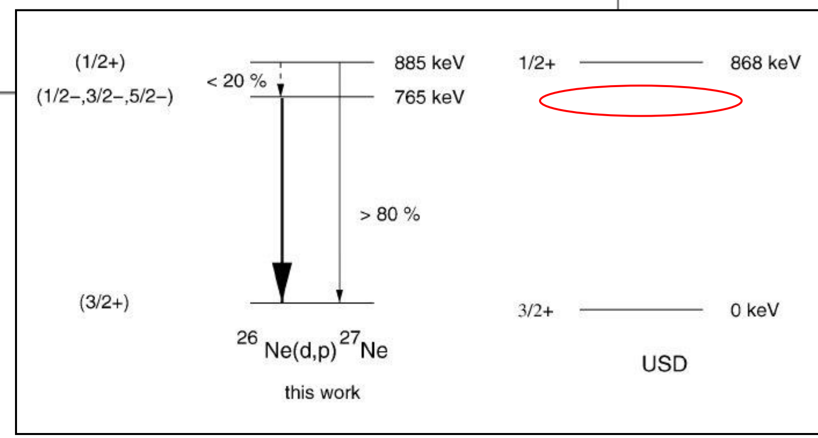

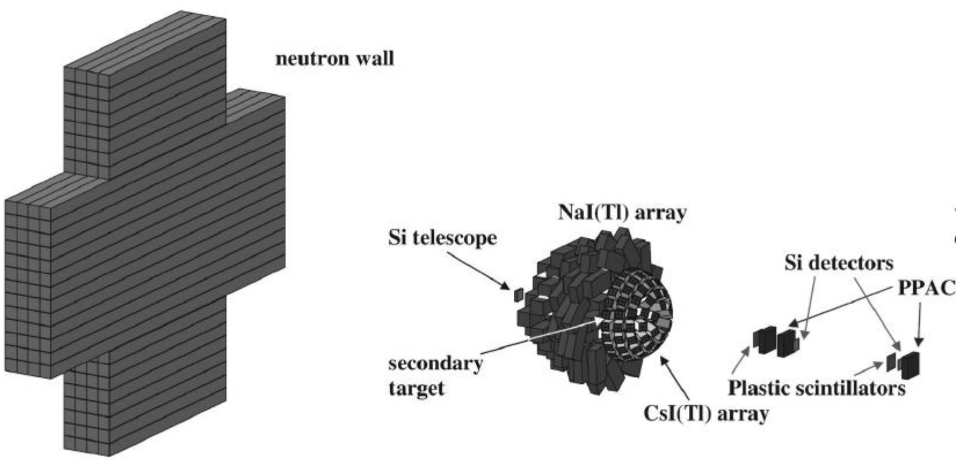

Also:

Elekes et al PRL 98 (2007) 102502

$^{22}O(d,p)$ to n-unbound ^{23}O SP states

And helium:

Especially $(\alpha,{}^{3}He)$ etc. at RIKEN

Experimental approaches largely depend on the beam intensity and resolution:

Below 10^4 pps MAYA, ACTAR…

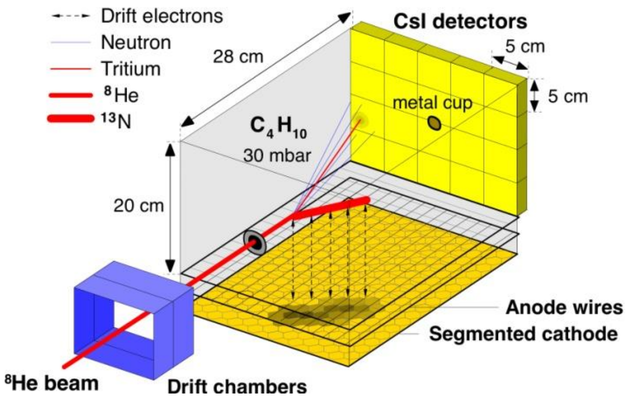

Below 10^6 pps SHARC, T-REX…

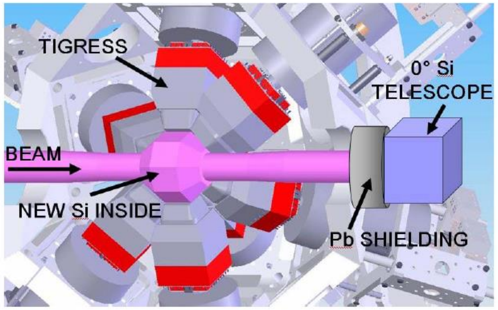

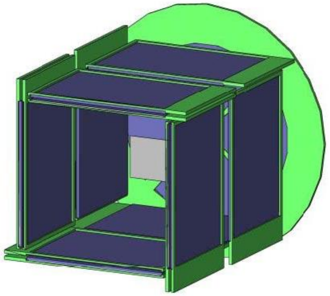

Up to 10^9 pps TIARA or alternatively…

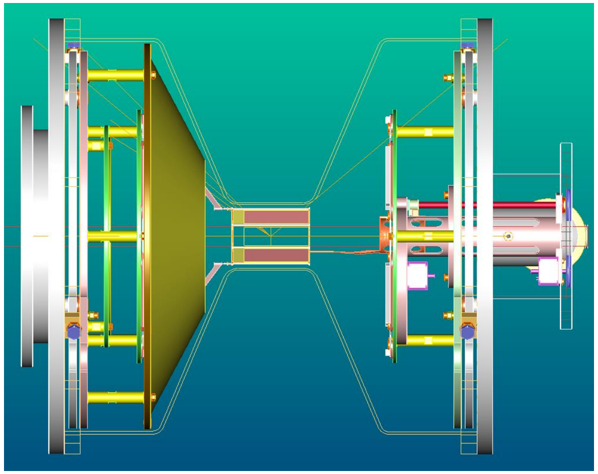

A solenoid device…

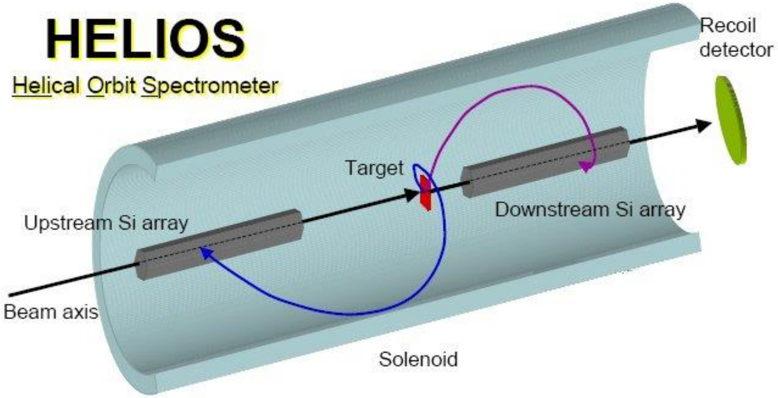

OUR EXPERIMENT TO STUDY $^{25}Ne\ d_{3/2}$

$^{24}Ne(d,p\gamma)$ N=16 replaces broken N=20

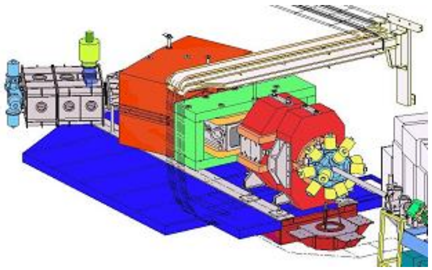

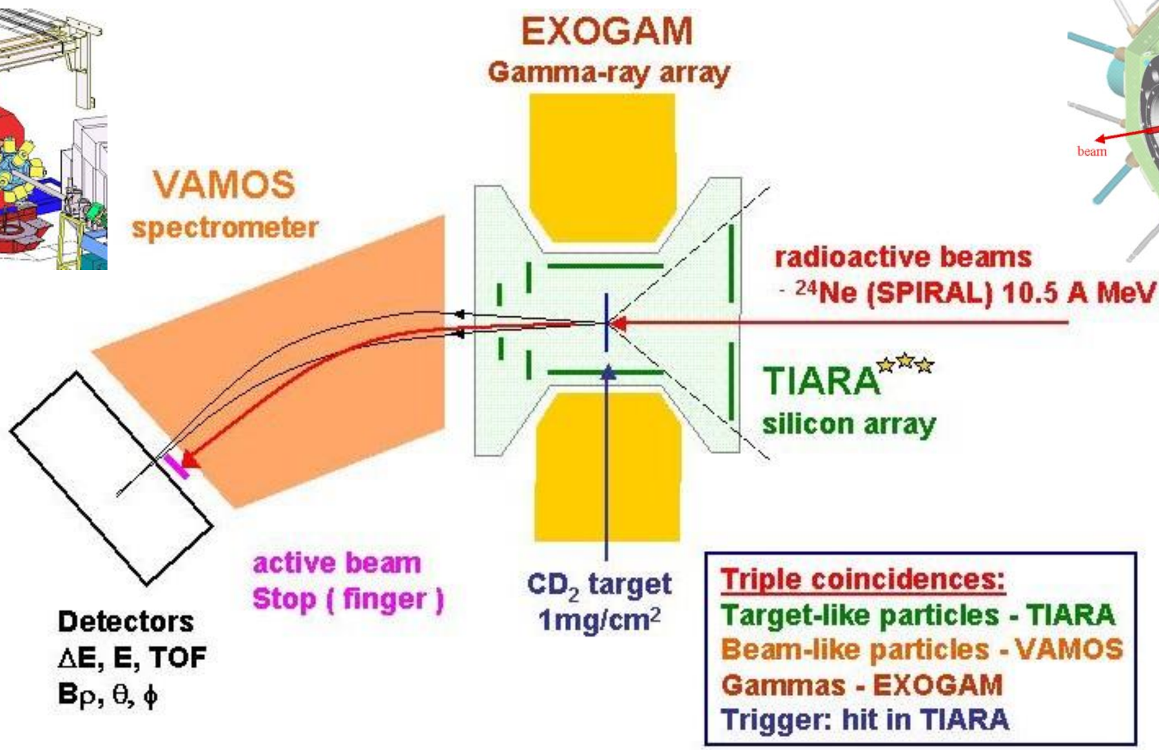

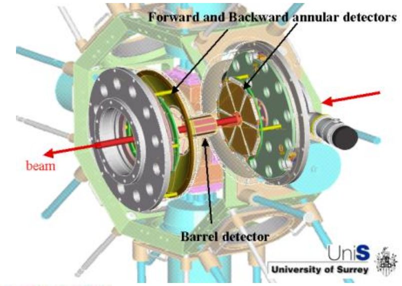

Schematic of the TIARA setup. A beam of 10^5 pps of ^{24}Ne at 10.5A MeV was provided from SPIRAL, limited to 8π mm.mrad to give a beam spot size of 1.5-2.0 mm. The target was 1.0 mg/cm² of $(CD_2)_n$ plastic. The TIARA array covered 90% of 4π with active silicon.

W.N. Catford *et al.*, Eur. Phys. J. **A25**, Suppl. 1, 245 (2005).

GANIL

GRAND ACCELERATEUR NATIONAL D'IONS LOURDS

LABORATOIRE COMMUN DSM/CEA-IN2P3/CNRS

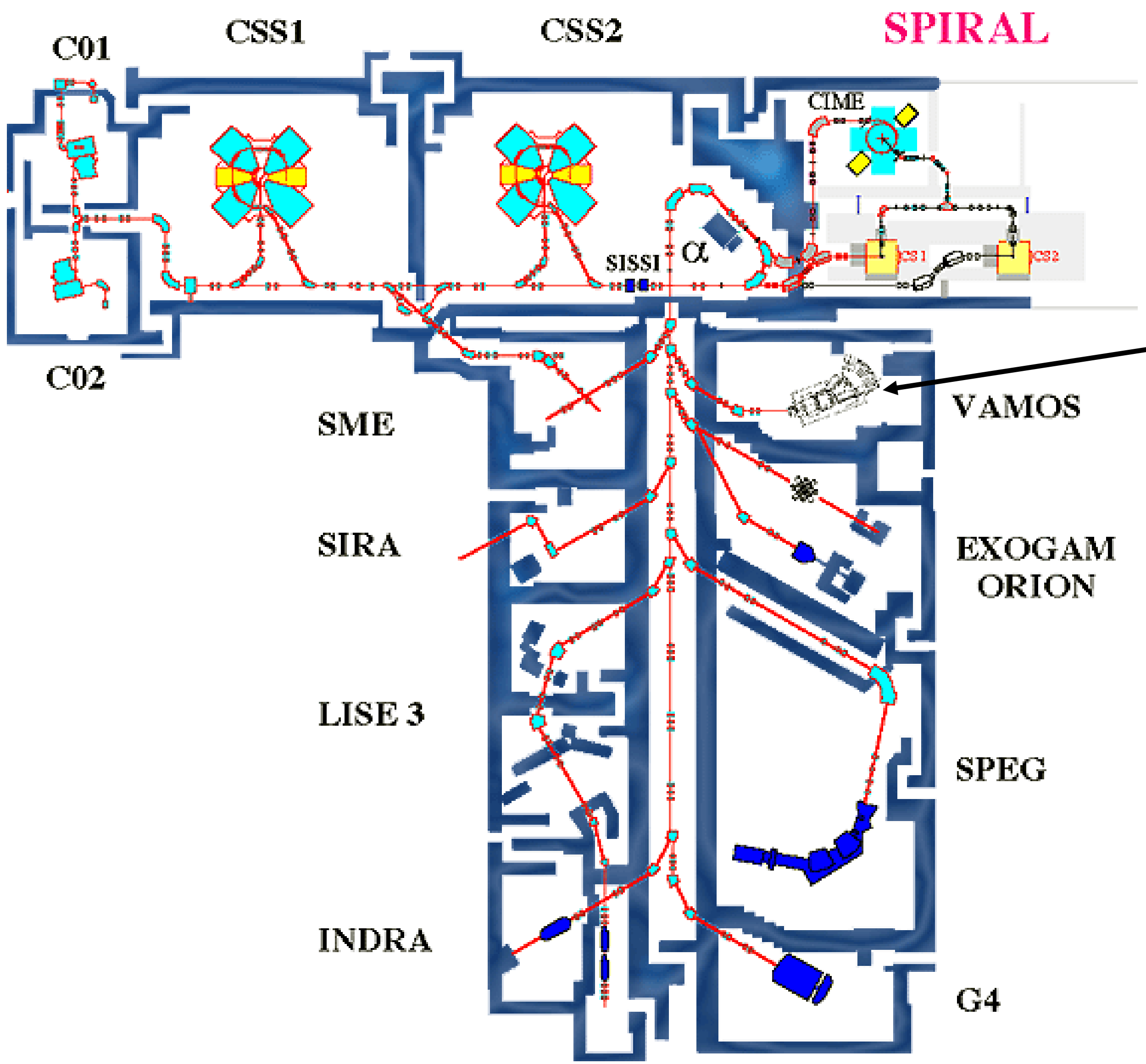

TIARA

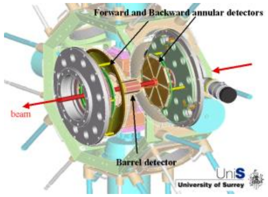

$^{24}Ne + d \rightarrow {}^{25}Ne + p$

$\tau = 3.38$ min

100,000 pps

EXOGAM + TIARA

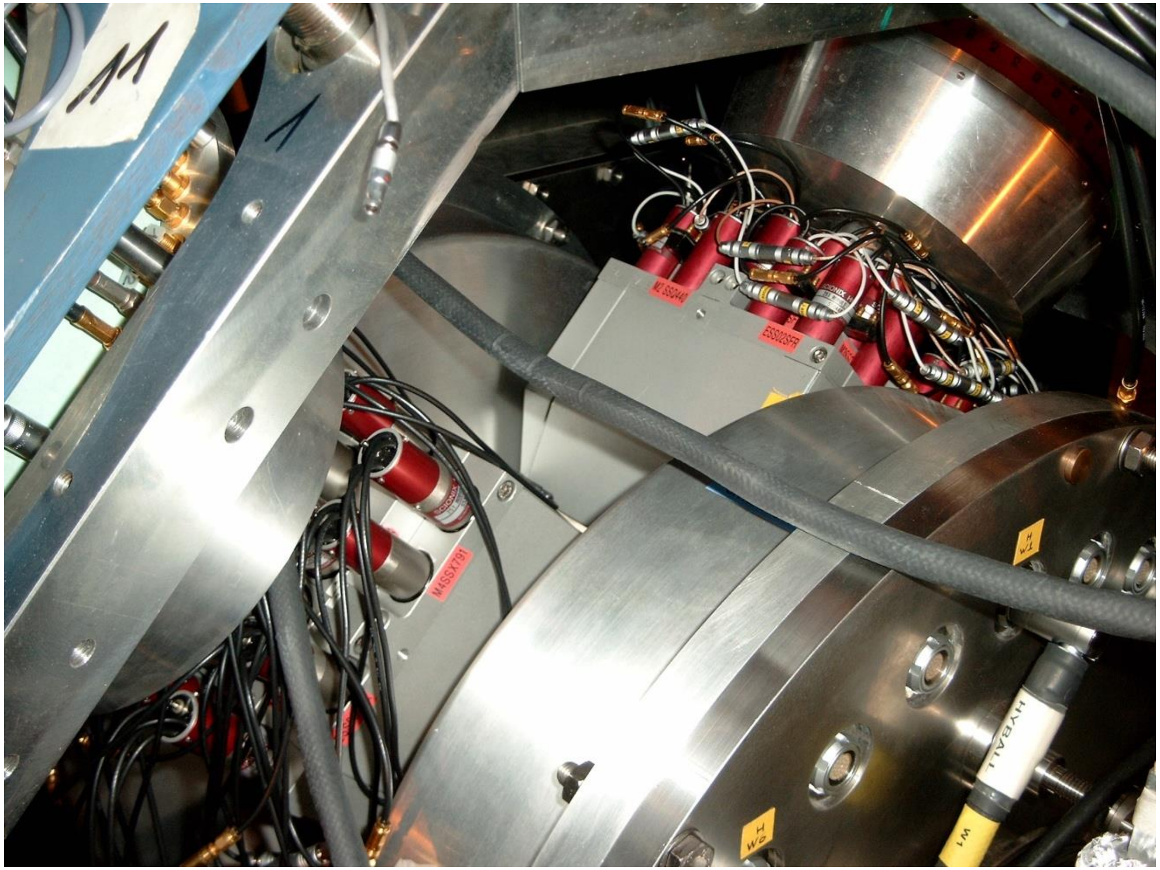

TIARA

Geant simulation: first interaction point for E(gamma) = 2.05 MeV

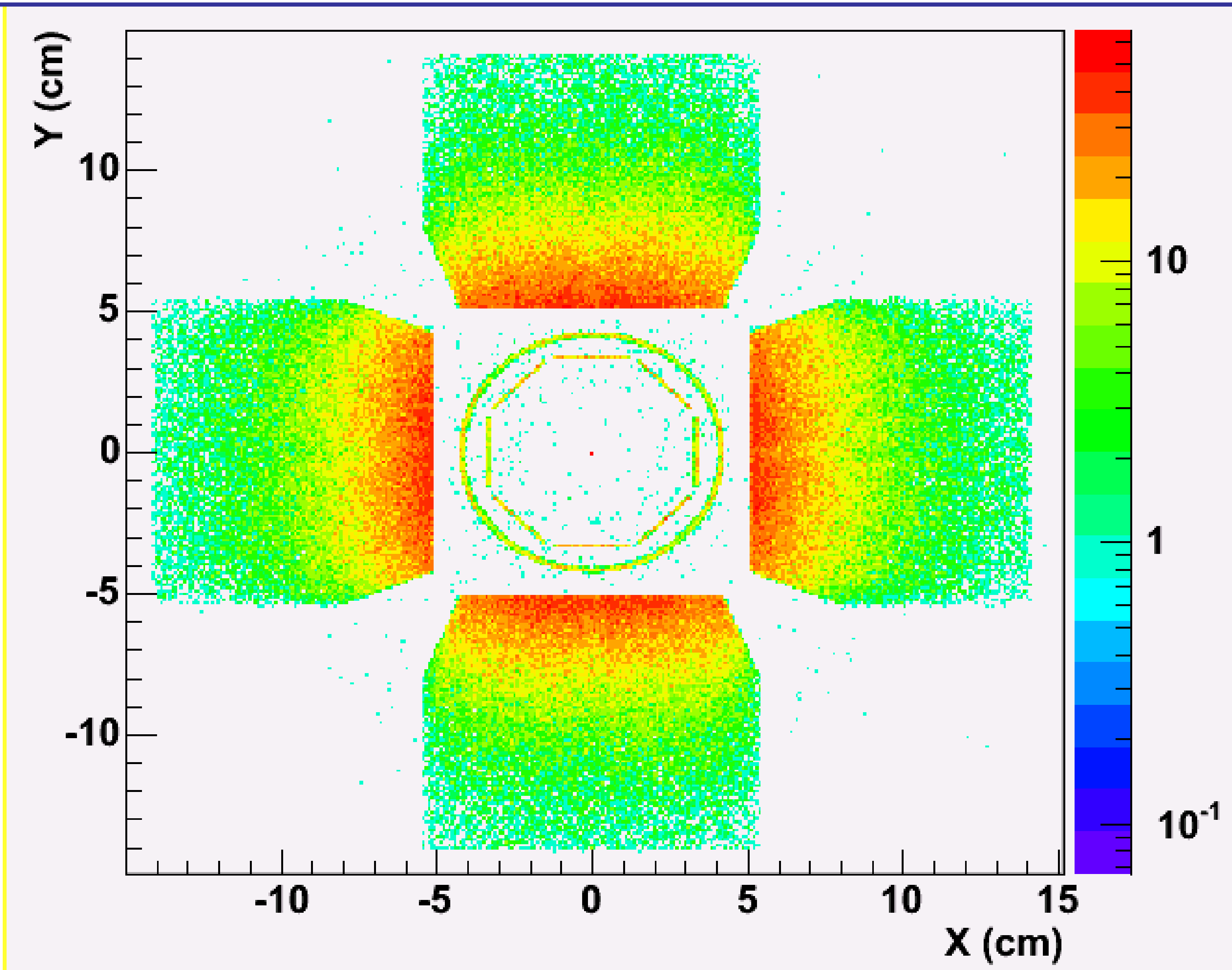

Results from the experiment to study ^{25}Ne

GAMMA RAY ENERGY SPECTRA

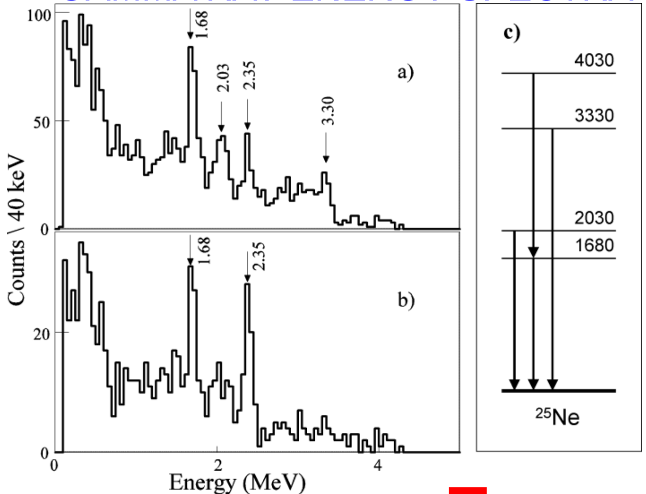

FIX E_x

EXCITATION E_x FROM PROTONS

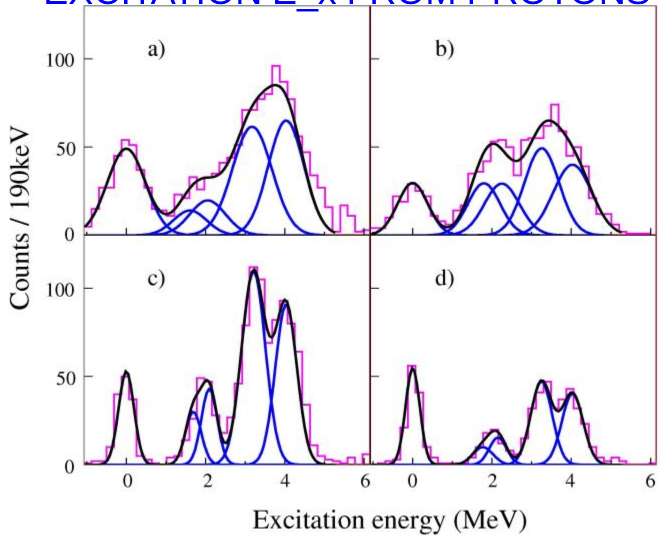

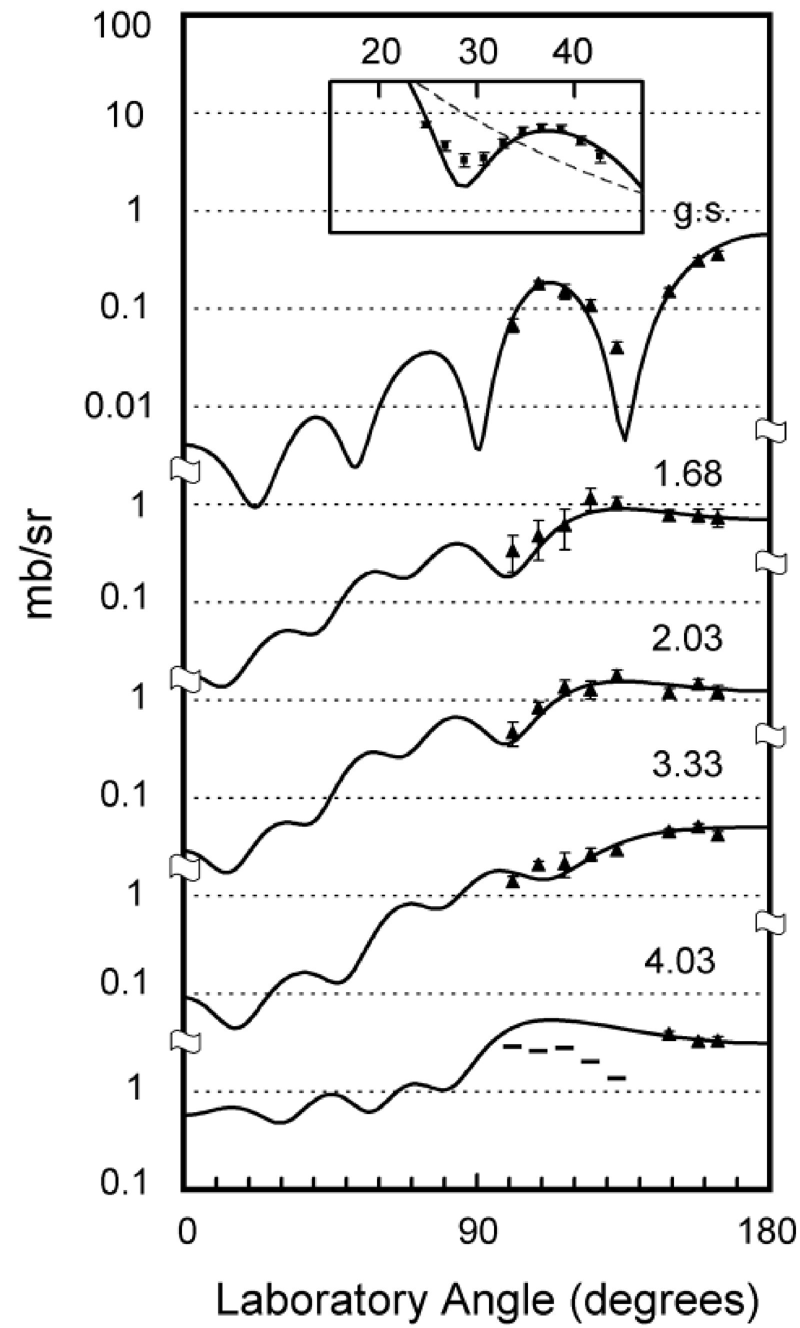

SOME RESULTS and PERSPECTIVES

In ^{25}Ne the $3/2^+$ state was far from a pure SP state due to other couplings at higher energies, but it was clear enough in its ID and could be used to compare with its SM partner to improve the USD interaction

It is not always necessary to map the full SP strength which may be very much split
and
with radioactive beams it may not often be possible

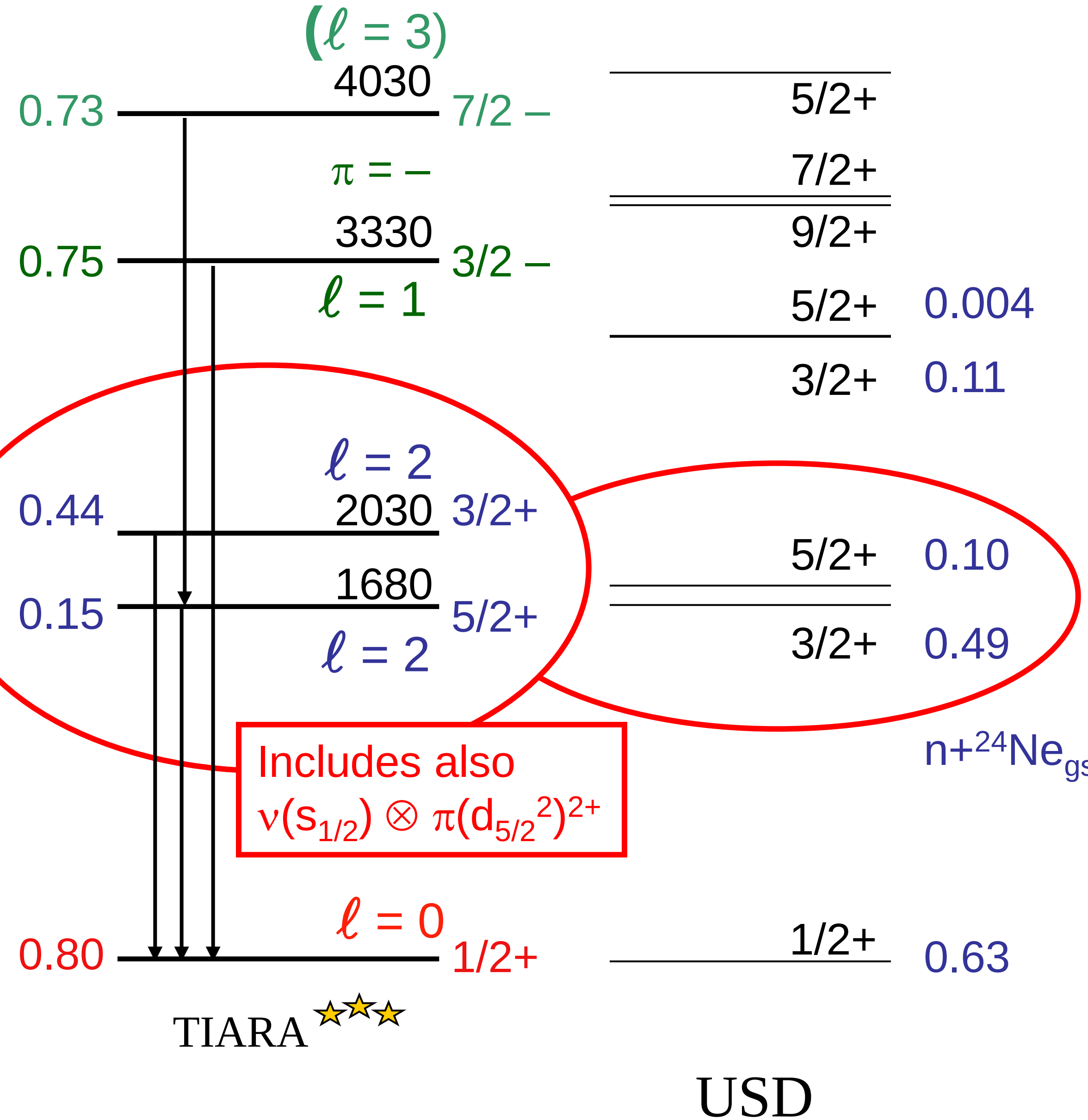

WILTON CATFORD JUNE 2008

E. SOME RESULTS and PERSPECTIVES

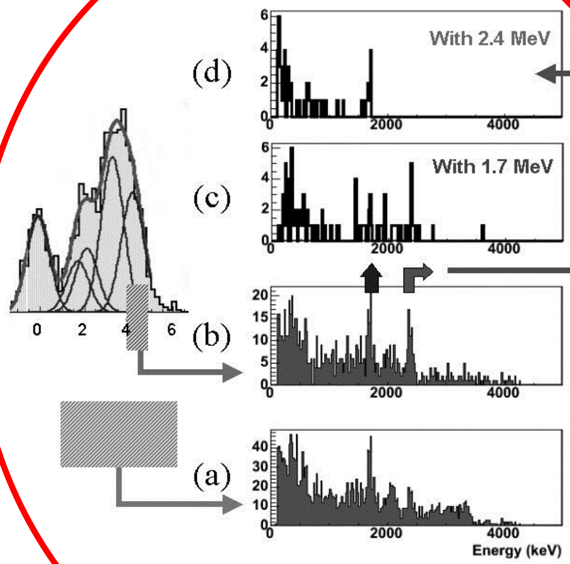

In ^{25}Ne we used gamma-gamma coincidences to distinguish spins and go beyond orbital AM

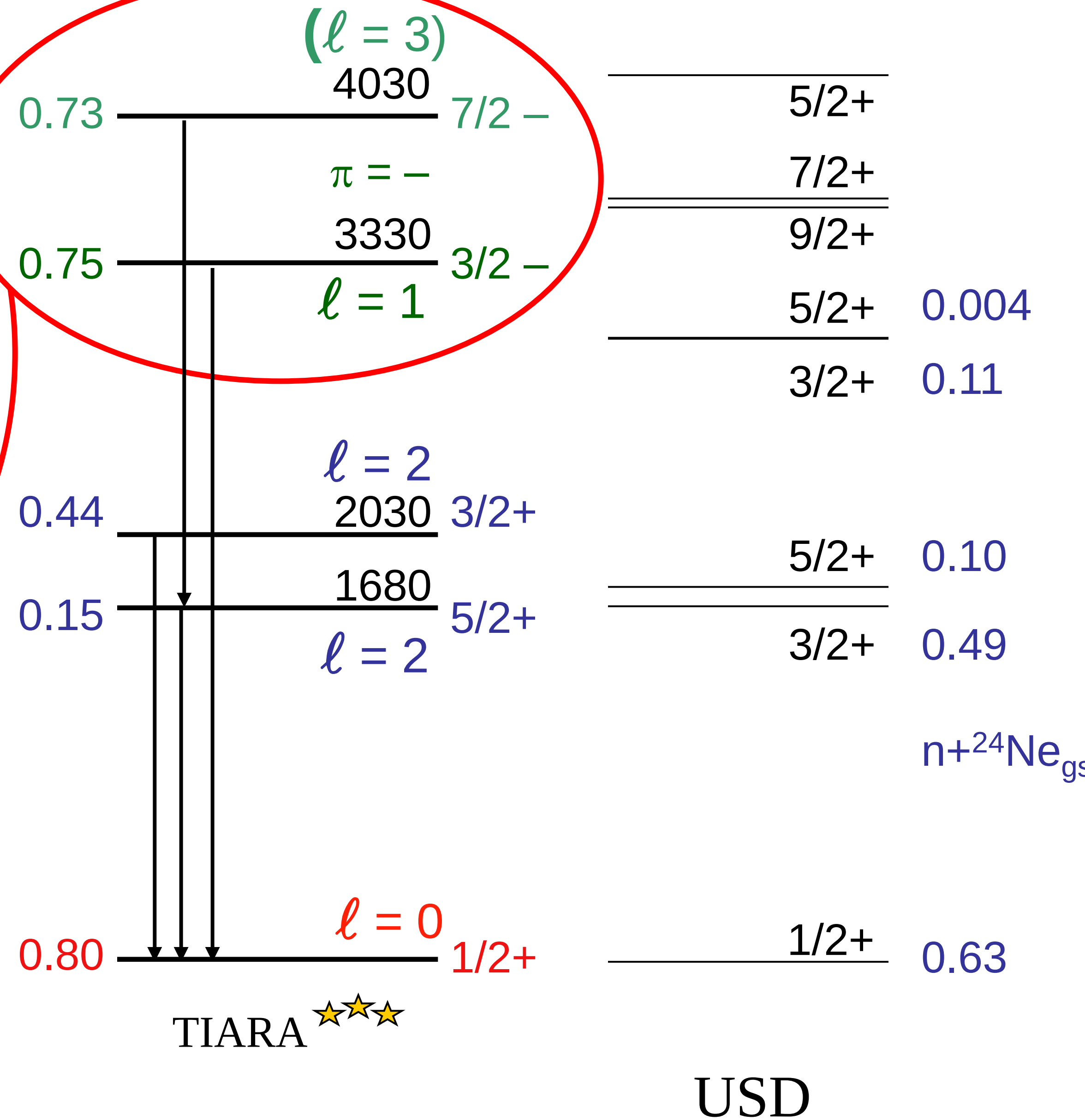

WILTON CATFORD JUNE 2008

Summary of 25Ne Measurements

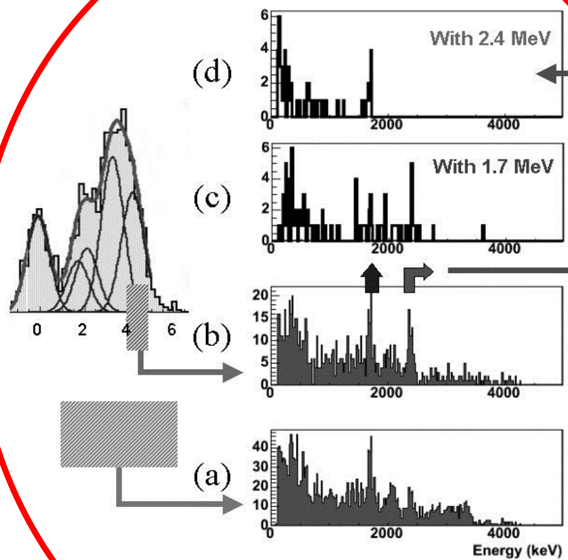

Negative parity states (cross shell) also identified

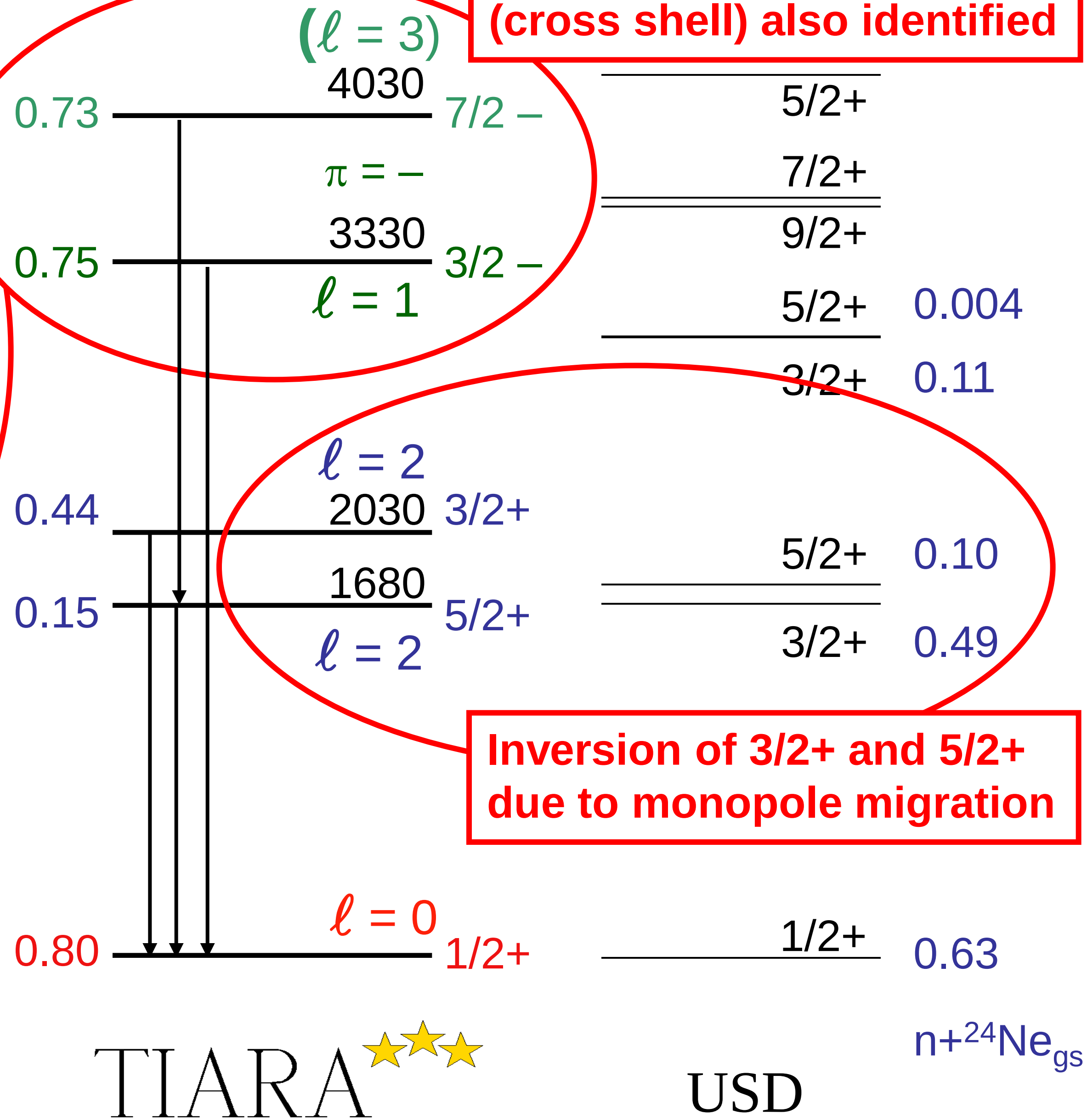

Inversion of 3/2+ and 5/2+ due to monopole migration

In ^{25}Ne we used gamma-gamma coincidences to **distinguish spins** and go beyond orbital AM
FIRST QUADRUPLE COINCIDENCE (p-HI-γ-γ) RIB TRANSFER DATA

Physics outcomes for ^{25}Ne study:

COZMIN TIMIS and WNC, SURREY

Identified lowest lying 3/2+ and 5/2+ excited states

Showed that 3/2+ is significantly raised due to monopole shift,
Supporting N=16 emerging as a shell gap

Identified lowest negative parity intruder states as 3/2– and 7/2–

Measured relative energy of negative parity intruder states,
Supporting N=20 disappearance as a shell gap, and also
Supporting N=28 disappearance as a shell gap

Provided quantitative input to measuring magnitude of monopole shift

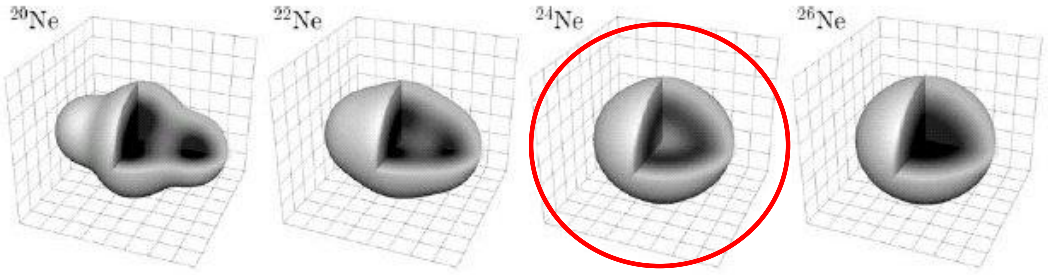

Fig. 12. Intrinsic single-particle density distribution $\rho(\mathbf{x})$ for different neon isotopes (cf. Fig. 11).

Roth, Neff et al., NPA 745 (2004) 3-33

We proceed from here by

- removing more protons from d5/2 – that is, looking at oxygen, namely ^{21}O

… there are important anomalies to resolve, regarding the ν(d3/2) energy

- also looking at the more exotic neon isotopes – namely ^{27}Ne, N=17

Oxygen 23 by (d,p) at 600 pps

PRL **98**, 102502 (2007) PHYSICAL REV

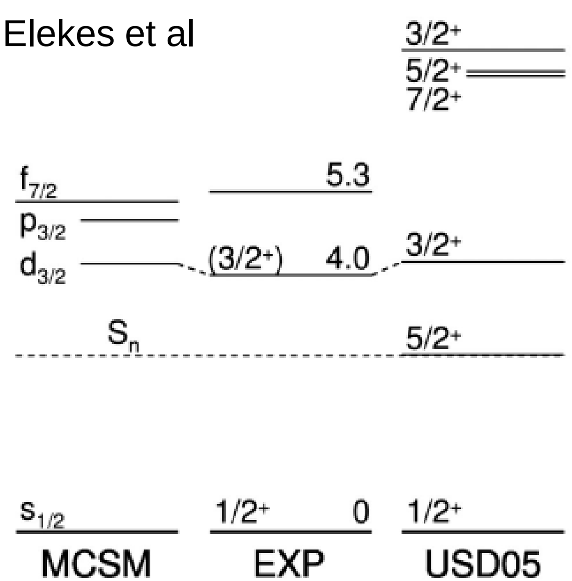

FIG. 4. Excited states of ^{23}O observed in the present experiment in comparison with the shell model calculation using the USD05 [11,12] interaction and the effective single particle energies taken from the Monte Carlo shell model (MCSM) calculation based on the SDPF-M interaction [15].

Oxygen 25 by ^{26}F – p at 20 pps

PRL **100**, 152502 (2008)

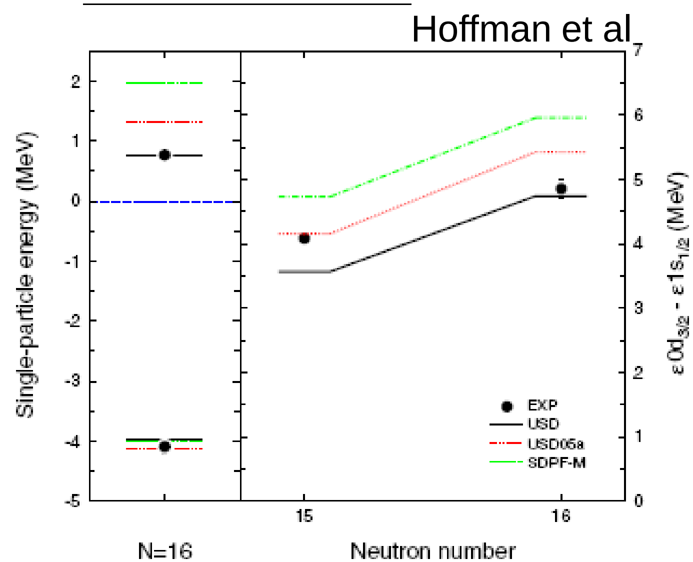

FIG. 3 (color online). The experimental (data points) and theoretical [13–15] (lines) single-particle energies (SPE) for the $\nu 1s_{1/2}$ and $\nu 0d_{3/2}$ orbitals at $N = 16$ are shown on the left. The difference between these SPEs is shown for $Z = 8$, $N = 15$ [12] and 16, giving the $N = 16$ shell gap size. Errors are shown if they are larger than the symbol size.

TIARA + MUST2 experiments at SPIRAL/GANIL:

Beam of ^{20}O at 10^5 pps and 10 MeV/A
(stripping at target to remove $^{15}N^{3+}$ with A/q = 5)
(This experiment not discussed, in these lectures).

Beam of ^{26}Ne at 10^3 pps (pure) and 10 MeV/A

The (d,p) could be studied to both BOUND and UNBOUND states

Gamma-ray coincidences were recorded for bound excited states

With MUST2 we could measure (d.t) at forward angles with good PID

The 16% of ^1H in the ^2H target allowed (p,d) measurements also

BEA FERNANDEZ DOMINGUEZ, LIVERPOOL (GANIL)
JEFFRY THOMAS, SURREY
SIMON BROWN, SURREY
ALEXIS REMUS, IPN ORSAY

TIARA+MUST2+VAMOS+EXOGAM @ SPIRAL/GANIL

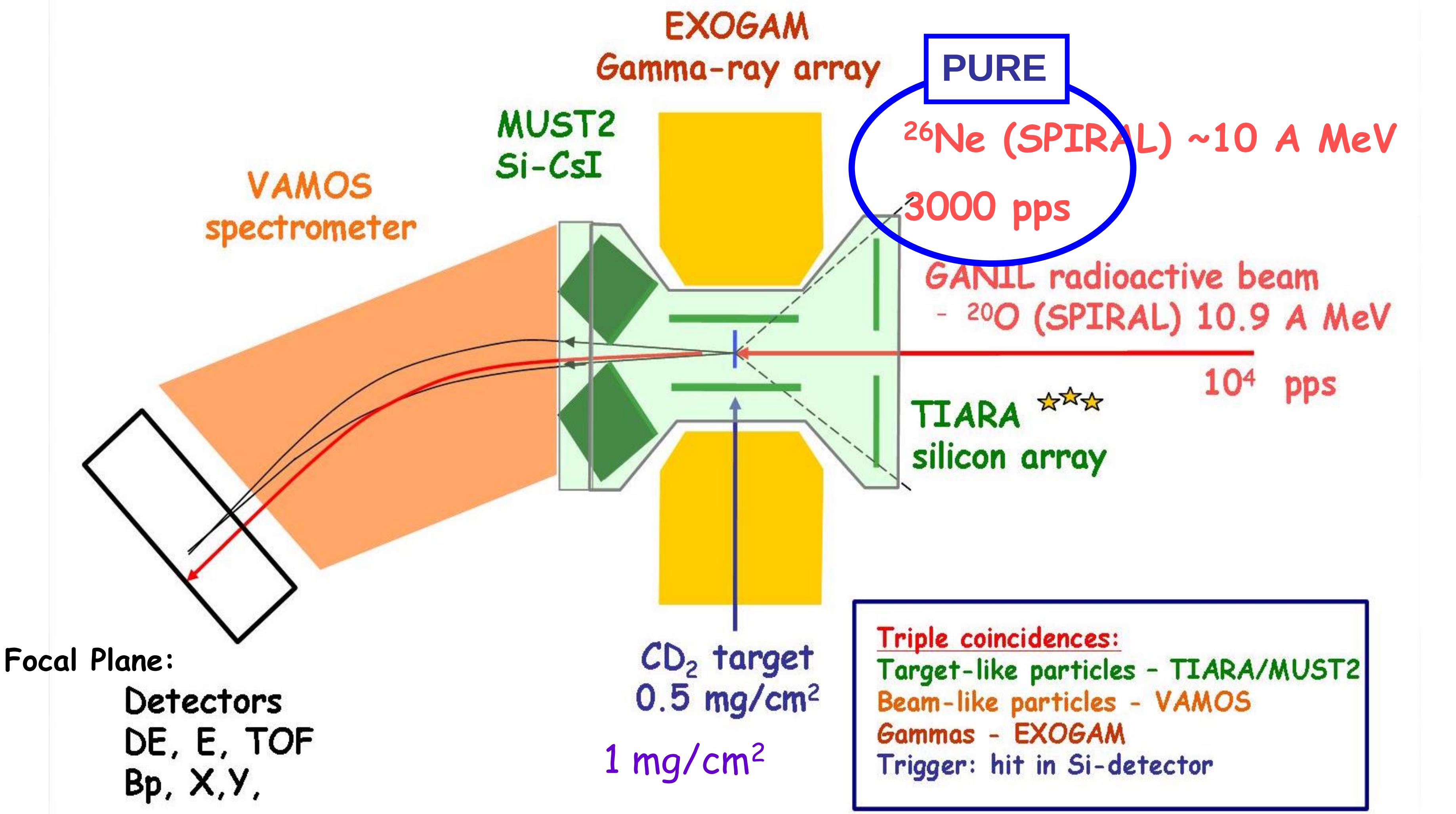

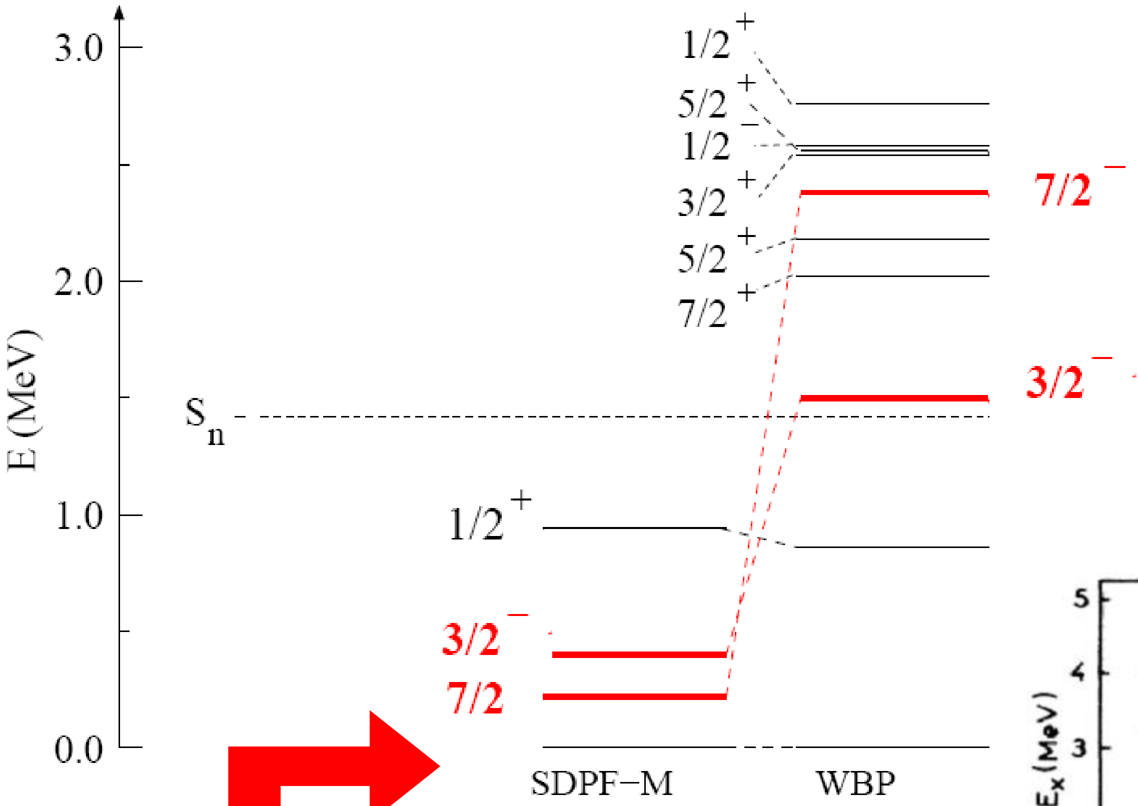

N=17 ISOTONES

Shell model predictions **vary wildly** for fp intruders

Systematics show region of **dramatic change**

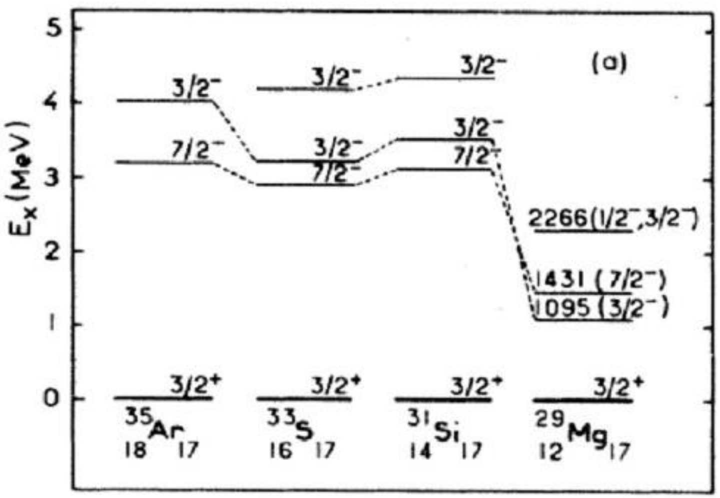

P. Baumann *et al.*, Phys. Rev. C36, 765 (1987).

^{27}Ne Predictions

7/2⁻ **never seen**
3/2⁻ known

^{27}Ne IS THE NEXT ISOTONE

^{27}Ne BOUND STATES

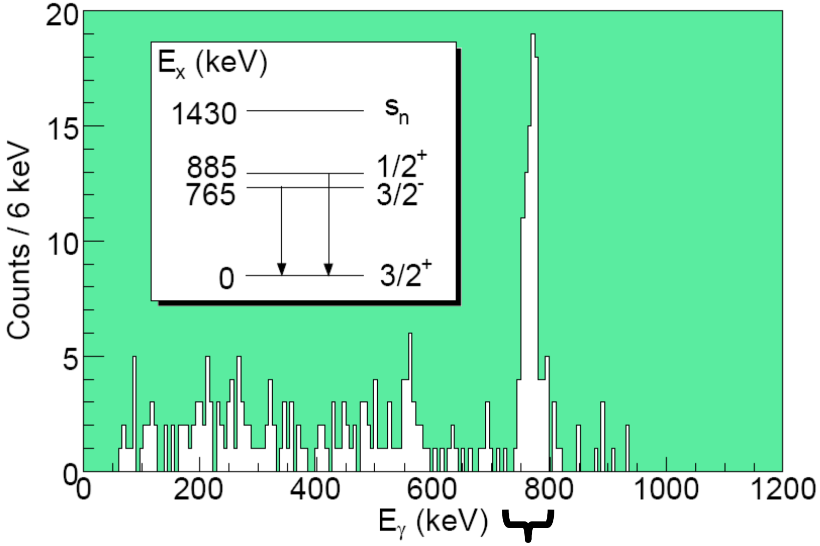

The target was 1 mg/cm^2 CD_2
(thick, to compensate for 2500 pps)

Known bound states were selected by gating on the decay gamma-ray (and the ground state by subtraction)

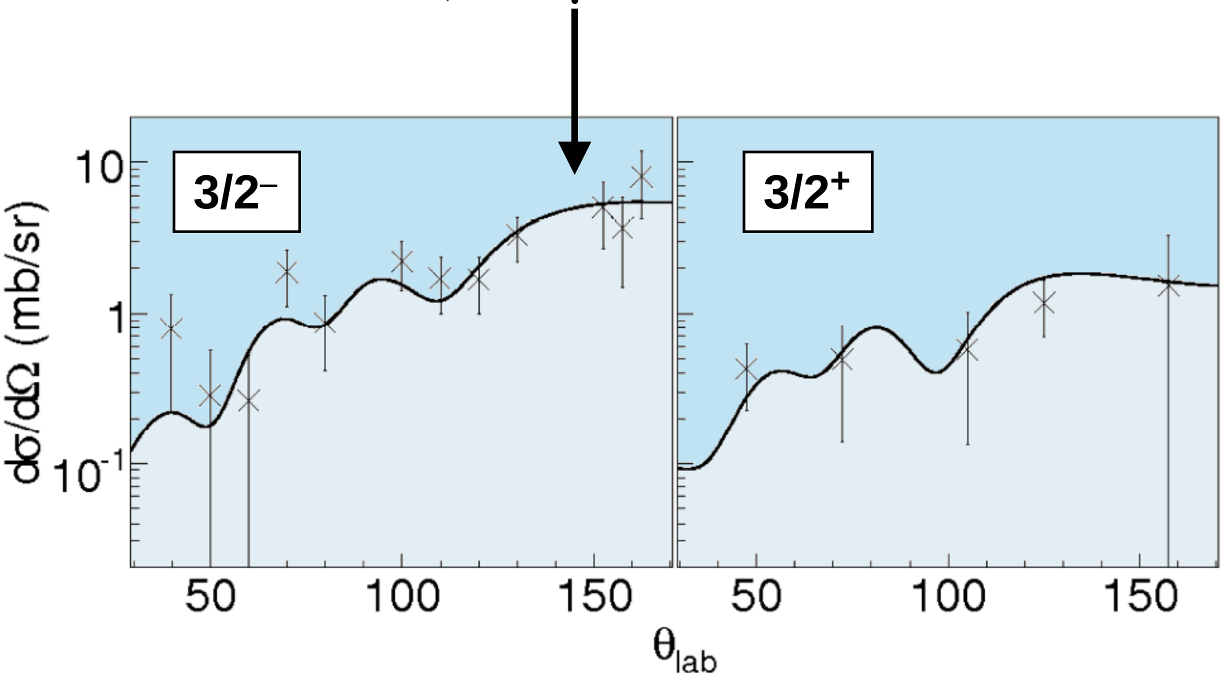

In these case, the spins were already known.

The magnitude was the quantity to be measured.

^{27}Ne UNBOUND STATES

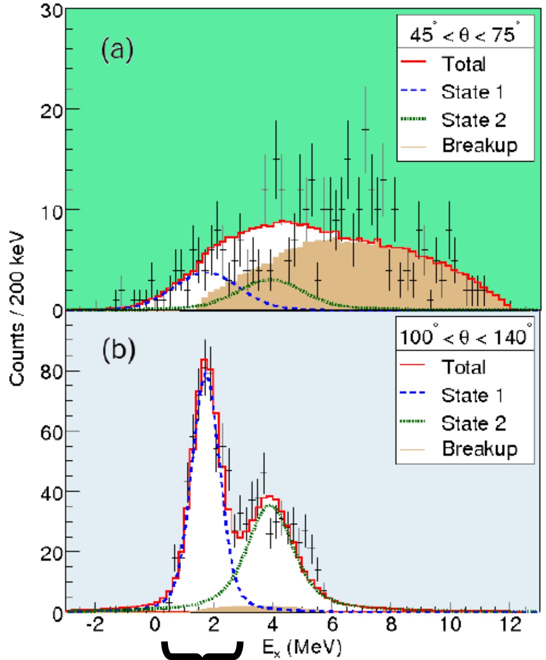

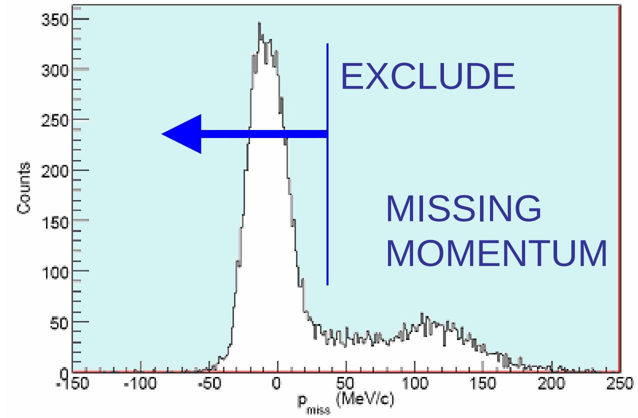

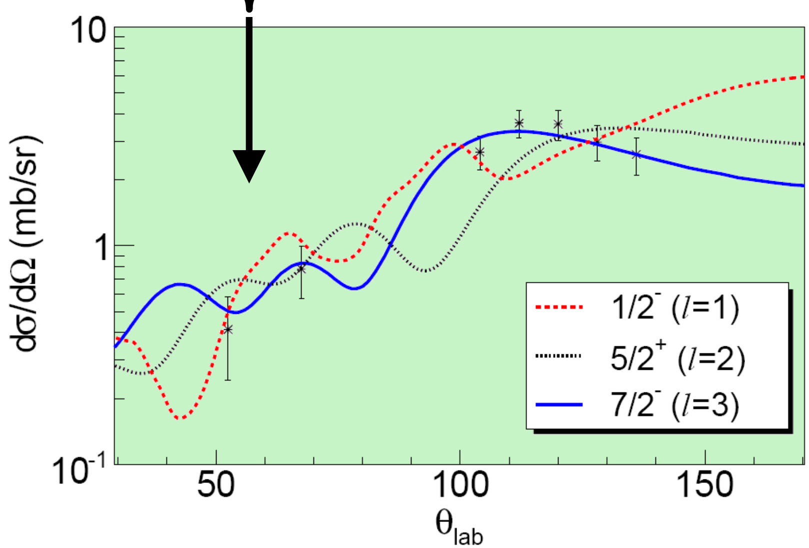

^{27}Ne results

- level with main $f_{7/2}$ strength is <u>unbound</u>
- excitation energy measured
- spectroscopic factor measured
- the $f_{7/2}$ and $p_{3/2}$ states are <u>inverted</u>
- this inversion also in ^{25}Ne experiment
- the natural width is just 3.5 ± 1.0 keV

^{27}Ne results

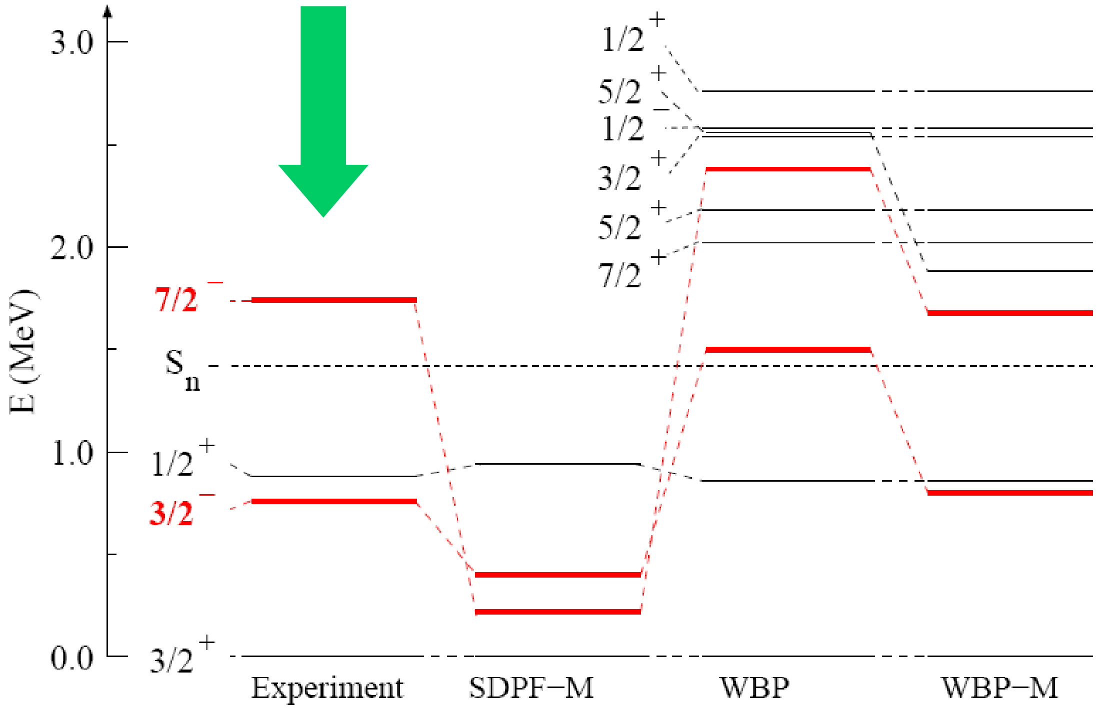

J^{π}	E^{*}_{exp} (MeV)	E^{*}_{WBP-M} (MeV)	C^2S		
			Ref. [9]	Present	WBP-M
$3/2^+$	0	0	0.2(2)	0.42(22)	0.63
$3/2^-$	0.765	0.809	0.6(2)	0.64(33)	0.67
$1/2^+$	0.885	0.869	0.3(1)	0.17(14)	0.17
$7/2^-$	1.74	1.686	-	0.35(10)	0.40

- we have been able to reproduce the observed energies with a modified WBP interaction, full 1hw SM calculation
- the SFs agree well also
- most importantly, the new interaction works well for ^{29}Mg, ^{25}Ne also
- so we need to understand why an *ad hoc lowering* of the fp-shell by 0.7 MeV is required by the data!

N=17 ISOTONES

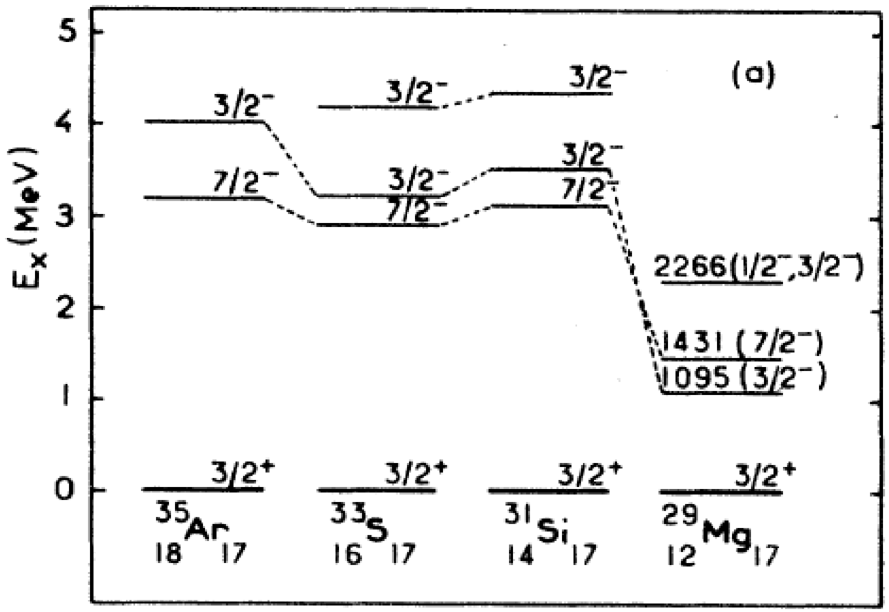

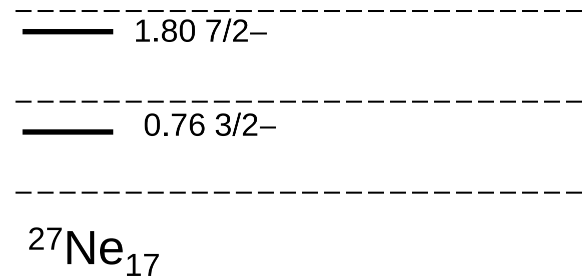

ISOTOPE CHAINS

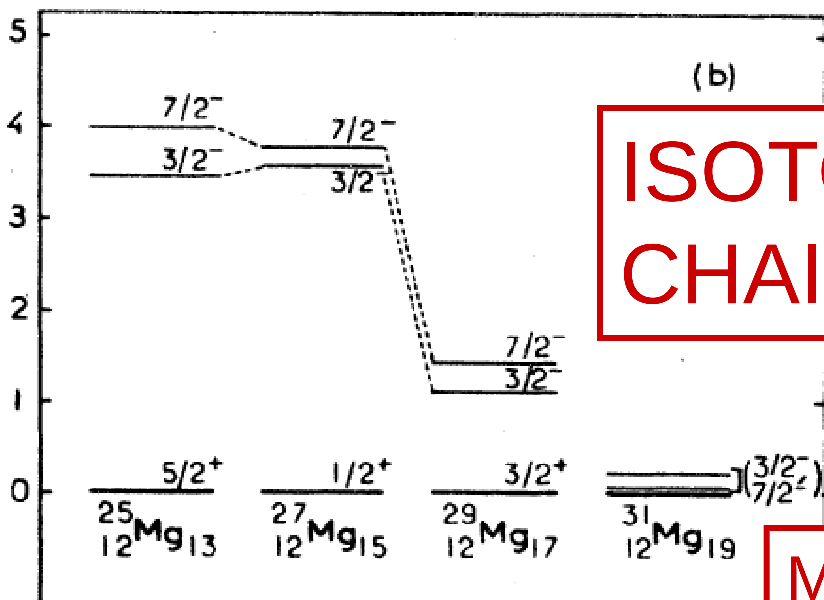

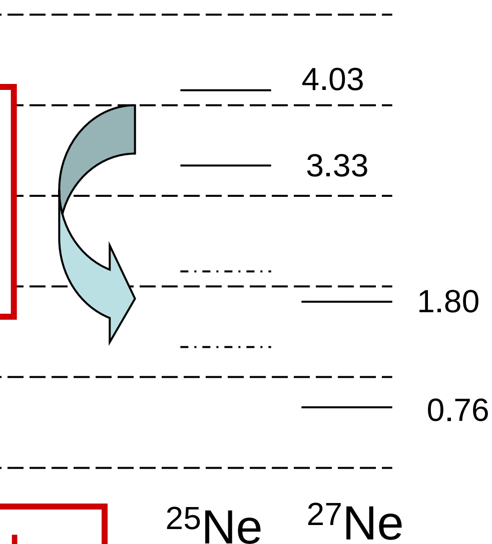

Mg

Ne

d3/2 level is 2.030 25Ne

Preliminary results for ^{26}Ne(d,t)^{25}Ne and also (p,d)

JEFFRY THOMAS, SURREY

^{26}Ne(d,t)^{25}Ne

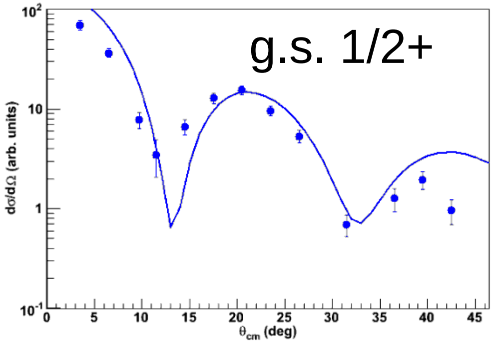

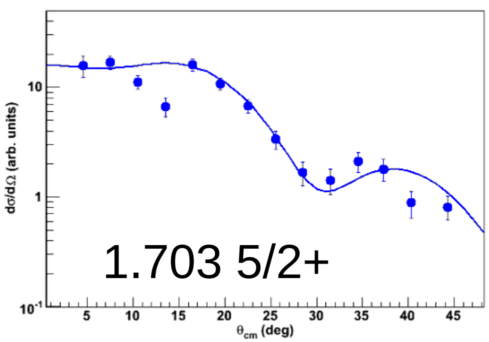

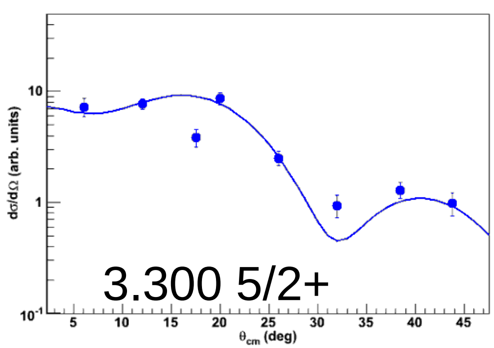

^{26}Ne(p,d)^{25}Ne

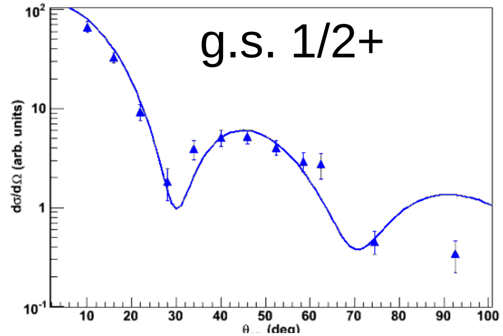

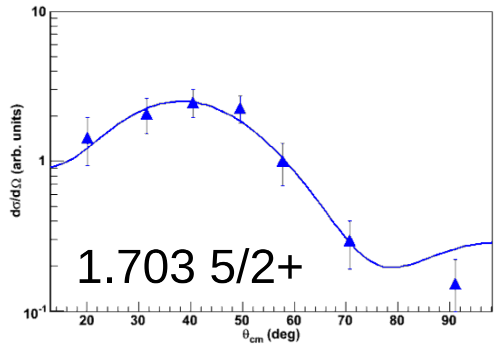

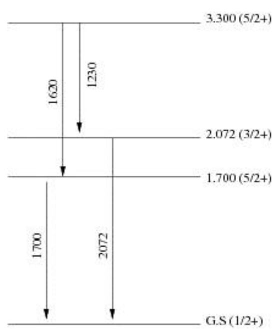

POSITIVE IDENTIFICATION OF EXCITED 5/2+ STATE

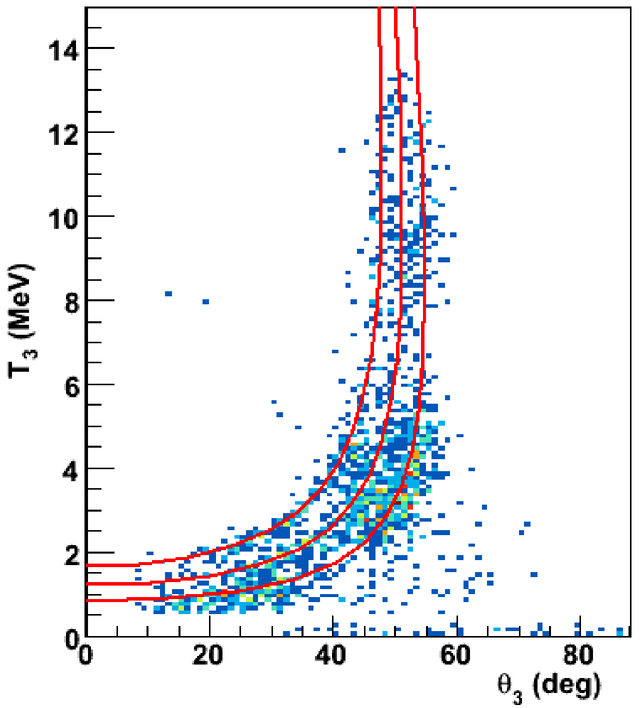

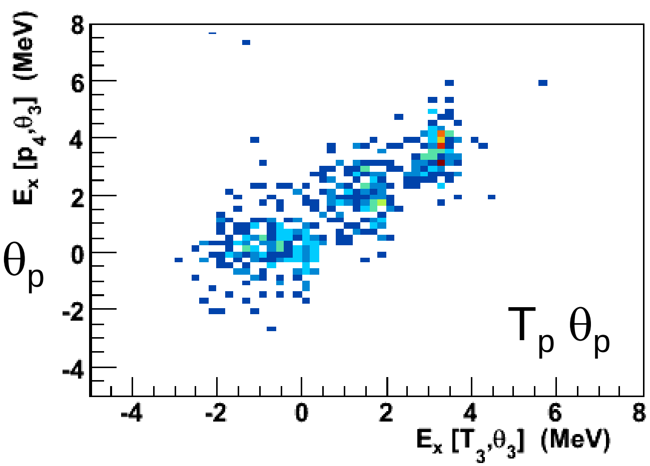

NEW ALGORITHM FOR ENERGY

Preliminary results for $^{26}Ne(d,t)^{25}Ne$ and also (p,d)

JEFFRY THOMAS, SURREY

$^{26}Ne(d,t)^{25}Ne$ | $^{26}Ne(p,d)^{25}Ne$

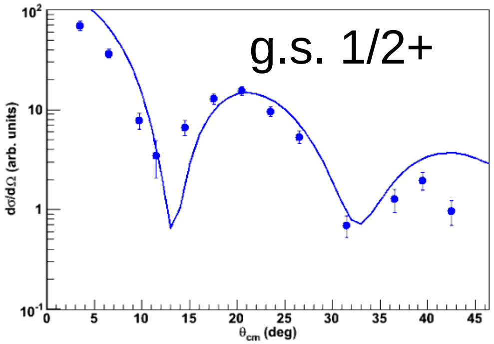

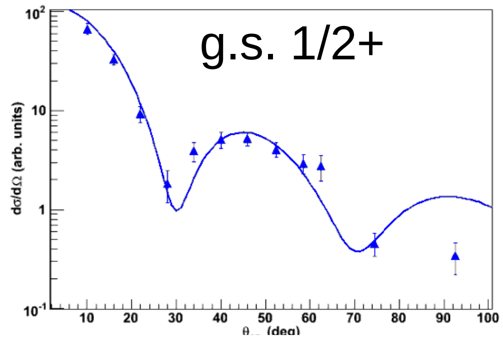

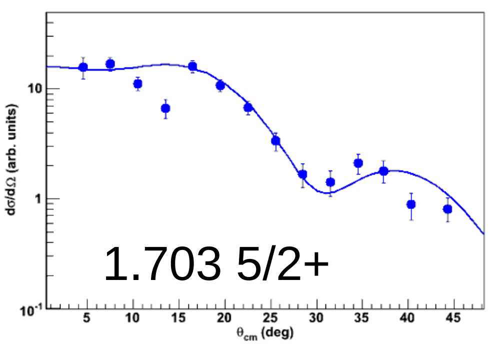

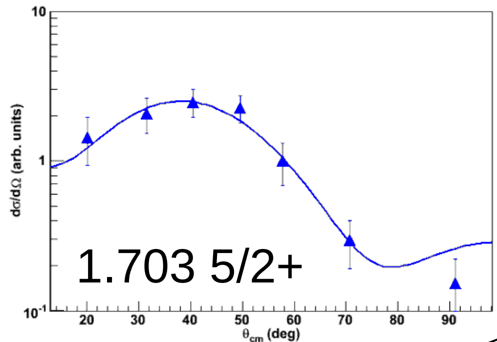

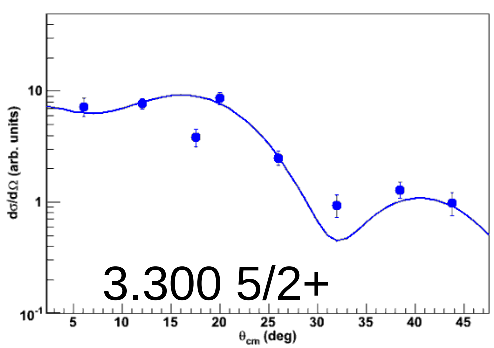

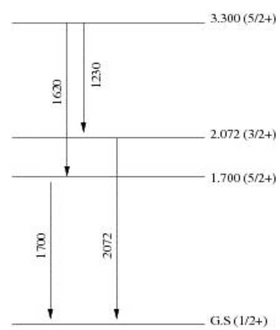

$^{26}Ne(d,t\gamma)^{25}Ne$

GAMMA ENERGY

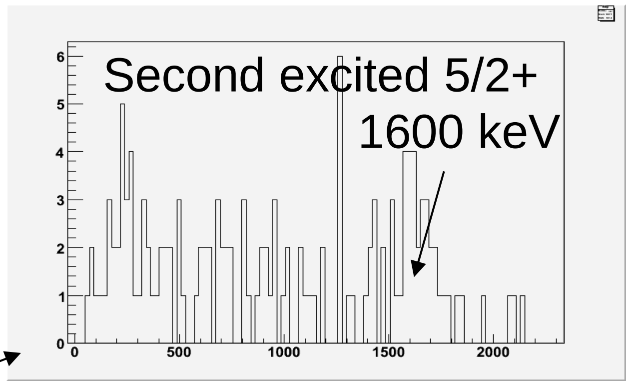

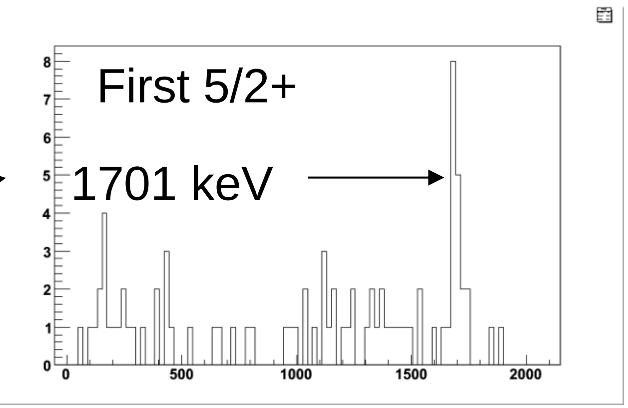

INDIVIDUAL DECAY SPECTRA OF EXCITED 5/2+ STATES

Migration of Levels as nuclei become more exotic, normalised to 7/2– energy

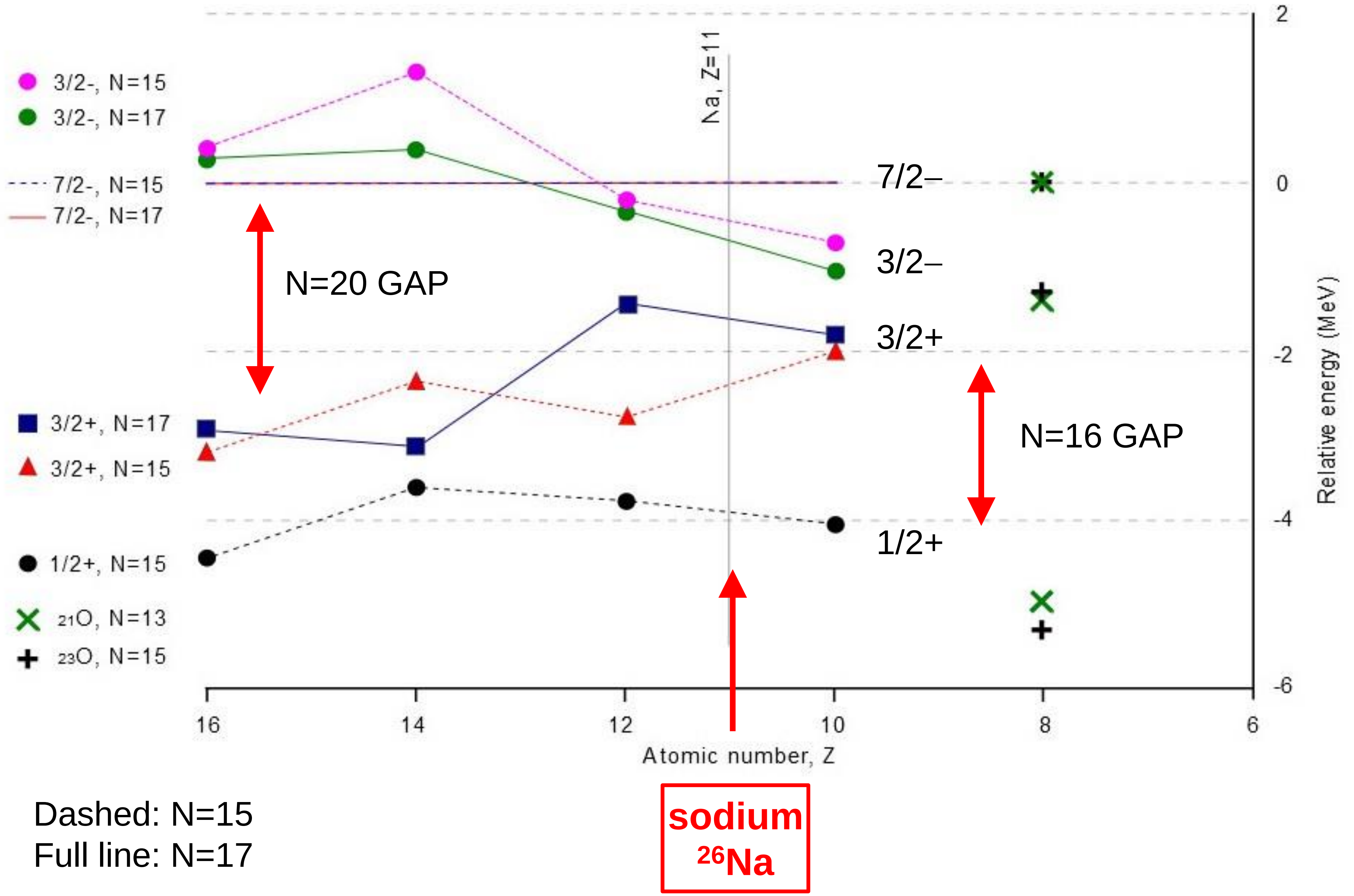

Dashed: N=15
Full line: N=17

The Next Step…

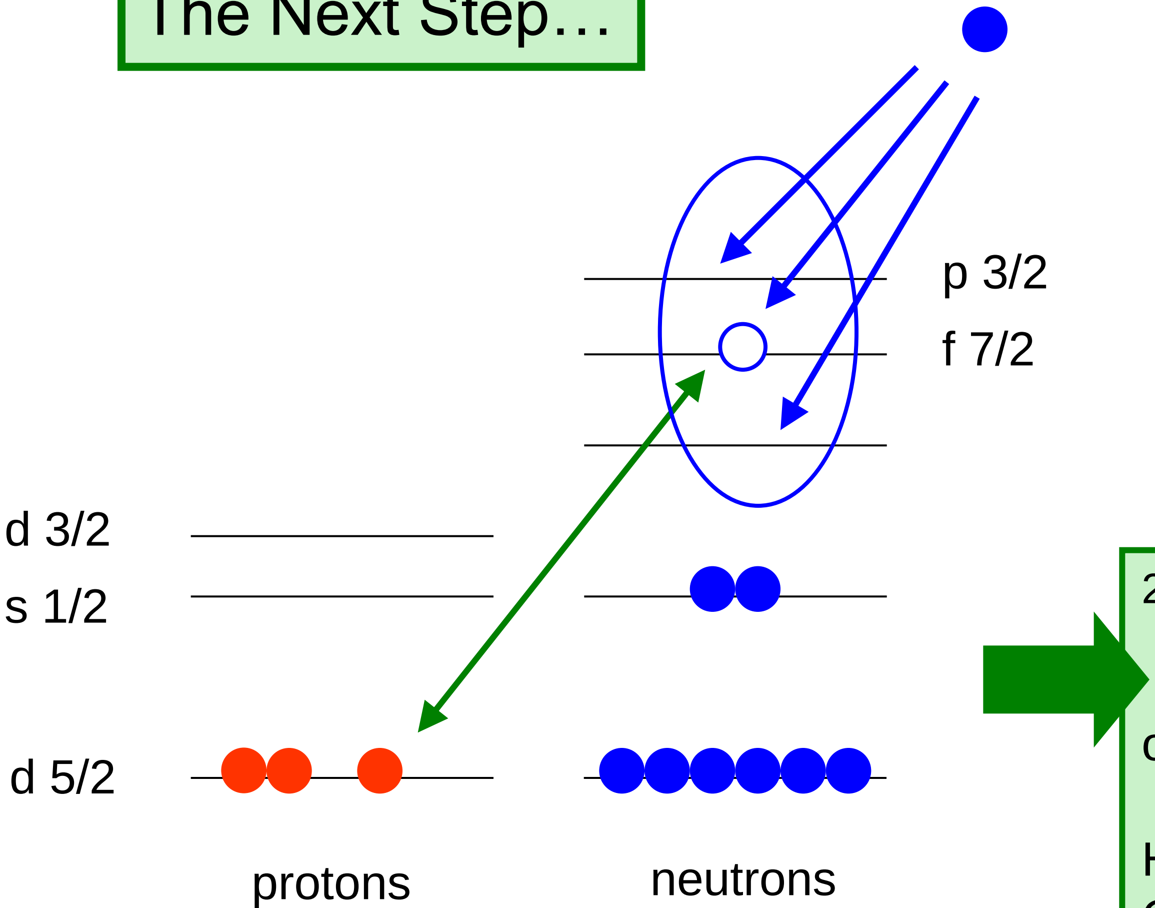

^{25}Na (d,p) ^{26}Na

odd-odd final nucleus

High density of states
Gamma-gating needed

MULTIPLETS e.g. $\pi(d_{5/2}) \otimes \nu(p_{3/2}) \rightarrow (1,2,3,4)^{-}$

Shell Model Predictions (modified WBP) for ^{26}Na states expected in (d,p)

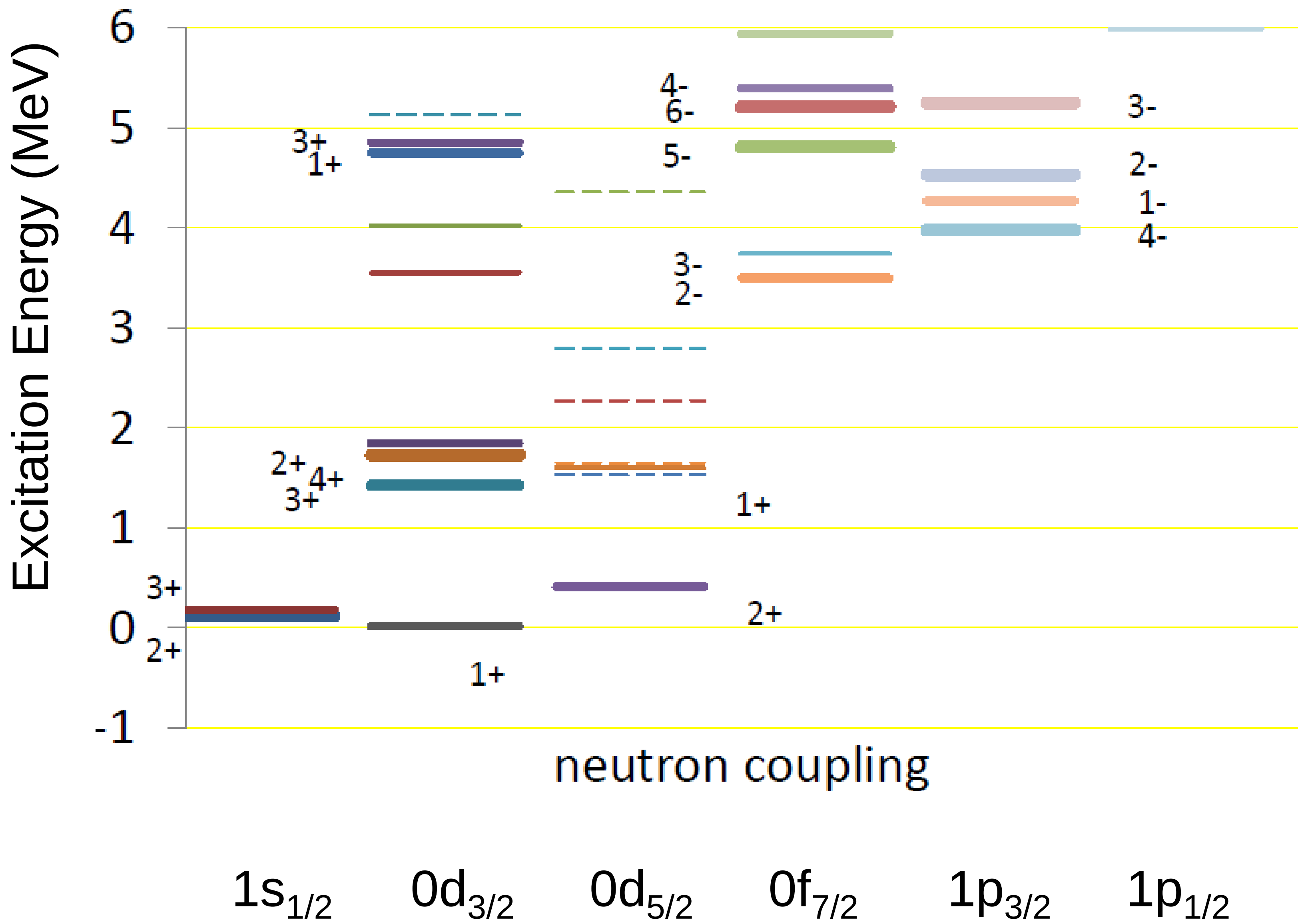

TRIUMF ISAC

ISAC2 TIGRESS

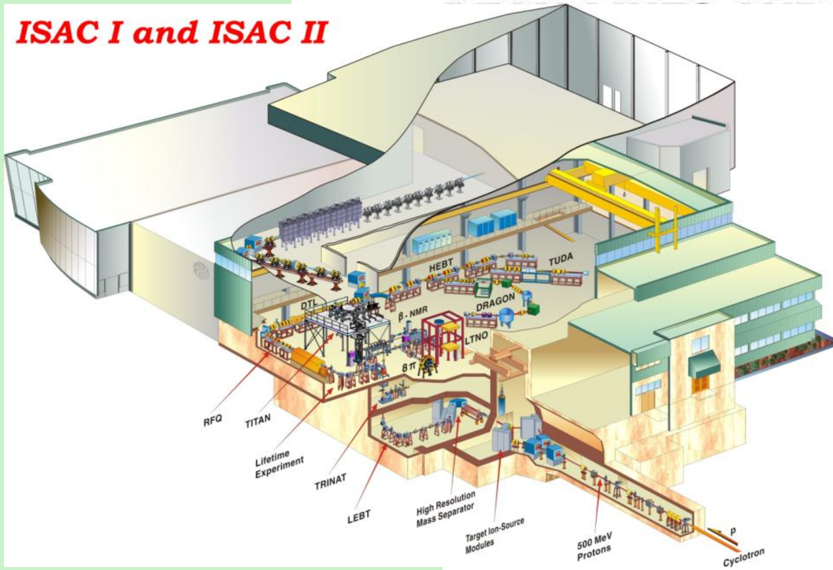

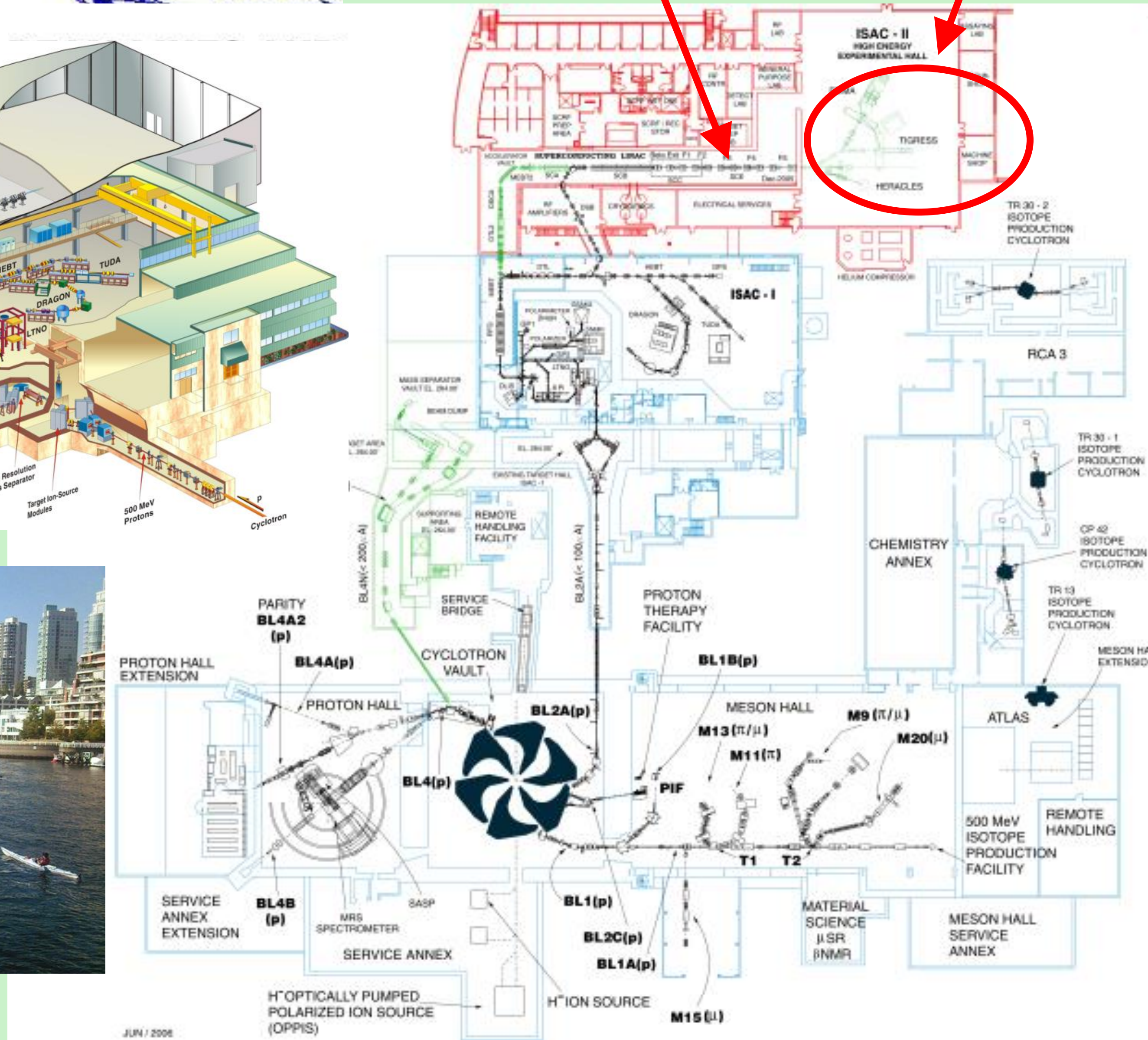

SHARC at ISAC2 at TRIUMF

Christian Diget

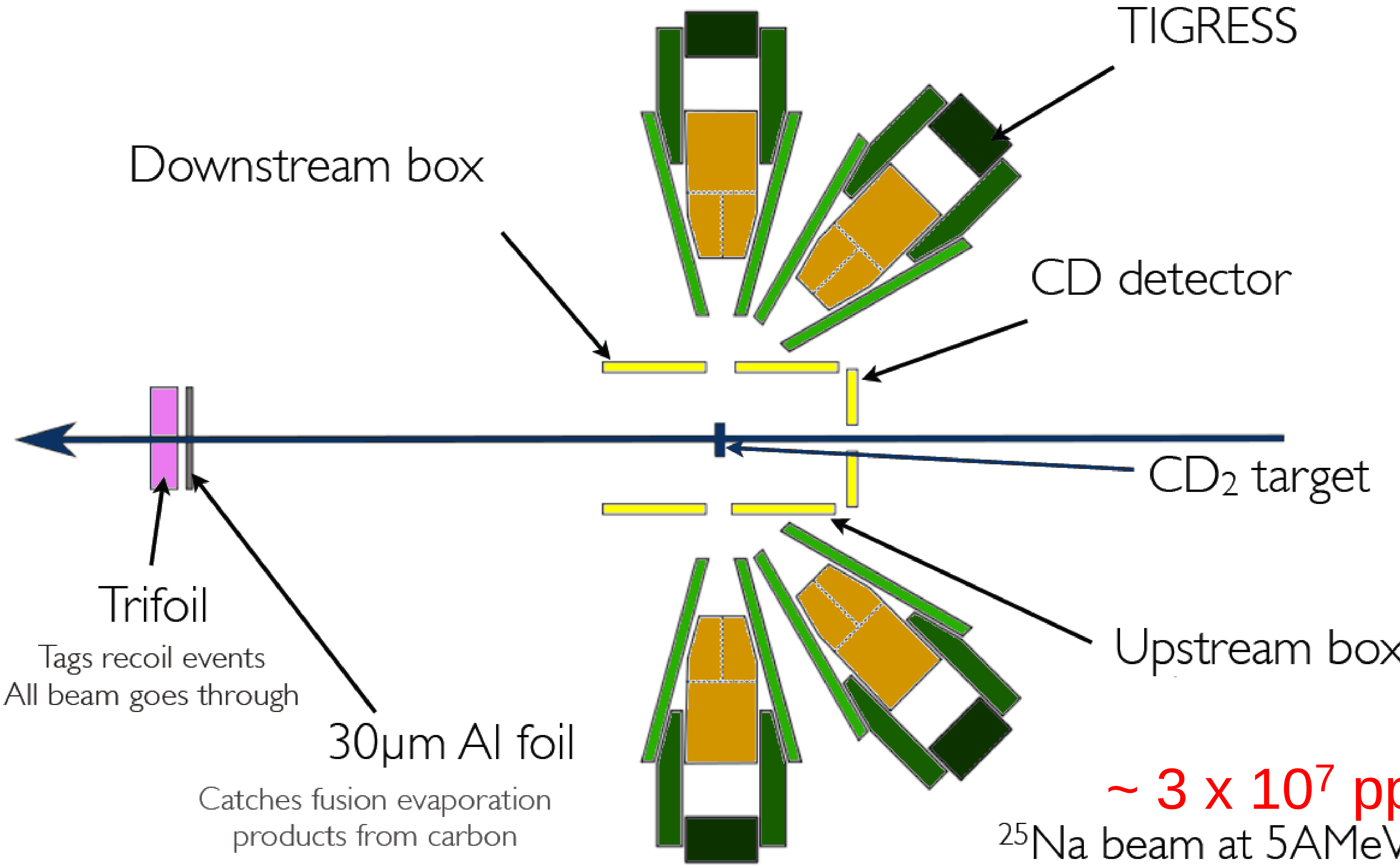

~ 3 x 10^7 pps

^{25}Na beam at 5AMeV

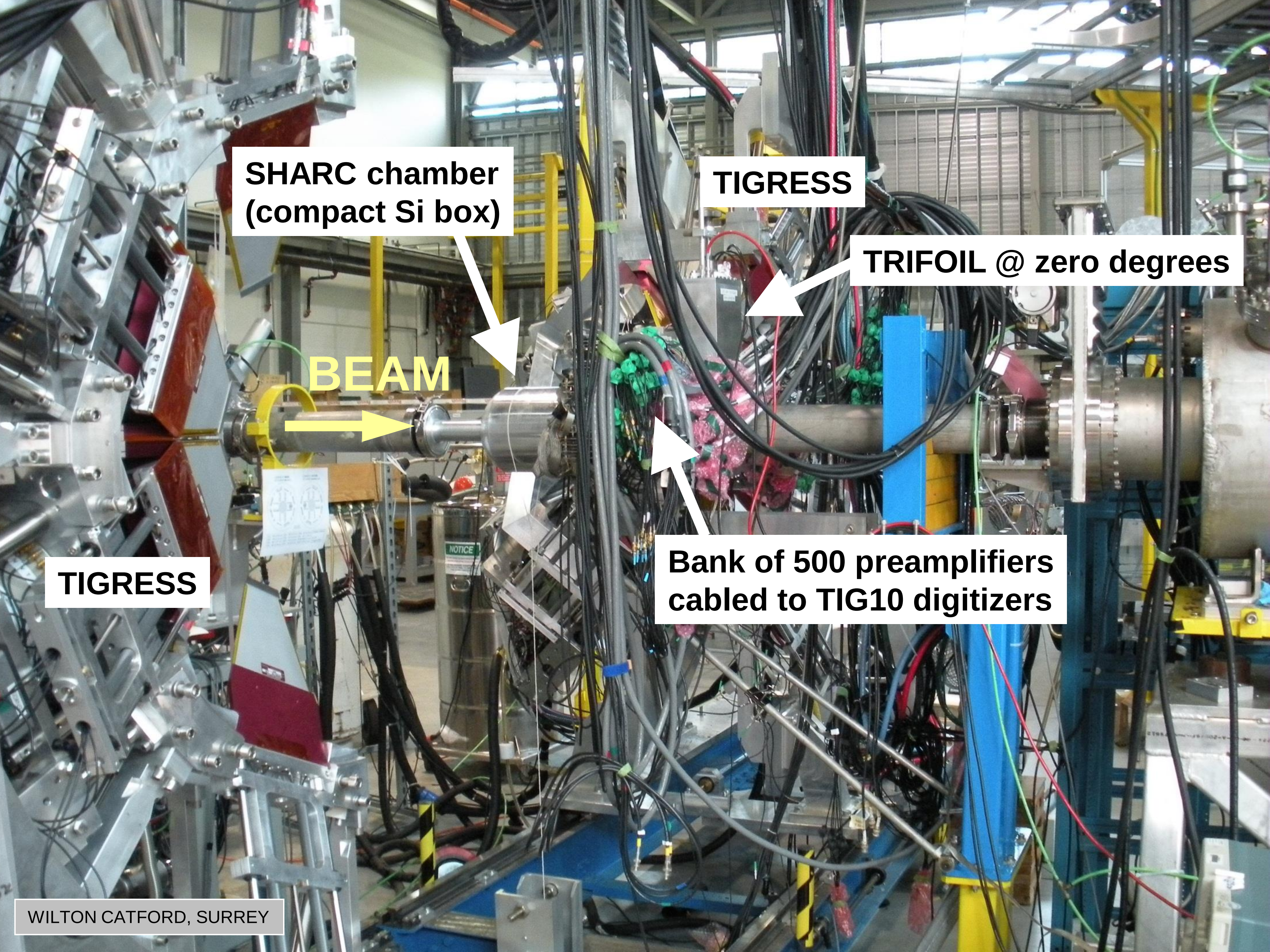
SHARC chamber
(compact Si box)
TIGRESS
TRIFOIL @ zero degrees
BEAM
Bank of 500 preamplifiers
cabled to TIG10 digitizers
TIGRESS
WILTON CATFORD, SURREY

Digital signal processing was used for **all Ge** and **all Si** signals, via TIG10 modules

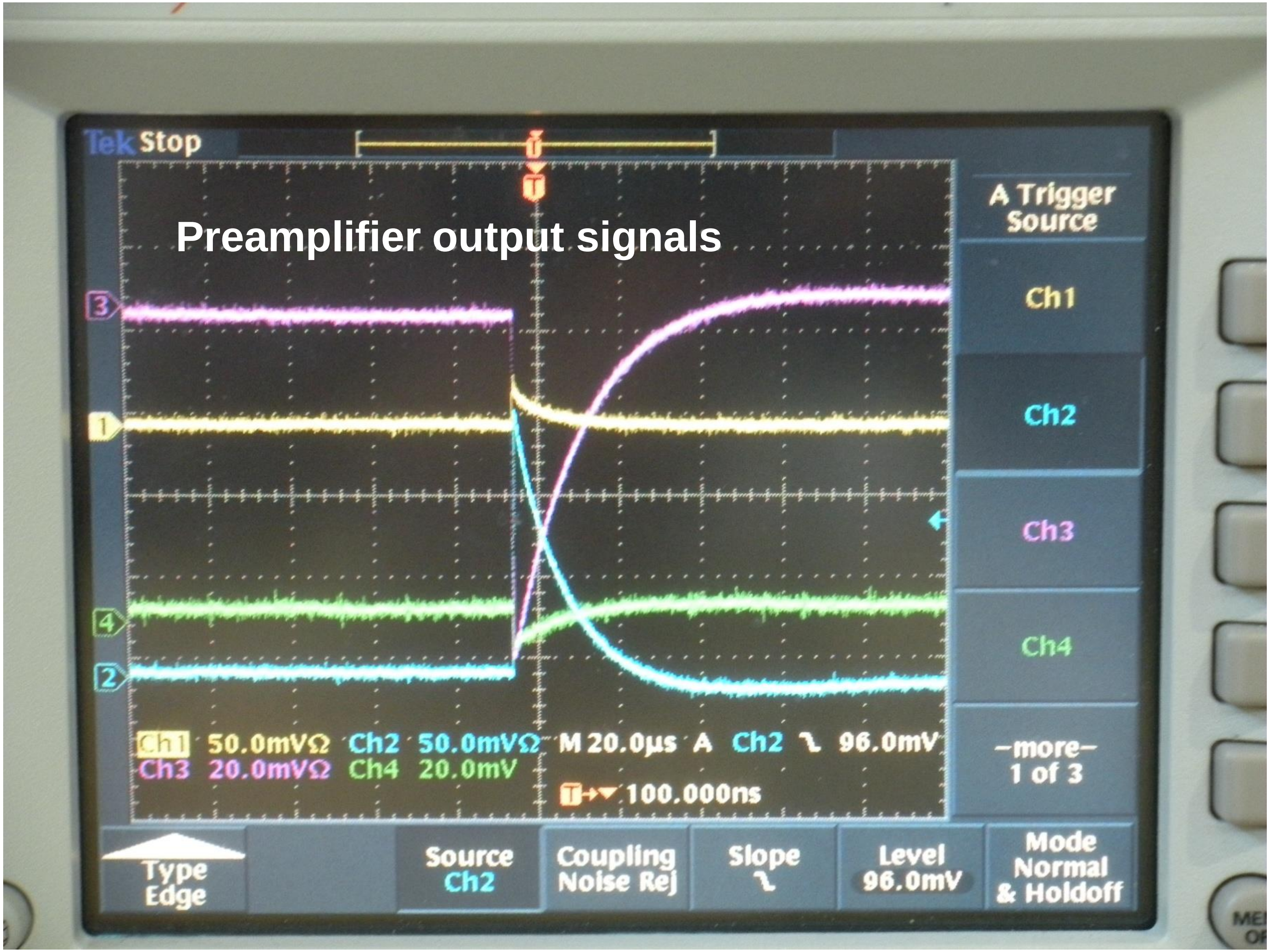

Preliminary Analysis: E vs θ

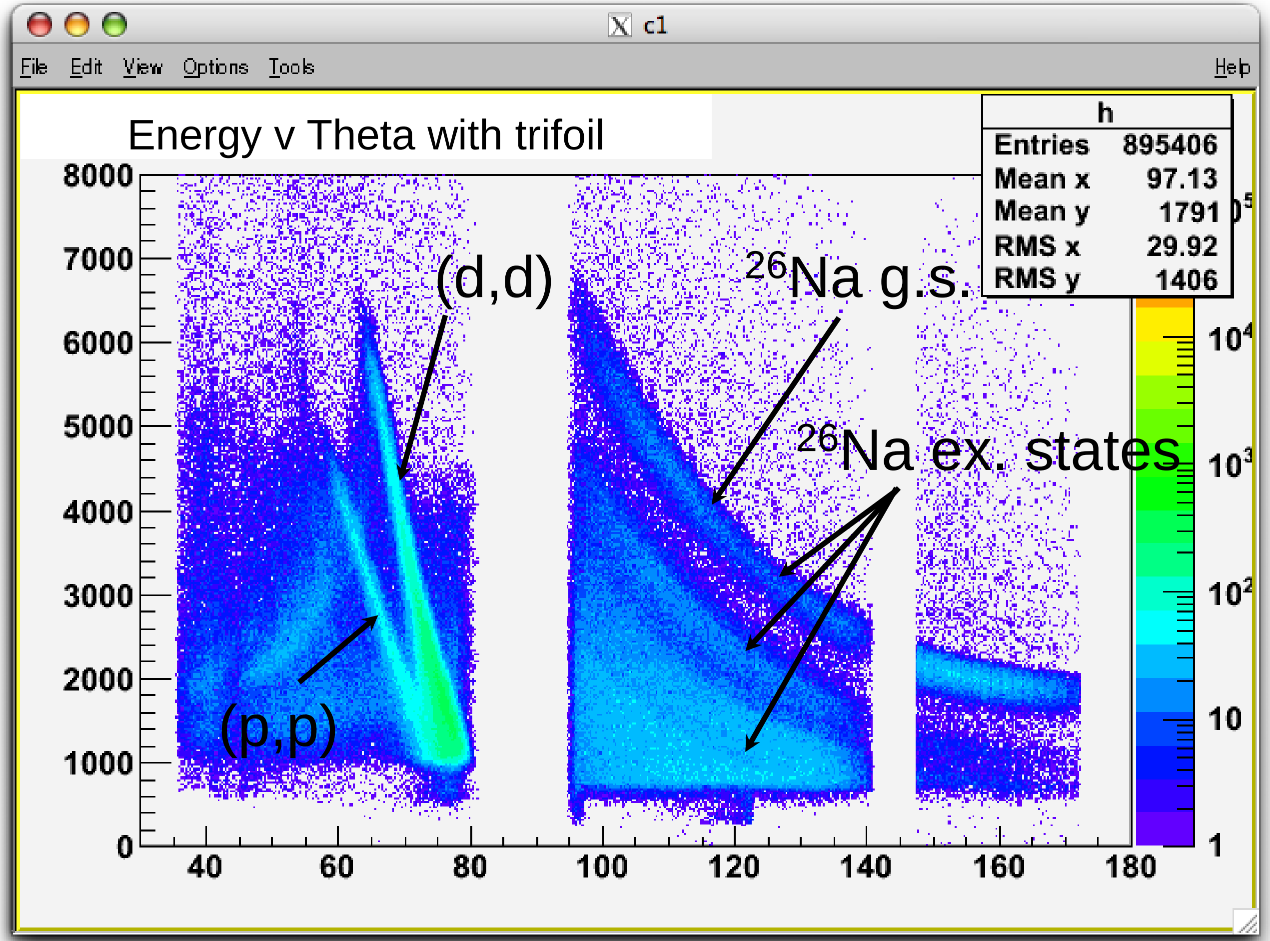

Preliminary Analysis: γ ray spectra

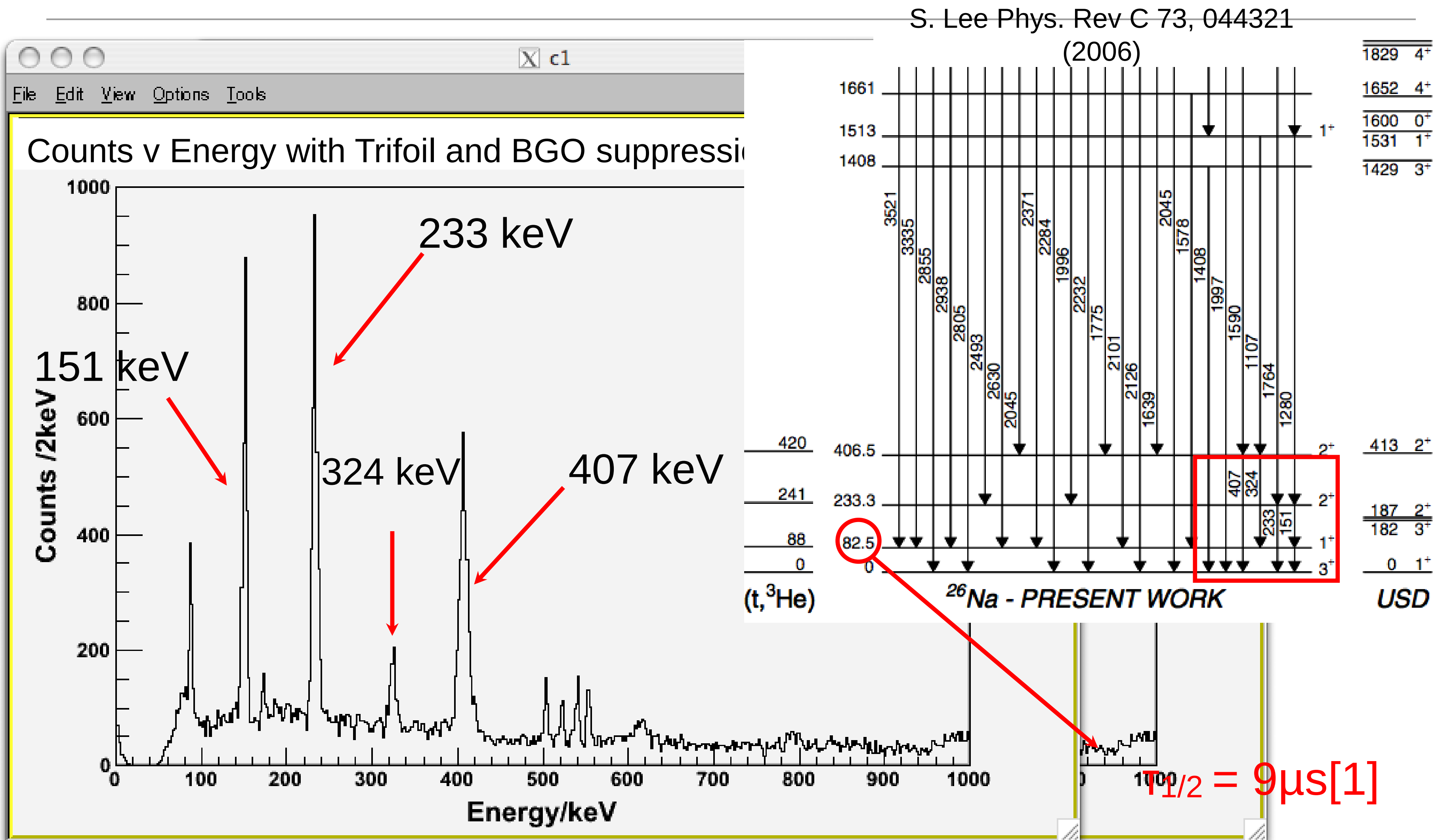

[1] Contrib.Proc. 5th Int.Conf.Nuclei Far from Stability, Rosseau Lake, Canada, D1 (1987)

Preliminary Analysis

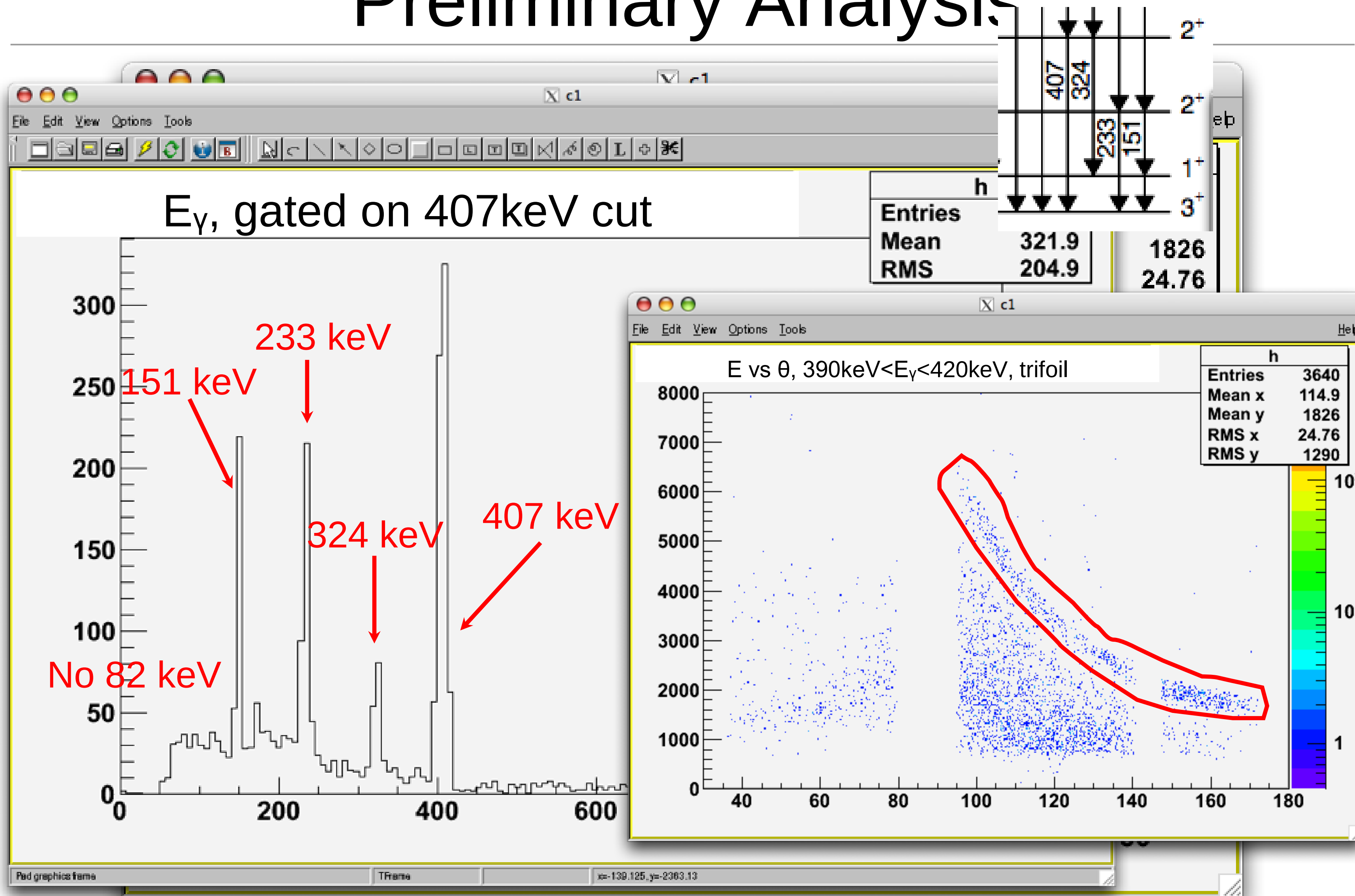

Measuring Trifoil performance

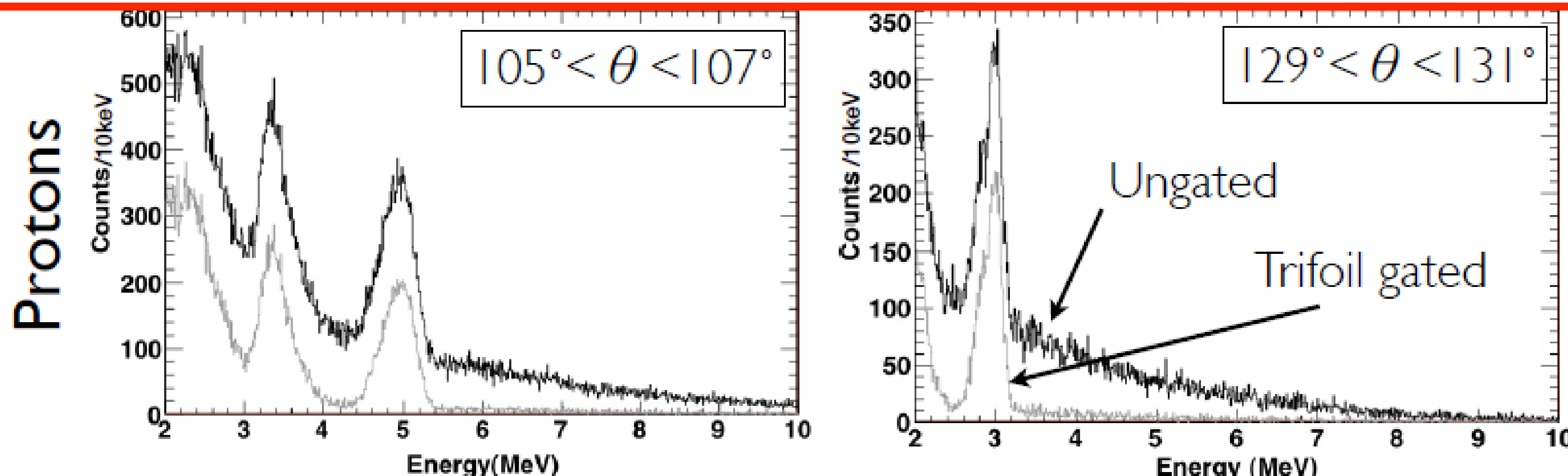

- 80% of protons tagged
- Signal to background improved by factor of 10

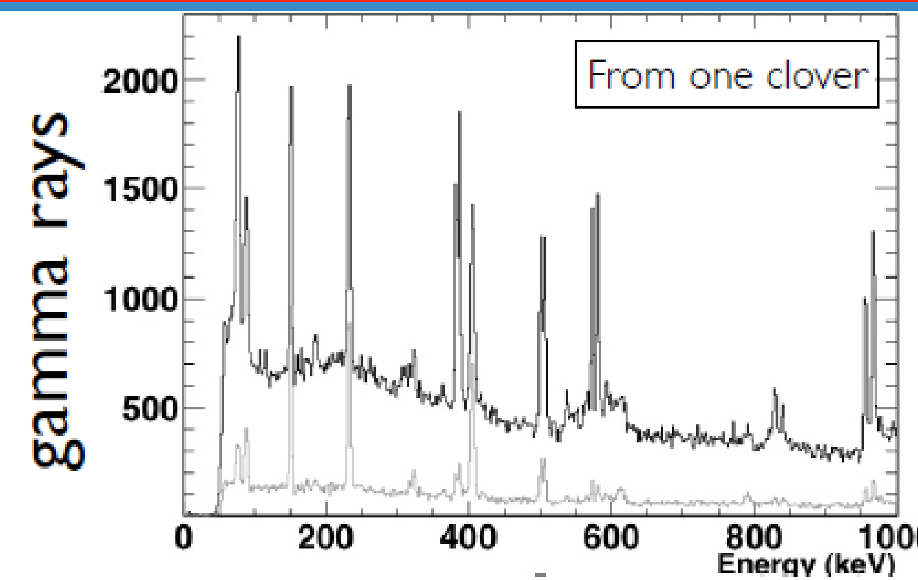

Data from d(^{25}Na,p)^{26}Na at 5 MeV/A using SHARC at ISAC2 at TRIUMF

Gemma Wilson, Surrey

Excitation energy deduced from proton energy and angle

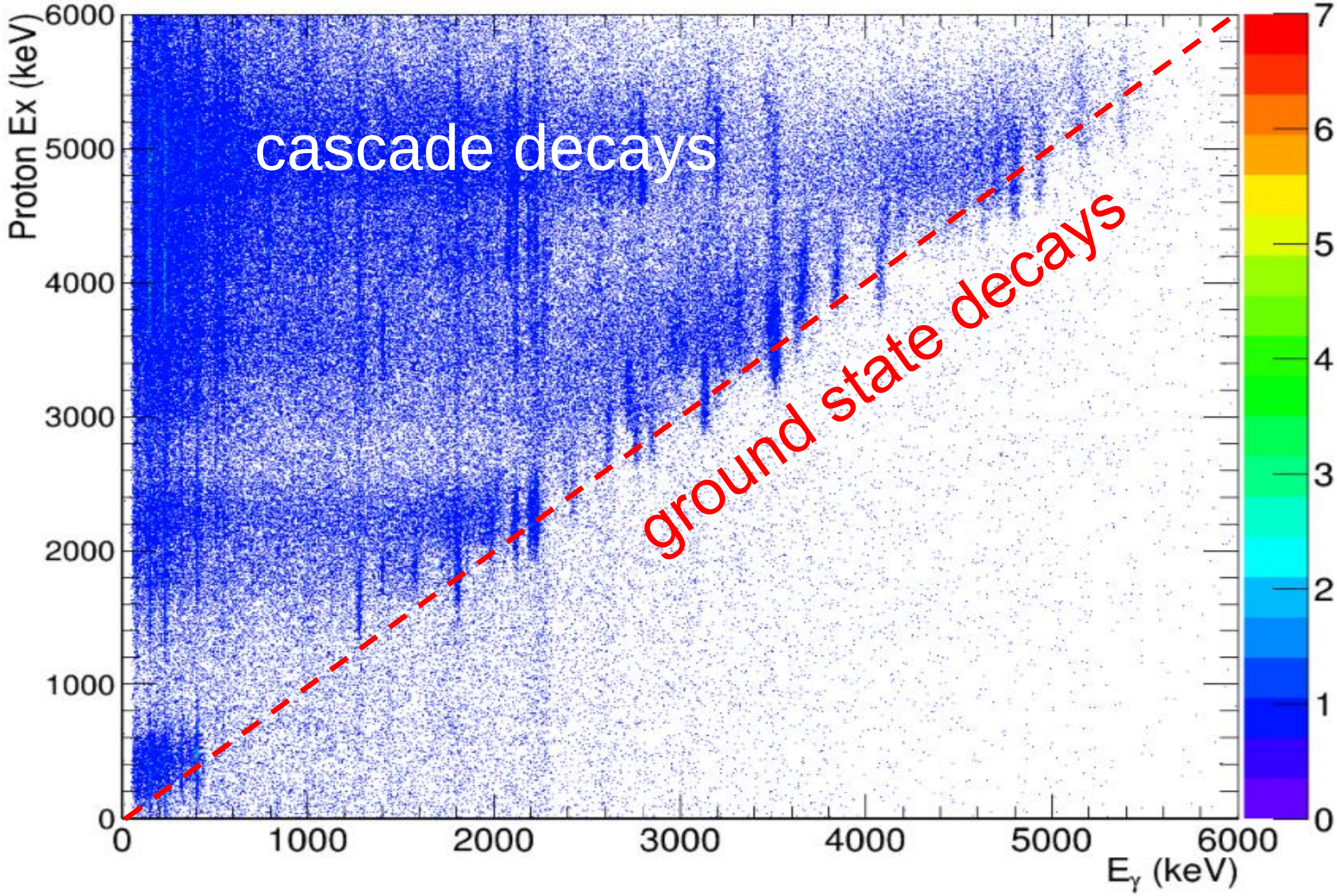

Doppler corrected (β=0.10) gamma ray energy measured in TIGRESS

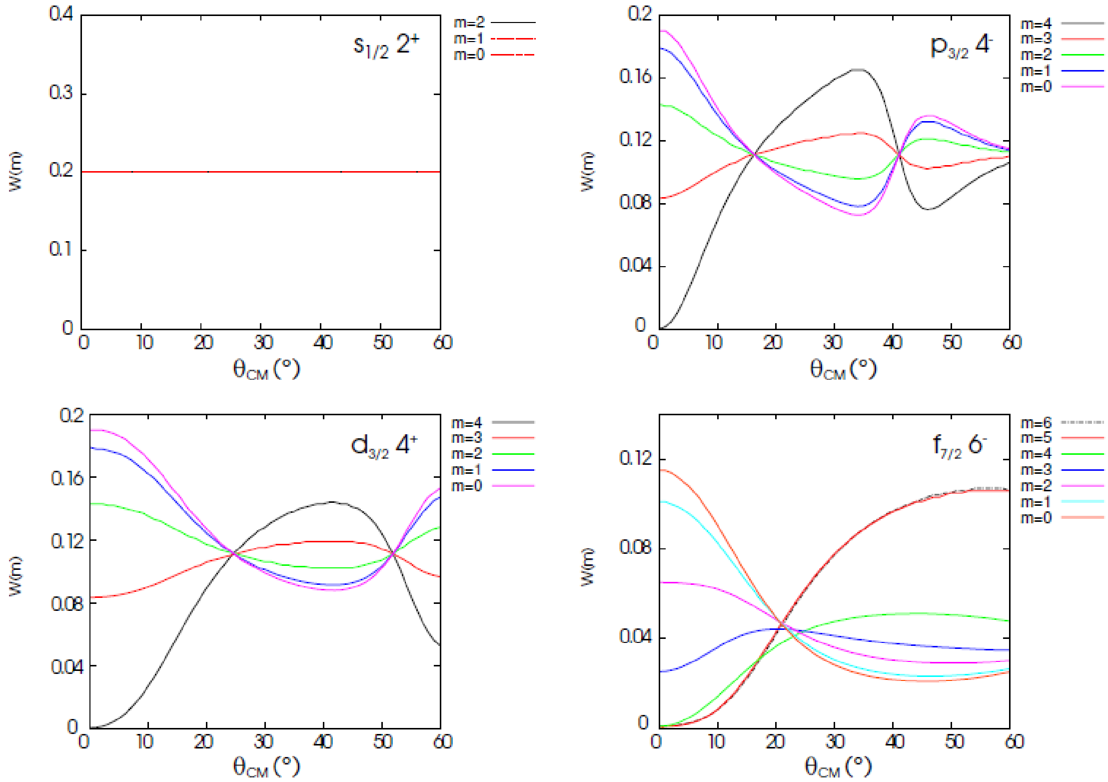

Substate populations over proton CM angle for a 2.2 MeV state in ^{26}Na

If we **gate** on a **gamma-ray**, then we **bias** our proton measurement, if the gamma **detection probability** depends on the **proton angle**.

And it does depend on the proton angle, because the gamma-ray correlation is determined by magnetic substate populations.

However, our **gamma-ray** angular coverage is sufficient that the integrated efficiency for gamma detection remains very similar and the SHAPE of the **proton** angular distribution is unchanged by gating.

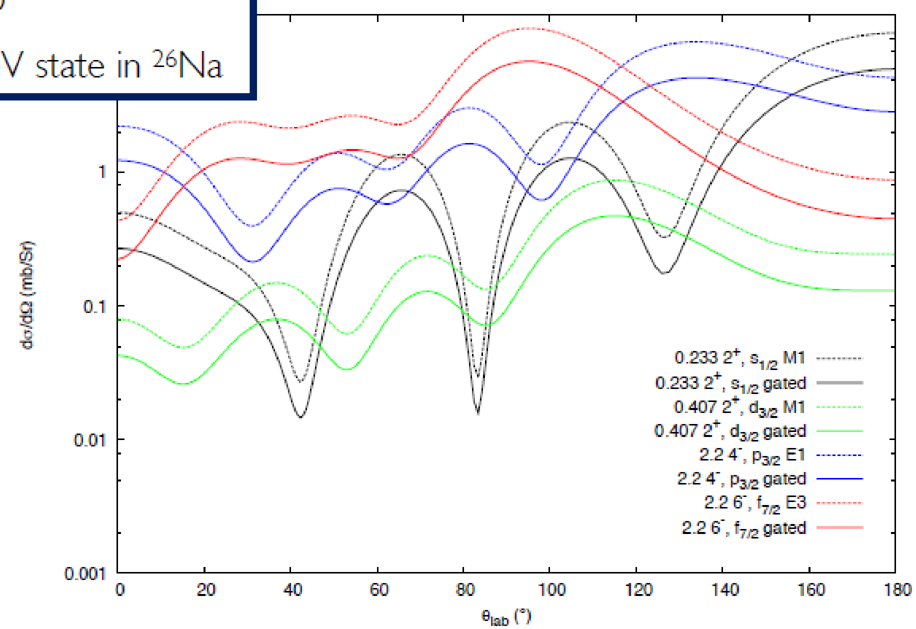

^{26}Na

This work

Energies in keV

Branching ratios in red

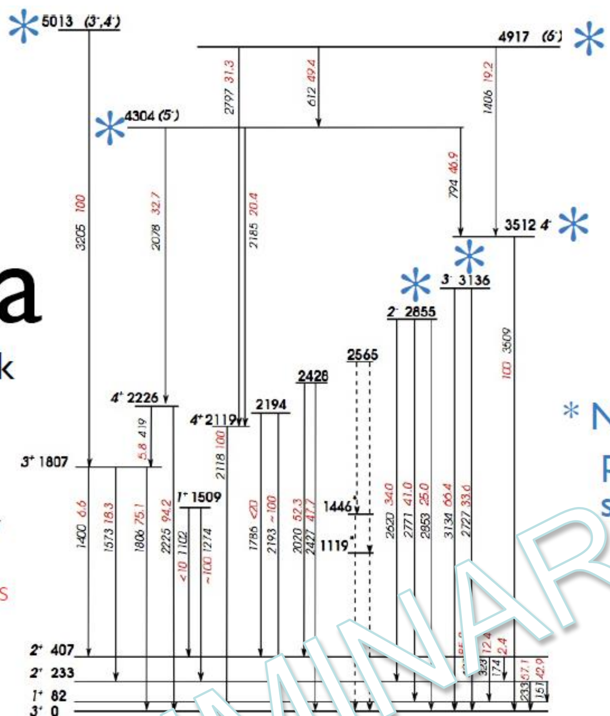

* Negative parity states

E_x [a] ([illegible])	J^π [b]	$n[illegible], j)$	S.F. [c] exp	ANC^2 [c]	E_x [d] (keV)	E_x [e] (keV)	n [f]	S.F. [g] theory
[illegible]33	2^+	$0s_{1/2}$	0.1[illegible]		233	187	1	0.22
[illegible]	2^+	$0s_{1/2}$	[illegible]		407	414	2	0.19
1509	1^+				1513	1532	1	[h]
1806	3^+	$0d_{3/2}$	0.2[illegible]			1430	2	0.32
2118	4^+	$0d_{3/2}$	0.34					
2225	4^+	$0d_{3/2}$	0.43			1830	2	0.59
2853	2^-		*			3499	1	0.23
3134	3^-	$0f_{7/2}$	0.10			3742	1	0.17
3509	4^-	$1p_{3/2}$	0.54			3977	1	0.43
4303	(5^-)	$0f_{7/2}$	*			4807	1	0.44
4915	(6^-)	$0f_{7/2}$	*			5208	1	0.64
5011	$(3,4)^-$		*					

* not possible to extract differential cross section

a) present work, from gamma-ray energies

b) inferred in present work

c) present work, using the indicated nucleon transfer

d) from fusion-evaporation study, ref. [22]

e) shell model using modified WBP interaction (see text)

f) numbering of shell model state (lowest = 1)

g) shell model value, for indicated nucleon transfer

h) mixed strength 0.08 $0d_{5/2}$ and 0.10 $0d_{3/2}$

3.512 MeV $p_{3/2}$

3.136 MeV $p_{3/2}$

2.226 MeV $d_{3/2}$

2.119 MeV $d_{3/2}$

1.807 MeV $d_{3/2}$

0.407 MeV $s_{1/2}$

0.233 MeV $s_{1/2}$

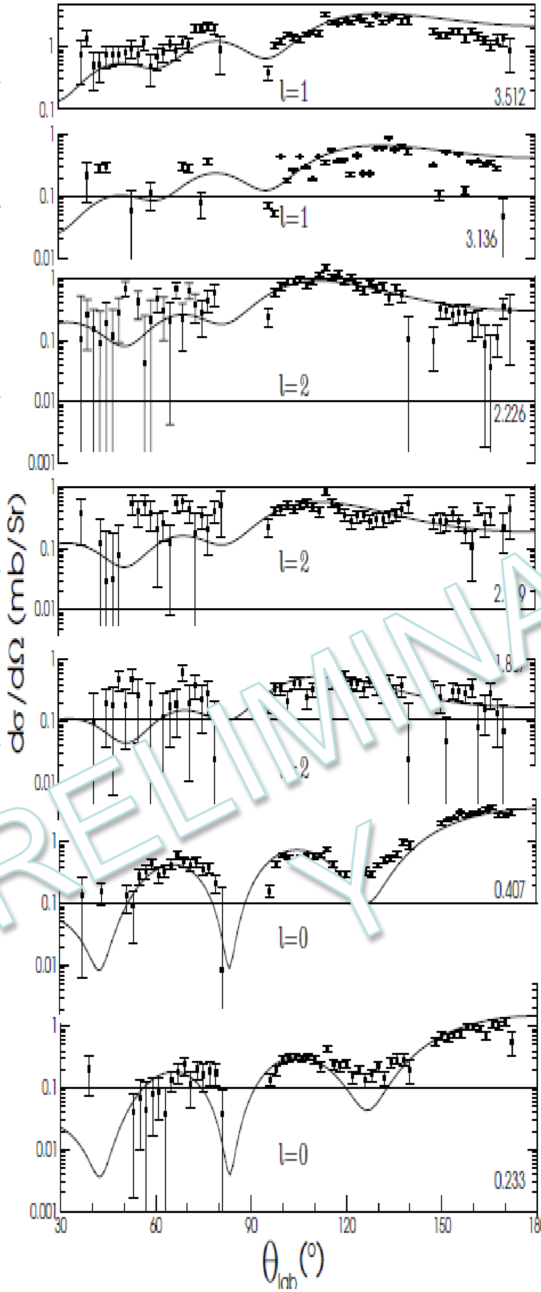

Shell Model Predictions (and new candidates) for ^{26}Na states expected in (d,p)

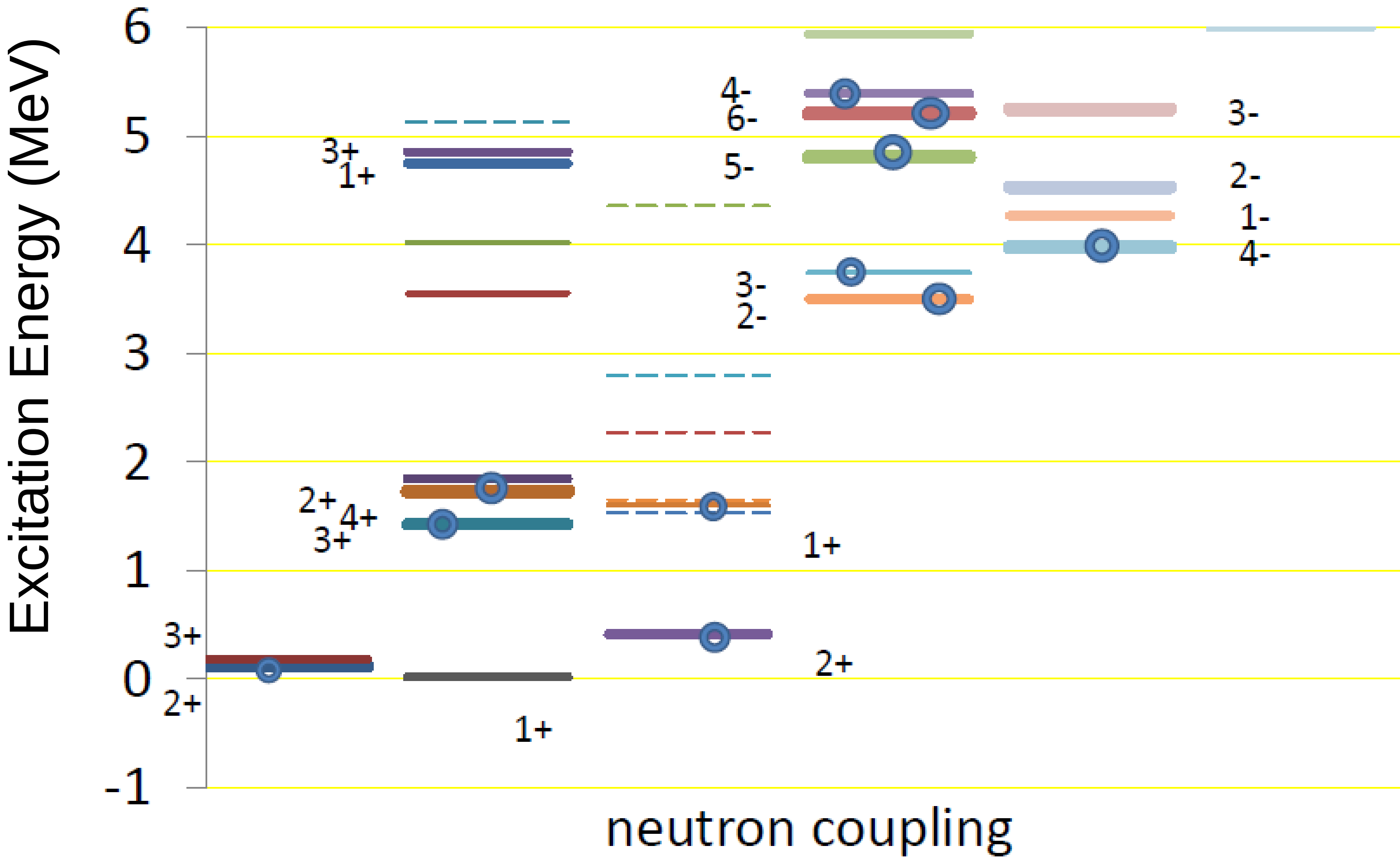

$1s_{1/2}$ $0d_{3/2}$ $0d_{5/2}$ $0f_{7/2}$ $1p_{3/2}$ $1p_{1/2}$

Shell Model Predictions (and new candidates) for ^{26}Na states expected in (d,p)…

Comparison of spectroscopic strength in theory and experiment

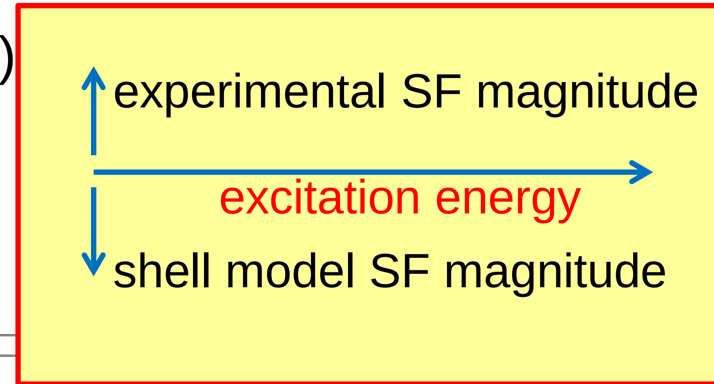

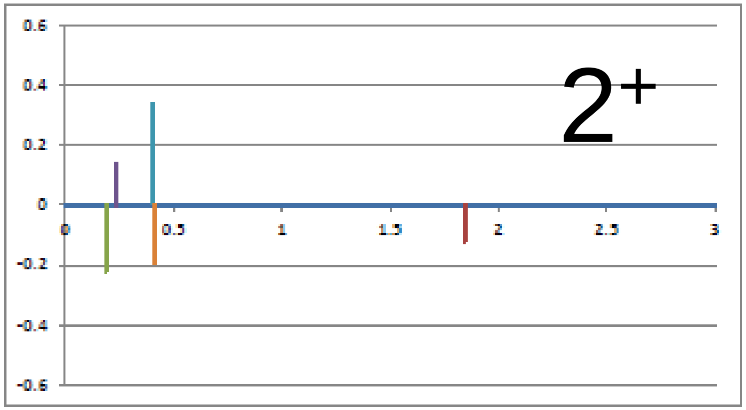

Above: s1/2 strength for 2+ states

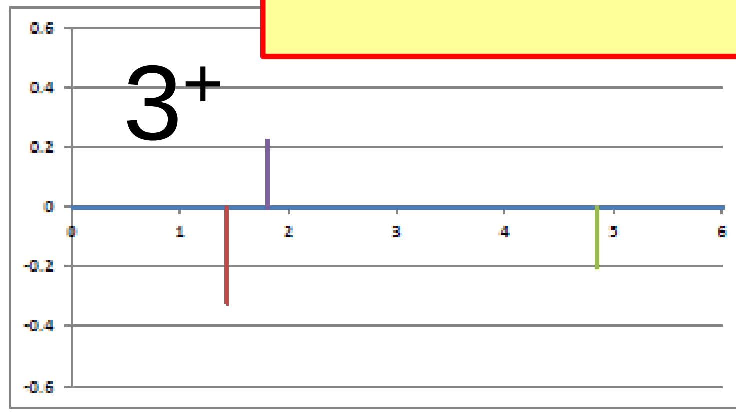

Above: d3/2 to 3+ states

Below: p3/2 to 4- states

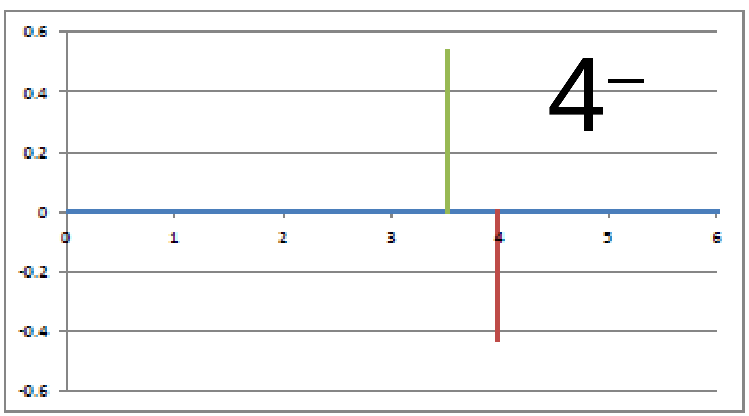

Below: d3/2 to 4+ states

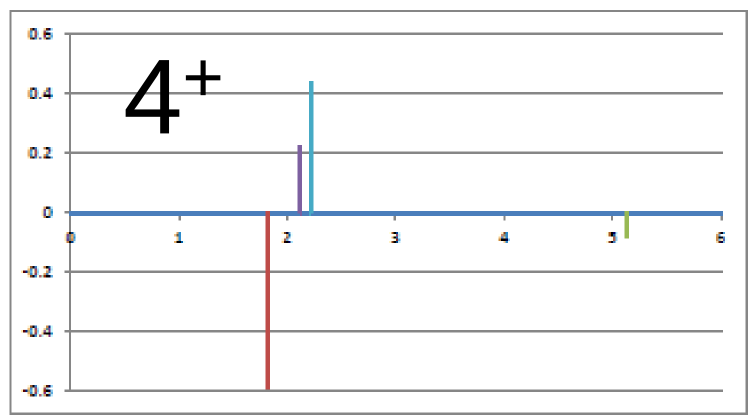

SOME FUTURE PERSPECTIVES

GASPARD

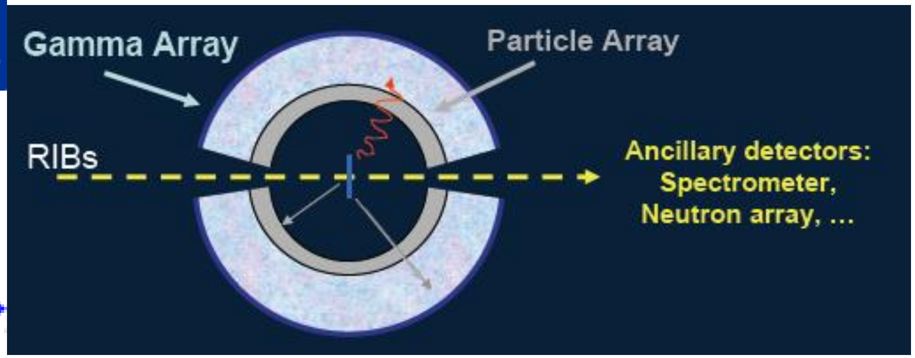

Spiral2

EURISOL

GRAPA

GAMMA RAY AND PARTICLE ARRAY

"… WORK IN PROGRESS"

FUTURE:

- We have experiments planned with ^{16}C, ^{64}Ge at GANIL & ^{28}Mg and others at TRIUMF
- Many other groups are also busy! T-REX at ISOLDE, ORRUBA at ORNL etc
- New and extended devices are planned for SPIRAL2, HIE-ISOLDE and beyond

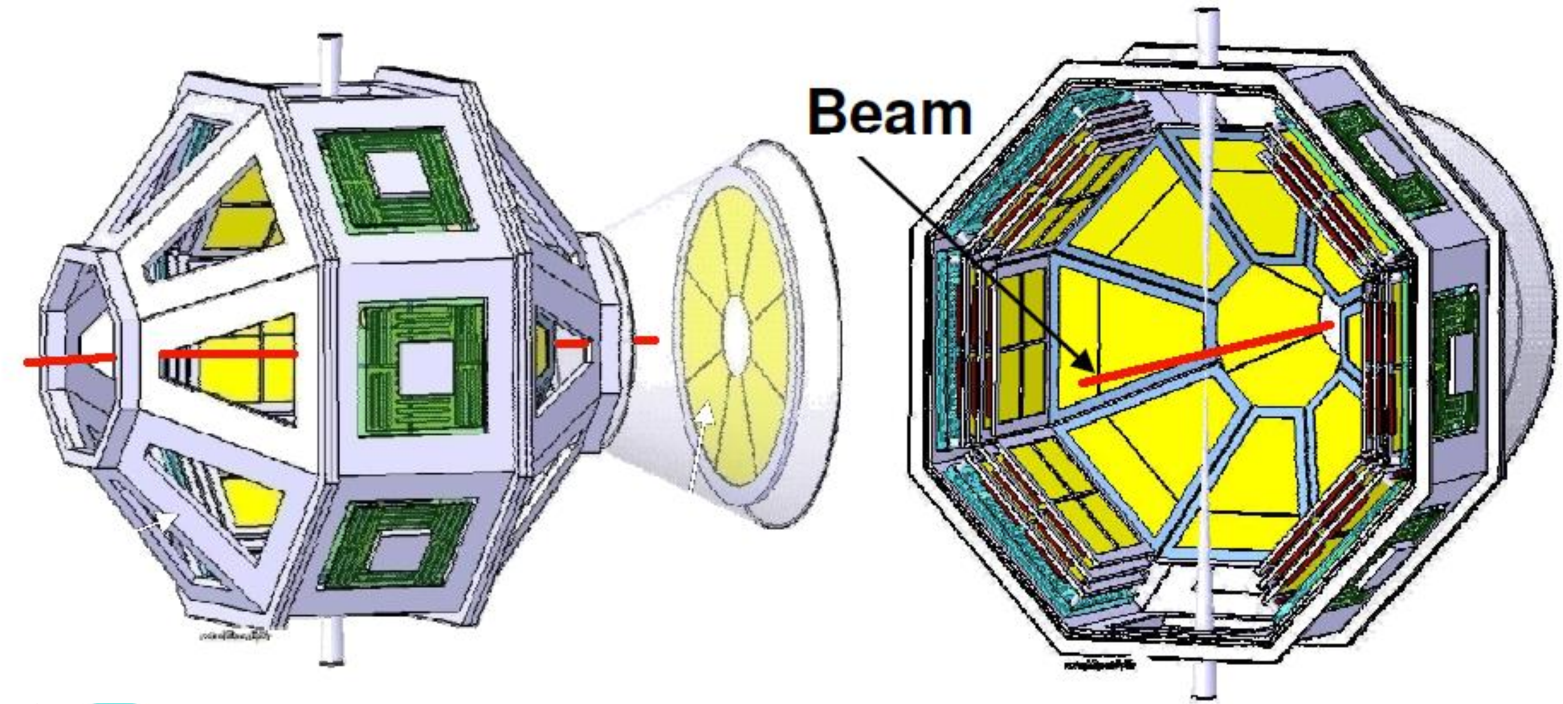

GASPARD

Designed to use cryogenic target CHyMENE and gamma-arrays PARIS, AGATA…

A development of the GRAPA concept originally proposed for EURISOL.

CHyMENE (Saclay/Orsay/…) SOLID Hydrogen TARGET

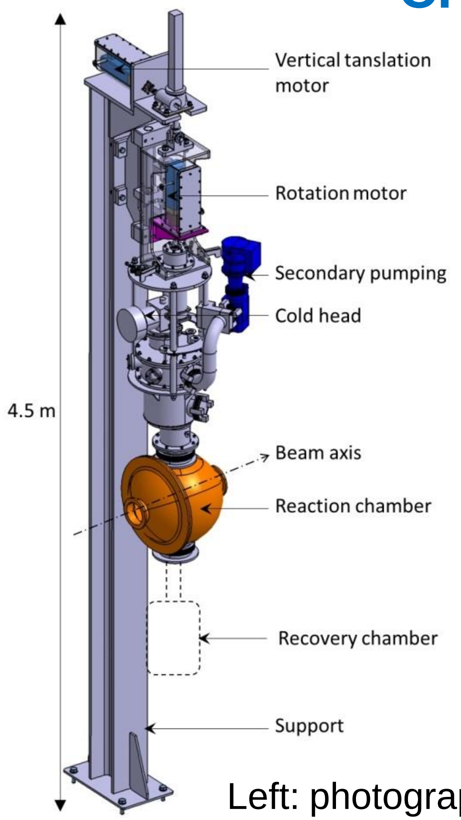

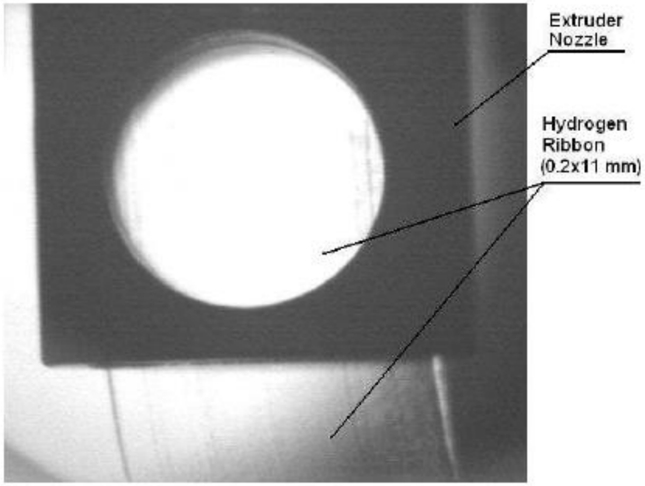

Left: photograph from 2007 of a 200μm pure solid hydrogen film being extruded.
Right: more recent photograph of 100μm pure solid hydrogen film being extruded.

The CHyMENE project has achieved 100μm and is designed to achieve 50μm uniform films.

For 100μm target, the energy loss by a typical beam is equivalent to a 1 mg/cm^2 CD_2 target.

For 100μm target, the number of hydrogen atoms is **<u>THREE TIMES</u>** that of a 1 mg/cm^2 CD_2.

GASPARD

TSR@ISOLDE

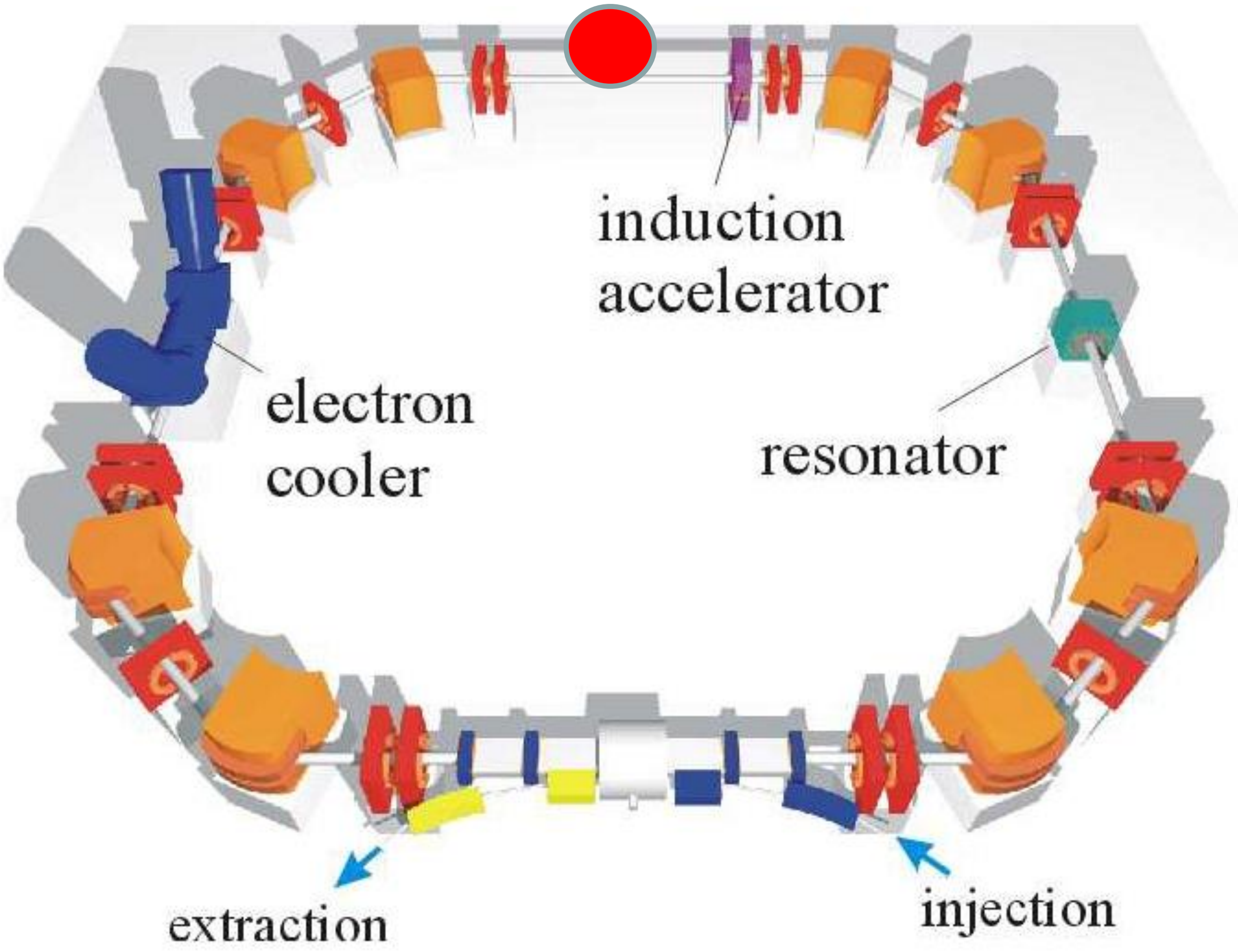

Circumference 55.4m

- Existing storage ring
- Re-deploy at ISOLDE
- Thin gas jet targets
- Light beams will survive
- Increased luminosity
- Supported by CERN
- In-ring initiative led by UK
- Also linked to post-ring helical spectrometer

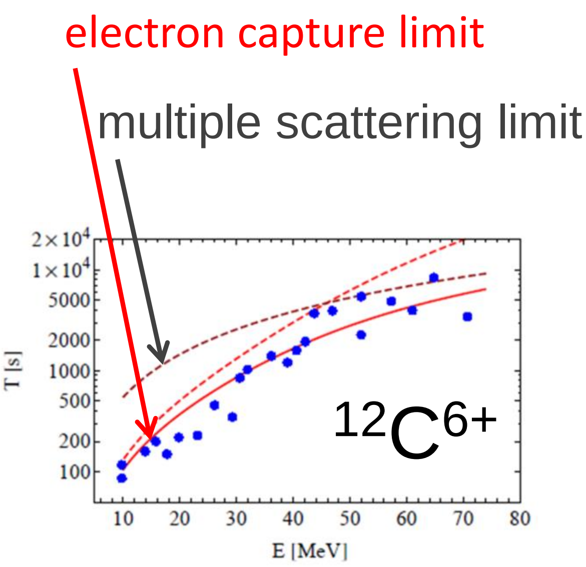

Ultimately, with single particle transfer reactions, we can certainly:

- make the measurements to highlight **strong** SP states

- measure the **spin/parity** for strong states

- **associate** experimental and Shell Model states and see

    - when the shell model **works** (energies and spectroscopic factors)
    - when the shell model **breaks down**
    - whether we can adjust the interaction and **fix** the calculation
    - how any such modifications can be interpreted in terms of NN interaction

And clearly:

- monopole shifts need to be measured and understood because the changes
  In energy gaps fundamentally affect nuclear structure (collectivity, etc.)

Heavy-Ion induced nucleon transfer reactions

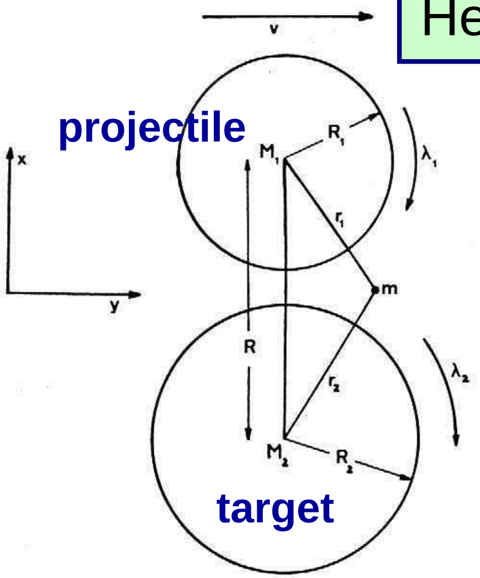

David M. Brink, *Phys. Lett.* **B40** (1972) 37
N. Anyas-Weiss *et al.*, *Physics Reports*, **12** (1974) 201

IDEA: for the transferred nucleon, we match the initial and final values of the **linear** momentum and of the **angular** momentum

Linear momentum in y-direction (relative motion), before and after:

$p_i = m\upsilon - \hbar\lambda_1 / R_1 \qquad p_f = \hbar\lambda_2 / R_2 \qquad \Delta p = p_f - p_i \approx 0$

Set $\Delta p=0$ within accuracy of Uncertainty Principle $\Delta p \sim \hbar/\Delta y$; $\Delta y \sim R/2$

k-matching: $\Delta k = k_0 - \lambda_1 / R_1 - \lambda_2 / R_2 \approx 0 \quad ; \quad \Delta k \leq 2\pi/R$

Angular momentum projected in the z-direction (perpendicular to relative motion) is given by

$L_{init} = L(\text{relative motion})_i + \lambda_1 \hbar = \mu\upsilon R + \lambda_1 \hbar$ and $L_{final} = L(\text{relative})_f + \lambda_2 \hbar$

$\Delta L \hbar = L_{final} - L_{init} = (\lambda_2 - \lambda_1)\hbar + \delta(\mu\upsilon R)$ where each of μ, υ and R changes

$\Delta L \hbar = (\lambda_2 - \lambda_1)\hbar + ½ m\upsilon (R_1 - R_2) + R\, Q_{eff} / \upsilon \; ; \; Q_{eff} = Q - (Z_1^f Z_2^f - Z_1^i Z_2^i)\, e^2 / R$

ℓ-matching

Q-value Coulomb-corrected for nucleon rearrangement

Set $\Delta L = 0$ precisely, in principle (in practice, classical treatment of $E_{rel} \Rightarrow$ allow $\Delta L \leq 2$)

And finally, there is a simple requirement that $\ell_1 + \lambda_1 = \text{even}$ and $\ell_2 + \lambda_2 = \text{even}$

Heavy-Ion induced nucleon transfer reactions - 2

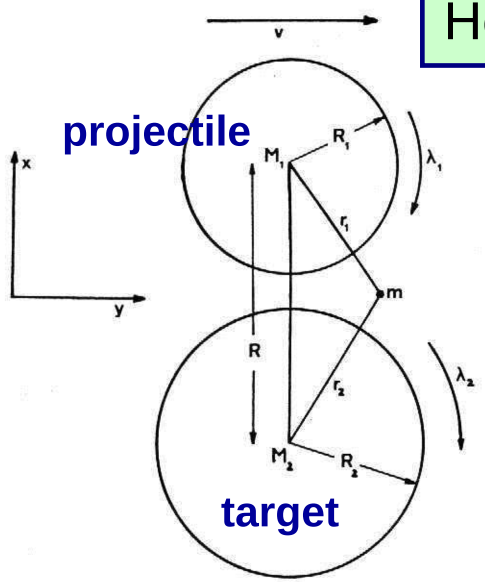

David M. Brink, *Phys. Lett.* **B40** (1972) 37
N. Anyas-Weiss *et al.*, *Physics Reports*, **12** (1974) 201

Linear momentum in y-direction (relative motion), before and after:

k-matching: $\Delta k = k_0 - \lambda_1 / R_1 - \lambda_2 / R_2 \approx 0$; $\Delta k \leq 2\pi/R$

Angular momentum projected in the z-direction (perpendicular):

$\Delta L \hbar = (\lambda_2 - \lambda_1)\hbar + \tfrac{1}{2} m\upsilon (R_1 - R_2) + R\, Q_{eff} / \upsilon$;

ℓ-matching $\qquad Q_{eff} = Q - (Z_1^f Z_2^f - Z_1^i Z_2^i)\, e^2 / R$

And finally, there is a simple requirement that $\ell_1 + \lambda_1 =$ even and $\ell_2 + \lambda_2 =$ even

Initial $\psi_1 = u_1(r_1)\, Y_{\ell 1, \lambda 1}(\theta_1, \phi_1)$
Final $\psi_2 = u_2(r_2)\, Y_{\ell 2, \lambda 2}(\theta_2, \phi_2)$

and the main contribution to the transfer is at the reaction plane:
$\Rightarrow \theta_1 = \theta_2 = \pi / 2$

But $Y_{\ell \lambda}(\pi/2, \phi) = 0$ *unless*
$\ell + \lambda =$ even

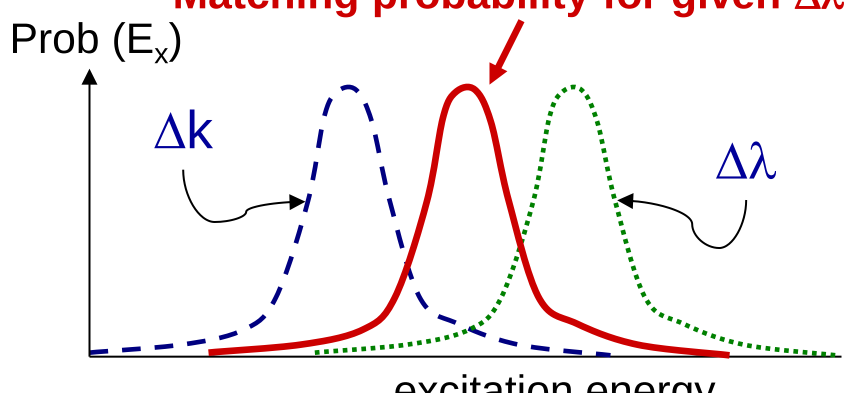

Example of Brink matching conditions

$^{12}C\ (\ ^{17}O,^{16}O\ )\ ^{13}C\ *$ $E_{beam} = 100$ MeV

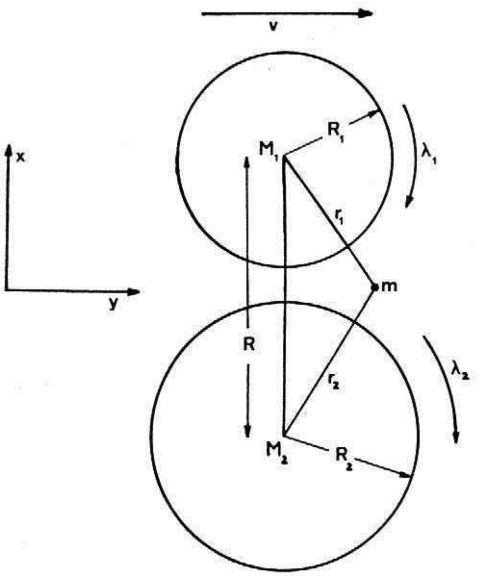

Projectile is ^{17}O which has transferred nucleon in $d_{5/2}$ orbital which can have $\lambda_1 = 0, \pm 2$ (π selection rules)

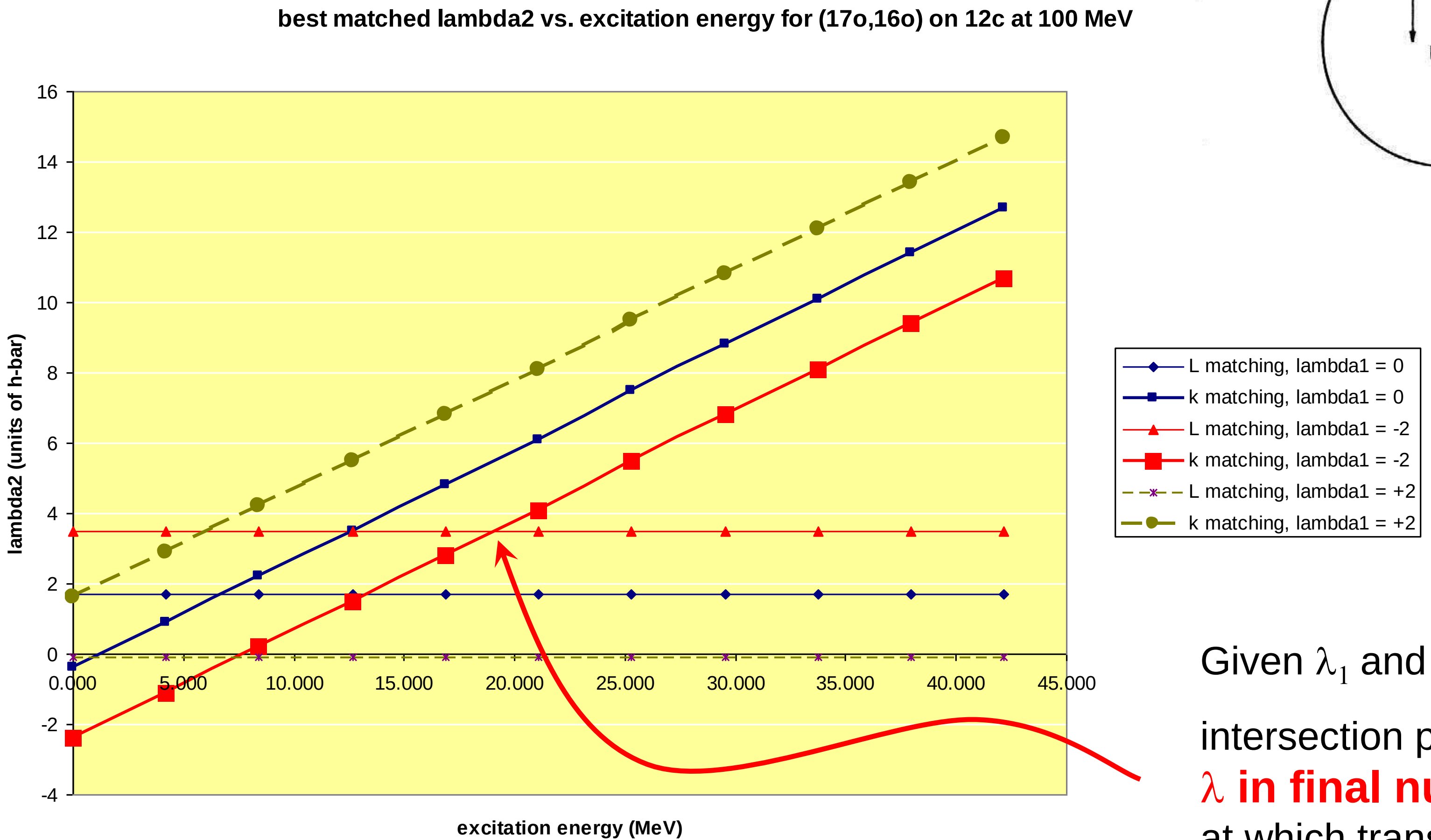

Given λ_1 and the reaction:

intersection point gives
λ in final nucleus and E_x
at which transfer is **matched**

$j_> / j_<$ selectivity

P.D. Bond, *Phys. Rev.*, **C22** (1980) 1539

P.D. Bond, *Comments Nucl. Part. Phys.*, **11** (1983) 231-240

The application of $j_> / j_<$ selectivity is difficult if considering experiments with complete kinematics with RNBs

However, detecting just the beam-like particle in coincidence with decay gamma-rays has much potential (recent experiments at ORNL, F. Liang)

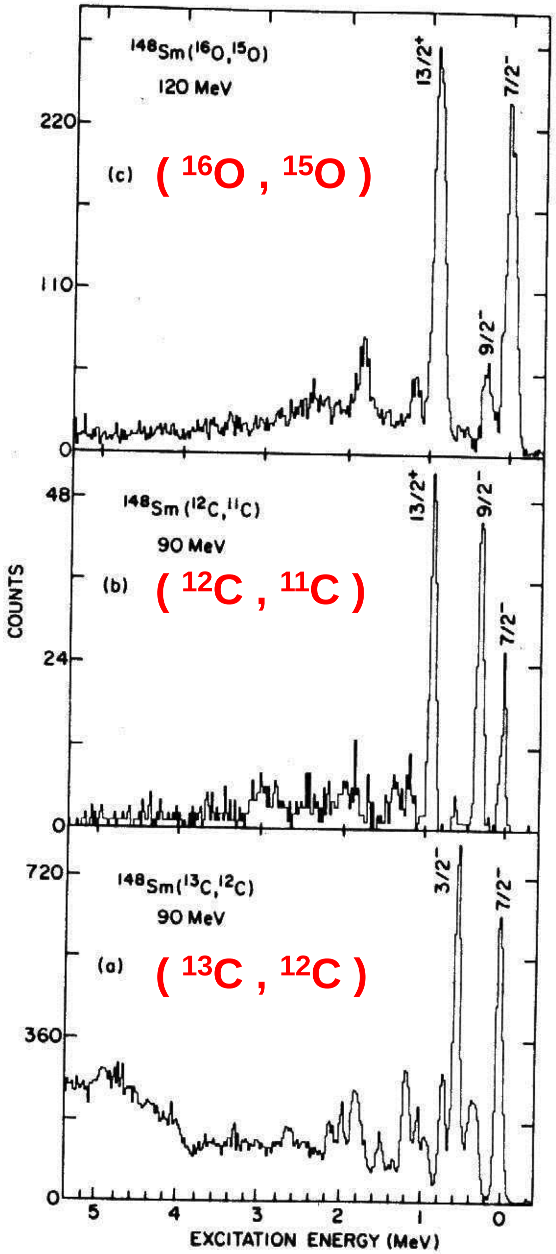

FIGURE 1 Single neutron transfer reactions for $^{148}Sm \rightarrow {}^{149}Sm$. Spectra were taken at the peaks of the bell-shaped angular distributions. Note the strong difference in the relative population of final states with (a) the (^{13}C, ^{12}C) reaction, (b) the (^{12}C, ^{11}C) reaction and (c) the (^{16}O, ^{15}O) reaction.

Q = – 9.8 MeV < < 0
high j values populated

Initial orbit $p_{1/2} = j_<$

favours $j_>$ e.g. $f_{7/2}$

Q = – 12.8 MeV < < 0
high j values populated

Initial orbit $p_{3/2} = j_>$

favours $j_<$ e.g. $h_{9/2}$

Q = 0.925 MeV ≈ 0
lower j values seen

Less $j_> / j_<$ selectivity

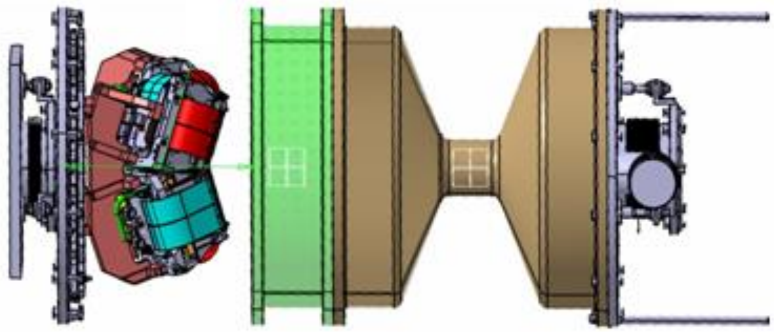

Thank you to all of the Collaborators…

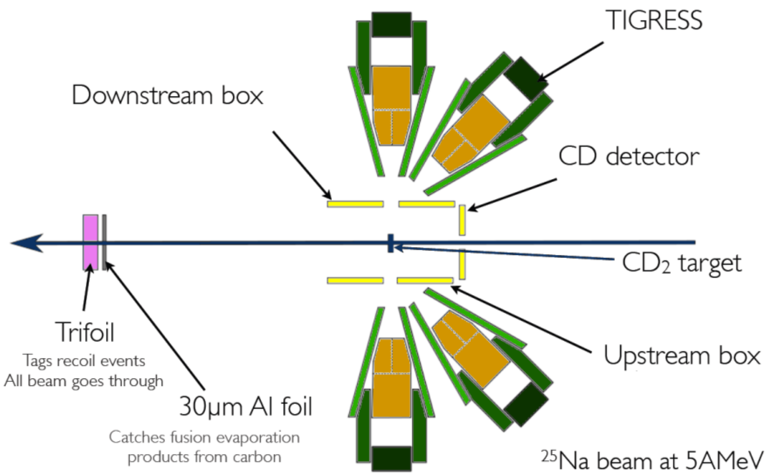

And thank you to all of the Audience…